



Measurement of photon–jet transverse momentum correlations in 5.02 TeV Pb + Pb and pp collisions with ATLAS



The ATLAS Collaboration *

ARTICLE INFO

Article history:

Received 19 September 2018
 Received in revised form 19 November 2018
 Accepted 10 December 2018
 Available online 13 December 2018
 Editor: W.-D. Schlatter

ABSTRACT

Jets created in association with a photon can be used as a calibrated probe to study energy loss in the medium created in nuclear collisions. Measurements of the transverse momentum balance between isolated photons and inclusive jets are presented using integrated luminosities of 0.49 nb^{-1} of Pb + Pb collision data at $\sqrt{s_{\text{NN}}} = 5.02 \text{ TeV}$ and 25 pb^{-1} of pp collision data at $\sqrt{s} = 5.02 \text{ TeV}$ recorded with the ATLAS detector at the LHC. Photons with transverse momentum $63.1 < p_T^{\gamma} < 200 \text{ GeV}$ and $|\eta^{\gamma}| < 2.37$ are paired with all jets in the event that have $p_T^{\text{jet}} > 31.6 \text{ GeV}$ and pseudorapidity $|\eta^{\text{jet}}| < 2.8$. The transverse momentum balance given by the jet-to-photon p_T ratio, $x_{j\gamma}$, is measured for pairs with azimuthal opening angle $\Delta\phi > 7\pi/8$. Distributions of the per-photon jet yield as a function of $x_{j\gamma}$, $(1/N_{\gamma})(dN/dx_{j\gamma})$, are corrected for detector effects via a two-dimensional unfolding procedure and reported at the particle level. In pp collisions, the distributions are well described by Monte Carlo event generators. In Pb + Pb collisions, the $x_{j\gamma}$ distribution is modified from that observed in pp collisions with increasing centrality, consistent with the picture of parton energy loss in the hot nuclear medium. The data are compared with a suite of energy-loss models and calculations.

© 2018 The Author(s). Published by Elsevier B.V. This is an open access article under the CC BY license (<http://creativecommons.org/licenses/by/4.0/>). Funded by SCOAP³.

1. Introduction

The energy loss of fast partons traversing the hot, deconfined medium created in nucleus–nucleus collisions can be studied in a controlled and systematic way through the analysis of jets produced in association with a high transverse momentum (p_T) prompt photon [1–7]. At leading order in quantum chromodynamics, the photon and leading jet are produced back-to-back in the azimuthal plane, with equal transverse momenta. Measurements of prompt photon production in Au + Au collisions at the Relativistic Heavy Ion Collider (RHIC) [8] and Pb + Pb collisions at the Large Hadron Collider (LHC) [9] have confirmed that, since photons do not participate in the strong interaction, their production rates are not modified by the medium [10]. Thus, photons provide an estimate of the p_T and direction of the parton produced in the initial hard-scattering before it has lost energy through interactions with the medium. Measurements of jet production with different requirements on the photon kinematics can therefore shed light on how the absolute amount of parton energy loss depends on the initial parton p_T .

Furthermore, photon–jet events offer a particularly useful way to probe the distribution of energy lost by jets in individual events,

and are complementary to measurements such as the dijet p_T balance [11–13]. Whereas those measurements report the ratio of the transverse momenta of two final-state jets, both of which may have lost energy, photon–jet events provide an alternative system in which one high- p_T object is certain to remain unaffected by the hot nuclear medium. Finally, jets produced in association with a photon are more likely to originate from quarks than those produced in dijet events at the same p_T . Thus, when considered together with measurements of dijets or of inclusive jet [14–16] and hadron [17–19] production rates in Pb + Pb collisions, analysis of photon–jet events can help to further constrain the flavour (i.e. quark versus gluon) dependence of parton energy loss.

Studies of photon–hadron correlations, in which high- p_T hadrons are used as a proxy for the jet, were first performed at RHIC [20–22], and measurements using fully reconstructed jets have since begun at the LHC [23,24]. In the LHC studies, the distribution of the photon–jet azimuthal separation, $\Delta\phi$, was found to be consistent with that in simulated photon–jet events embedded into a heavy-ion background, and the jet-to-photon transverse momentum ratio, $x_{j\gamma} = p_T^{\text{jet}}/p_T^{\gamma}$, was studied for inclusive photon–jet pairs. The per-photon jet yield $(1/N_{\gamma})(dN/dx_{j\gamma})$ distribution was shifted to significantly smaller values in Pb + Pb data.

In these previous measurements, the $x_{j\gamma}$ distributions in Pb + Pb events were not corrected for detector resolution effects, which led to a substantial broadening of the reported distribu-

* E-mail address: atlas.publications@cern.ch.

tions in data. As a result, qualitative comparisons with models or even with the analogous distributions in proton–proton (pp) data could only be accomplished by applying an additional smearing to the comparison distributions to introduce detector effects. Recent measurements of dijet p_T correlations [12] and inclusive jet fragmentation functions at large longitudinal momentum fraction [25] in $Pb + Pb$ collisions used unfolding procedures to correct for bin-migration effects and return the distributions to the particle level, i.e. free from detector effects.

This Letter reports a study of photon–jet correlations in $Pb + Pb$ collisions at a nucleon–nucleon centre-of-mass energy $\sqrt{s_{NN}} = 5.02$ TeV and pp collisions at the same centre-of-mass energy $\sqrt{s} = 5.02$ TeV. The data were recorded in 2015 with the ATLAS detector at the LHC and correspond to integrated luminosities of 0.49 nb^{-1} and 25 pb^{-1} , respectively. Events containing a prompt photon with $63.1 < p_T^\gamma < 200 \text{ GeV}$ and pseudorapidity $|\eta^\gamma| < 2.37$ (excluding the region $1.37 < |\eta^\gamma| < 1.52$) are studied. The p_T balance of photon–jet pairs for jets with $p_T^{\text{jet}} > 31.6 \text{ GeV}$ and $|\eta^{\text{jet}}| < 2.8$ which are approximately back-to-back with the photon in the transverse plane, $\Delta\phi > 7\pi/8$, is analysed through the per-photon yield of jets as a function of $x_{J\gamma}$, with all jets that meet this selection requirement counted separately. In Monte Carlo simulations, the fraction of photons paired with more than one jet rises from 1% to $\approx 15\%$ over the reported photon p_T ranges. The particular photon and jet p_T ranges used in the measurement are chosen to be evenly spaced on logarithmic scales to facilitate the unfolding procedure described below.

The yields are corrected via data-driven techniques for background arising from combinatoric pairings of each photon with unrelated jets in $Pb + Pb$ events and from the contamination by neutral mesons in the photon sample. The resulting $x_{J\gamma}$ distributions are corrected for the effects of the experimental resolution on the photon and jet p_T via a two-dimensional unfolding procedure similar to that used in Ref. [12]. Due to higher-order effects, photon–jet events do not generally have the back-to-back leading order topology mentioned above. Thus the pp data, which includes these effects, provides the reference distributions against which to interpret the results in $Pb + Pb$ events. This Letter directly compares photon–jet data in $Pb + Pb$ and pp events, and with Monte Carlo event generators and analytic calculations [26–29].

2. Experimental set-up

The ATLAS experiment [30] is a multipurpose particle detector with a forward–backward symmetric cylindrical geometry and nearly 4π coverage.¹ This analysis relies on the inner detector, the calorimeter and the data acquisition and trigger system.

The inner detector comprises three major subsystems: the pixel detector and the silicon microstrip tracker, which extend out to $|\eta| = 2.5$, and the transition radiation tracker which extends to $|\eta| = 2.0$. The inner detector covers the full azimuth and is immersed in a 2 T axial magnetic field. The pixel detector consists of four cylindrical layers in the barrel region and three disks in each endcap region. The silicon microstrip tracker comprises four cylindrical layers (nine disks) of silicon strip detectors in the barrel (endcap) region.

The calorimeter is a large-acceptance, longitudinally-segmented sampling detector covering $|\eta| < 4.9$ with electromagnetic (EM) and hadronic sections. The EM calorimeter is a lead/liquid-argon sampling calorimeter with an accordion-shaped geometry. It is divided into a barrel region, covering $|\eta| < 1.475$, and two endcap regions, covering $1.375 < |\eta| < 3.2$. The EM calorimeter has three primary sections, longitudinal in shower depth, called “layers”, in the barrel region and up to $|\eta| = 2.5$ in the end cap regions. In the barrel and first part of the end cap ($|\eta| < 2.4$), with the exception of the regions $1.4 < |\eta| < 1.5$, the first layer has a fine segmentation in η ($\Delta\eta = 0.003\text{--}0.006$) to allow the discrimination of photons from the two-photon decays of π^0 and η mesons. Over most of the acceptance, the total material upstream of the EM calorimeter ranges from 2.5 to 6 radiation lengths. In the transition region between the barrel and endcap regions ($1.37 < |\eta| < 1.52$), the amount of material rises to 11.5 radiation lengths, and thus this region is not used for the detection of photons. The hadronic calorimeter is located outside the EM calorimeter. It consists of a steel/scintillator-tile sampling calorimeter covering $|\eta| < 1.7$ and a liquid-argon calorimeter with copper absorber covering $1.5 < |\eta| < 3.2$.

The forward calorimeter (FCal) is a liquid-argon sampling calorimeter located on either side of the interaction point. It covers $3.1 < |\eta| < 4.9$ and each half is composed of one EM and two hadronic sections, with copper and tungsten serving as the absorber material, respectively. The FCal is used to characterise the centrality of $Pb + Pb$ collisions as described below. Finally, zero-degree calorimeters (ZDC) are situated at large pseudorapidity, $|\eta| > 8.3$, and are primarily sensitive to spectator neutrons.

A two-level trigger system is used to select events, with a first-level trigger implemented in hardware followed by a software-based (high-level) trigger. Data for this measurement were acquired using a high-level photon trigger [31] covering the central region ($|\eta| < 2.5$). At the first-level trigger stage, the transverse energy of EM showers is computed within regions of $\Delta\phi \times \Delta\eta = 0.1 \times 0.1$, and those showers which satisfy an E_T threshold are used to seed the high-level trigger stage. At this next stage, reconstruction algorithms similar to those applied in the offline analysis use the full detector granularity to form the final trigger decision. The trigger was configured with an online photon- p_T threshold of 30 GeV (20 GeV) in the pp ($Pb + Pb$) running period and required the candidate photon to satisfy a set of loose criteria for the electromagnetic shower shape [31]. For the $Pb + Pb$ data-taking, the high-level trigger included a procedure to estimate and subtract the underlying event (UE) contribution to the E_T measured in the calorimeter [9], ensuring high efficiency in high-activity $Pb + Pb$ events.

In addition to the photon trigger, $Pb + Pb$ data were recorded with minimum-bias triggers; these events are used to characterise the centrality of $Pb + Pb$ collisions as described in Section 3. The minimum-bias triggers are based on the presence of a minimum amount of approximately 50 GeV of transverse energy in all sections of the calorimeter system ($|\eta| < 3.2$) or, for events that do not meet this condition, on substantial energy deposits in both ZDC modules and an inner-detector track identified by the high-level trigger system.

3. Data selection and Monte Carlo samples

Photon–jet events in pp and $Pb + Pb$ collisions are initially selected for analysis by the high-level triggers described above. The typical number of interactions per bunch crossing in the pp and $Pb + Pb$ data-taking were one and smaller than 10^{-4} , respectively. Events are required to satisfy detector and data-quality requirements, and to contain a vertex reconstructed from tracks in the

¹ ATLAS uses a right-handed coordinate system with its origin at the nominal interaction point (IP) in the centre of the detector and the z -axis along the beam pipe. The x -axis points from the IP to the centre of the LHC ring, and the y -axis points upward. Cylindrical coordinates (r, ϕ) are used in the transverse plane, ϕ being the azimuthal angle around the z -axis. The pseudorapidity is defined in terms of the polar angle θ as $\eta = -\ln \tan(\theta/2)$. Transverse momentum and transverse energy are defined as $p_T = p \sin\theta$ and $E_T = E \sin\theta$, respectively. ΔR is defined as $\sqrt{(\Delta\eta)^2 + (\Delta\phi)^2}$.

inner detector. An additional requirement in Pb + Pb collisions, based on the correlation of the signals in the ZDC and the FCal, is used to reject a small number of recorded events consistent with two Pb + Pb interactions in the same bunch crossing (pile-up) [32]. The pile-up rate is largest in the most central events, where it is at most 0.1% and rejected with an efficiency greater than 98%. No pile-up rejection is applied in pp collisions.

The centrality of Pb + Pb events is defined using the total transverse energy measured in the FCal, evaluated at the electromagnetic scale and denoted by $\sum E_T$. The same observable was used to characterise 2010 and 2011 Pb + Pb data at $\sqrt{s_{NN}} = 2.76$ TeV [33] and a similar procedure, based on Monte Carlo Glauber modeling [34], is followed in 2015 data [35]. In this analysis, Pb + Pb events within five centrality ranges are considered that represent 0–10% (largest $\sum E_T$ values and degree of nuclear overlap), 10–20%, 20–30%, 30–50% and 50–80% (smallest $\sum E_T$ values and degree of nuclear overlap) of the population. The mean number of participating nucleons in minimum-bias Pb + Pb collisions, N_{part} , ranges from 33.3 ± 1.5 in 50–80% events to 358.8 ± 2.3 in 0–10% events.

Monte Carlo simulations of $\sqrt{s} = 5.02$ TeV pp photon-jet events are used to correct the data for bin migration and inefficiency effects, and for comparison with distributions measured in pp collision data. For all the samples described below, the generated events were passed through a full GEANT 4 simulation [36,37] of the ATLAS detector under the same conditions present during data-taking and were digitised and reconstructed in the same way as the data.

For the primary simulation samples, the PYTHIA 8.186 [38] generator was used with the NNPDF23LO parton distribution function (PDF) set [39], and generator parameters which were tuned to reproduce a set of minimum-bias data (the “A14” tune) [40]. Both the direct and fragmentation photon contributions are included in the simulation. Six million pp events were generated with a generator-level photon in the p_T range 50 GeV to 280 GeV. Additionally, a sample of 18 million events were produced with the same generator, tune and PDF, and were overlaid at the detector-hit level with minimum-bias Pb + Pb events recorded during the 2015 run. The relative contribution of events in this “data-overlay” sample were reweighted on an event-by-event basis to match the $\sum E_T$ distribution observed in the photon-jet events in Pb + Pb data selected for analysis. Thus the Pb + Pb simulation samples contain underlying-event activity levels and kinematic distributions of jets (used in the combinatoric photon-jet background estimation) identical to those in data.

Additional samples of 0.3 million pp events and 6 million events overlaid with Pb + Pb data were produced with the SHERPA 2.1.1 [41] generator using the CT10 PDF set [42], as were 0.6 million pp HERWIG 7 [43] events with the MMHT UE tune and PDF set [44]. The SHERPA samples were generated with leading-order matrix elements for photon-jet final states with up to three additional partons, which were merged with the SHERPA parton shower. The HERWIG events were generated in a way that includes the direct and fragmentation photon contributions. Both the SHERPA and HERWIG samples were filtered for the presence of a photon in the required kinematic region, and are used because they contain different photon + multijet topological distributions and jet-flavour compositions.

At generator level, photons are required to be isolated by requiring the sum of the transverse energy carried by primary particles² in a cone of size $\Delta R = 0.3$ around the photon, E_T^{iso} , to be

smaller than 3 GeV. In the analysis, the background subtraction, described below, removes photons which pass the isolation cut in data but fail this isolation requirement at the particle level. Jets are defined by applying the anti- k_t algorithm [45,46] with radius parameter $R = 0.4$ to primary particles within $|\eta| < 4.9$. In simulation, the jet flavour, i.e. whether it is quark- or gluon-initiated, is defined as the flavour of the highest- p_T parton that points to the generator-level jet [47].

4. Event reconstruction

4.1. Photon reconstruction

Photon candidates are reconstructed from clusters of energy deposited in EM calorimeter cells, following a procedure used for previous measurements of isolated prompt photon production in Pb + Pb collisions [9]. The procedure is similar to that used extensively in pp collisions [48,49], but is applied to the calorimeter cells after an event-by-event estimation and subtraction of the pile-up and UE contribution to the deposited energy in each cell [14]. In Pb + Pb collisions, all photon candidates are treated as if they were unconverted photons. Photon identification is based primarily on shower shapes in the calorimeter [50], selecting those candidates which are compatible with originating from a single photon impacting the calorimeter. The measurement of the photon energy is based on the energy collected in a small region of calorimeter cells centred on the photon ($\Delta\eta \times \Delta\phi = 0.075 \times 0.175$ in the barrel and $\Delta\eta \times \Delta\phi = 0.125 \times 0.125$ in the endcaps), and is corrected via a dedicated calibration [51], which accounts for upstream losses and both lateral and longitudinal leakage. The sum of transverse energy in calorimeter cells inside a cone size of $\Delta R = 0.3$ centred on the photon candidate, excluding a small central area of size $\Delta\eta \times \Delta\phi = 0.125 \times 0.175$, is used to compute the isolation energy E_T^{iso} . It is corrected for the expected leakage of the photon energy into the isolation cone.

Reconstructed photon candidates are required to satisfy identification and isolation criteria. The identification working point (called “tight”) includes requirements on each of several shower-shape variables [50]. These criteria reject two-photon decays of neutral mesons using information in the finely segmented first calorimeter layers, and reject hadrons which began showering in the EM section using information from the hadronic calorimeter. The isolation energy is required to be $E_T^{\text{iso}} < 3$ GeV in pp collisions. In Pb + Pb collisions, where UE fluctuations significantly broaden the distribution of E_T^{iso} values, this requirement is set to approximately one standard deviation of the Gaussian-like part of the distribution centred at zero, $E_T^{\text{iso}} < 8$ GeV.

In simulation, prompt photons in pp collisions have a total reconstruction and selection efficiency greater than 90%. At low $p_T \approx 60$ GeV in the most central Pb + Pb collisions, this efficiency is $\approx 60\%$, rising with increasing p_T and in less central collisions. In all events, the p_T scale, defined as the mean ratio of measured photon p_T to the generator-level p_T , for photons which satisfy these criteria is within 0.5% (1%) of unity in the barrel (endcap). The p_T resolution decreases from 3% to 2% over the measured p_T range.

4.2. Jet reconstruction

Jets are reconstructed following the procedure previously used in 2.76 TeV and 5.02 TeV pp and Pb + Pb collisions [14,15,52], which is briefly summarised here. The anti- k_t algorithm [46] with $R = 0.4$ is applied to energy deposits in the calorimeter grouped into towers of size $\Delta\eta \times \Delta\phi = 0.1 \times 0.1$. An iterative procedure,

² Primary particles are defined as those with a proper mean lifetime, τ , exceeding $c\tau = 10$ mm. For the jet and isolation E_T measurements, muons and neutrinos are excluded from the definition.

based entirely on data, is used to obtain an event-by-event estimate of the average η -dependent UE energy density, including that from pile-up, while excluding from the estimate the contribution from jets arising from a hard scattering. An updated estimate of the jet four-momentum is obtained by subtracting the UE energy from the constituent towers of the jet. This procedure is also applied to pp data. The p_T values of the resulting jets are corrected for the average calorimeter response using an η - and p_T -dependent calibration derived from simulation. An additional correction, derived from *in situ* studies of events with a jet recoiling against a photon or Z boson and from the differences between the heavy-ion reconstruction algorithm and that normally used in the 13 TeV pp data [53], is applied. A final correction at the analysis level is applied to correct for a deficiency in jet calibration due to it being derived from an event sample with a different jet flavour composition.

The distribution of reconstructed jet p_T values was studied in simulation as a function of generator-level jet p_T . In pp and $Pb + Pb$ collisions, the jet p_T scale is within 1% of unity. In pp collisions, the jet p_T resolution decreases from 15% at $p_T \approx 30$ GeV to 10% at $p_T \approx 200$ GeV. In $Pb + Pb$ collisions, the resolution at fixed jet p_T becomes worse in more central collisions in a way consistent with the increasing magnitude of UE fluctuations in the jet cone. In the most central events and at the lowest jet- p_T values, the resolution reaches 50%. At high p_T , the resolution asymptotically becomes centrality-independent and, at 200 GeV, consistent with that in pp collisions. More information about the jet reconstruction and jet performance in this dataset may be found in Ref. [54].

5. Data analysis

5.1. Photon purity and yield

After applying the identification and isolation selection criteria in pp collisions, approximately 19 500, 7800, 4100 and 400 photons are selected with $p_T^\gamma = 63.1\text{--}79.6$ GeV, 79.6–100 GeV, 100–158 GeV and 158–200 GeV, respectively. In $Pb + Pb$ collisions, the analogous yields are 15 400, 6300, 3500 and 300. These raw yields are determined as a function of p_T^γ and are then corrected for background and for the effects of p_T bin migration.

First, the selected photon sample is corrected for the background contribution, primarily from misidentified neutral hadrons. For each p_T^γ and centrality range, the purity of prompt photons within this range is estimated with a double-sideband approach [9, 48,49], which is summarised in the following.

In addition to the nominal selection, background-enhanced samples of photon candidates are defined by selecting photons failing at least one of four specific shower-shape requirements (referred to as the “non-tight” selection), or by requiring that they are not isolated such that $E_T^{\text{iso}} > 5$ GeV in pp collisions or $E_T^{\text{iso}} > 10$ GeV in $Pb + Pb$ collisions. Regions A and B are defined as those containing tight photons which are isolated and non-isolated, respectively, with region A corresponding to the signal photon selection. Regions C and D contain non-tight photons which are isolated and non-isolated, respectively. The number of photon candidates in each region is generally a mixture of signal and background photons, i.e. those arising from neutral mesons inside jets. The E_T^{iso} distribution for background photons is expected to be the same for the tight and non-tight selections such that the distribution of background photons “factorises” along isolation and identification axes. Separately, the probability that a prompt photon is found in regions B , C or D is determined from simulation. This information and the background factorisation assumption is

then applied to the data to determine the purity of photons in region A , defined as the ratio of the number of signal photons to all selected photons. The purity increases systematically with p_T^γ over the measured p_T range. In pp collisions, it rises from $\approx 85\%$ at $p_T^\gamma = 80$ GeV to more than 95% at 100 GeV, while in $Pb + Pb$ collisions it is typically $\approx 75\text{--}90\%$ over the same kinematic range.

The background-corrected prompt photon yields are then corrected for the resolution of the p_T^γ measurement. This is performed by comparing the yields, evaluated separately as a function of reconstructed and generator-level p_T , in simulation. Given the good p_T resolution, these differ by 2% at most, and this small resulting correction is applied to the yields in data.

5.2. Jet background subtraction

The raw jet yields, measured as a function of $x_{j\gamma}$, are corrected for two background components using data-driven methods. The corrections are performed separately for each p_T^γ interval and separately in pp collisions and $Pb + Pb$ collisions of different centrality ranges.

The first background arises from the combination of a high- p_T photon with jets unrelated to the photon-producing hard scattering. These include jets from separate hard parton-parton scatterings and UE fluctuations reconstructed as jets. This background is negligible in pp collisions. Because of the inclusive jet selection in the analysis, the combinatoric background is purely additive and can be statistically subtracted after scaling to the total photon yield. The combinatoric jet yields are determined in the data-overlay simulation, by examining the yield of reconstructed jets separated from a generator-level photon by $\Delta\phi > 7\pi/8$. Reconstructed jets that are not consistent with a generator-level jet, i.e. no generator-level jet with $p_T > 20$ GeV within $\Delta R < 0.4$, are deemed to arise from the original $Pb + Pb$ data event and are thus labelled as “combinatorial” jets. The combinatoric jet yields are subtracted from the measured $x_{j\gamma}$ distributions in data.

The second background is related to the estimated purity of the selected photons. The $x_{j\gamma}$ yields for photon candidates in region A contain an admixture of dijets, specifically jets correlated with misidentified neutral mesons. Since these hadrons pass experimental isolation requirements, they may be, for example, the leading fragment inside a jet. The shape of this background in the $x_{j\gamma}$ distribution is determined by repeating the analysis for photon candidates in region C , since this region contains mostly neutral mesons that remain isolated at the detector level. The resulting per-photon $x_{j\gamma}$ distributions are scaled to match the number of background photons, as determined above in Section 5.1, and their yields are statistically subtracted from the jet yields for photons in region A .

Fig. 1 shows the size of these backgrounds in the lowest- p_T^γ interval, where they are the largest. The combinatoric jet background for $Pb + Pb$ collisions contributes primarily to kinematic regions populated by $p_T^{\text{jet}} < 50$ GeV. It also depends strongly on centrality, being largest in 0–10% collisions but nearly negligible already in 30–50% collisions. The dijet background contributes to a broad range of p_T^γ values including the region $x_{j\gamma} > 1$, since the p_T ratio of a jet to one of the hadrons in the balancing jet can generally be above unity. This background has a similar shape in all event types. However, since the photon purity is lower in $Pb + Pb$ events than in pp events, this correction is larger in the former.

5.3. Unfolding

The background-subtracted $x_{j\gamma}$ yields are corrected for bin-migration effects due to detector resolution via a Bayesian unfolding procedure [55,56]. To accomplish this, the reconstructed

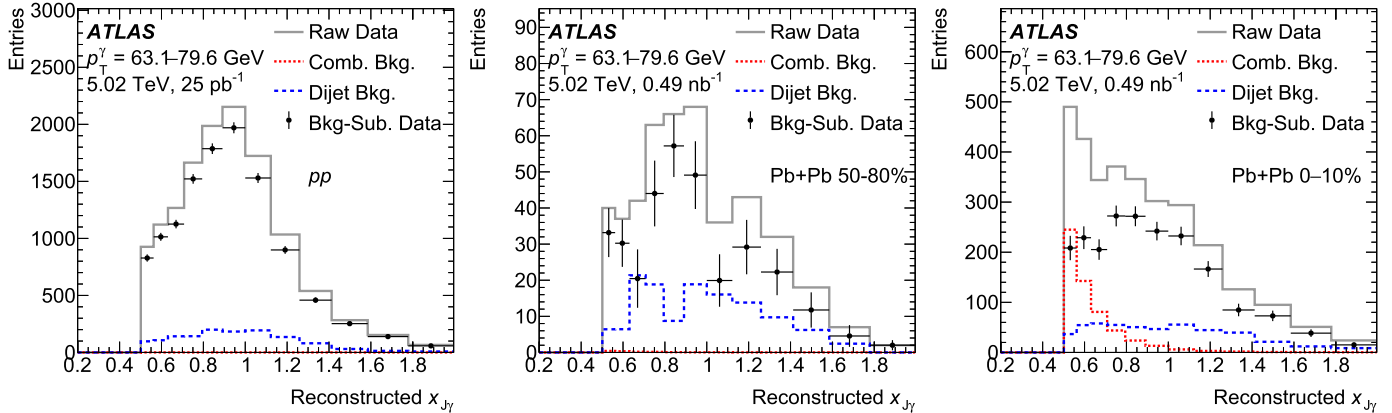


Fig. 1. Distributions of the photon-jet p_T -balance $x_{J\gamma}$ for the photon transverse momentum interval $p_T^\gamma = 63.1\text{--}79.6 \text{ GeV}$ for (left) pp , (centre) 50–80% centrality and (right) 0–10% centrality $\text{Pb} + \text{Pb}$ events. Solid grey, dotted red, and dashed blue histograms show the raw jet yields, the estimate of the combinatoric background (non-existent for pp events), and the dijet background, respectively. Black points show the background-subtracted data before unfolding, with the vertical bars representing the combined statistical uncertainty from the data and background subtraction procedure.

yields are arranged in a two-dimensional ($p_T^\gamma, x_{J\gamma}$) matrix with bin edges that are evenly spaced on logarithmic scales (and with values matching those used in previous jet measurements), and a two-dimensional unfolding is performed similar to that for dijet p_T correlations in Ref. [12]. The unfolding is performed in $x_{J\gamma}$ directly to preserve the fine correlation between p_T^{jet} and p_T^γ which would be washed out if the unfolding were performed in $(p_T^\gamma, p_T^{\text{jet}})$. Although the migration along the p_T^γ axis is small, it is necessary to include it since the degree of bin migration in $x_{J\gamma}$ depends on the p_T of the jets.

To fully account for the effects of bin migration across the analysis selection, the axes of the matrix are extended over a larger range of p_T^γ and $x_{J\gamma}$ than the fiducial region in which the results are reported. A response matrix is determined by matching each pair of ($p_T^\gamma, x_{J\gamma}$) values at the generator level to their counterparts at the reconstruction level, separately for pp events and for each $\text{Pb} + \text{Pb}$ centrality.

The Bayesian unfolding method requires a choice for the number of iterations, n_{iter} , and an assumption for the prior for the initial particle-level distribution. The PYTHIA simulation does not include the effects of jet energy loss, and thus the underlying particle-level distribution in data is expected to have a shape different from the default prior in the simulation. An initial unfolding using the default PYTHIA prior is performed for each centrality selection, and the ratios of the unfolded distributions to the generator-level priors in PYTHIA are fitted with a smooth function in $x_{J\gamma}$ in each p_T^γ interval. This function is evaluated to give a weight $w = w(x_{J\gamma}, p_T^\gamma)$ that is used to reweight the generator-level distribution in simulation and thus construct a nominal prior. Alternative reweightings, used in evaluating the sensitivity to the choice of prior, are determined by applying \sqrt{w} (the geometric mean of the nominal reweighting and no reweighting) and $w^{3/2}$ to the sample. The reconstruction-level $x_{J\gamma}$ distributions in simulation after each of these reweightings were examined to ensure that they span a reasonable range of values compared to that observed at the reconstruction level in data.

Before applying the unfolding procedure to data, it was tested on simulation. After the nominal reweighting, the Monte Carlo samples were split into two statistically independent subsamples. One subsample was used to populate the response matrix, which was then used to unfold the reconstruction-level distribution in the other subsample. The unfolded result was compared with the original generator-level distribution in the latter sample, which

were found to be recovered within the limits of the statistical precision of the samples.

The values of n_{iter} used for the nominal results are chosen following the same procedure as in Ref. [12]. For each centrality selection, the unfolded distributions are examined as a function of n_{iter} . For each value of n_{iter} , a total uncertainty is formed by adding two components in quadrature: (1) the statistical uncertainty of the unfolded data, which grows slowly with n_{iter} , and (2) the sum of square differences between the results and those obtained with an alternative prior, which decreases quickly with n_{iter} . The final values of n_{iter} are chosen to minimise the total uncertainty, and are between two and four.

The unfolded $x_{J\gamma}$ results are corrected for the jet reconstruction efficiency, evaluated in simulation as the p_T^γ -dependent probability that a generated jet at the given $x_{J\gamma}$ is successfully reconstructed within the total ($p_T^\gamma, x_{J\gamma}$) range used in the unfolding. This efficiency is typically $> 99\%$ for all events in the kinematic regions populated by jets with $p_T > 50 \text{ GeV}$. In pp collisions, this efficiency falls to $\approx 96\%$ in the lowest- $x_{J\gamma}$ region for each p_T^γ interval. In $\text{Pb} + \text{Pb}$ collisions, the efficiency at fixed $x_{J\gamma}$ decreases monotonically in increasingly central events, reaching a minimum of $\approx 75\%$ in the lowest- $x_{J\gamma}$ region in 0–10% centrality events.

6. Systematic uncertainties

The primary sources of systematic uncertainty can be grouped into three major categories: the measurement of p_T^{jet} ; the selection of the photon and measurement of p_T^γ ; the modelling and subtraction of the combinatoric background; and the unfolding procedure. For each variation described below, the entire analysis is repeated including the background correction steps and unfolding. The differences between the resulting $x_{J\gamma}$ values and the nominal ones are taken as an estimate of the uncertainty from each source.

A standard set of uncertainties in the jet p_T scale and resolution, following the strategy described in Ref. [57] and commonly used for measurements in 2015 $\text{Pb} + \text{Pb}$ and pp data [54,58], are used in this analysis. The impact of the uncertainties is evaluated by modifying the response matrix according to the given variations in the reconstructed jet p_T . These include uncertainties in the p_T scale derived from *in situ* studies of the calorimeter response [47,59], an uncertainty in the resolution derived using data-driven techniques [60], and uncertainties in both which result from a small relative energy-scale difference between the heavy-ion jet reconstruction procedure and that used in $\sqrt{s} = 13 \text{ TeV}$

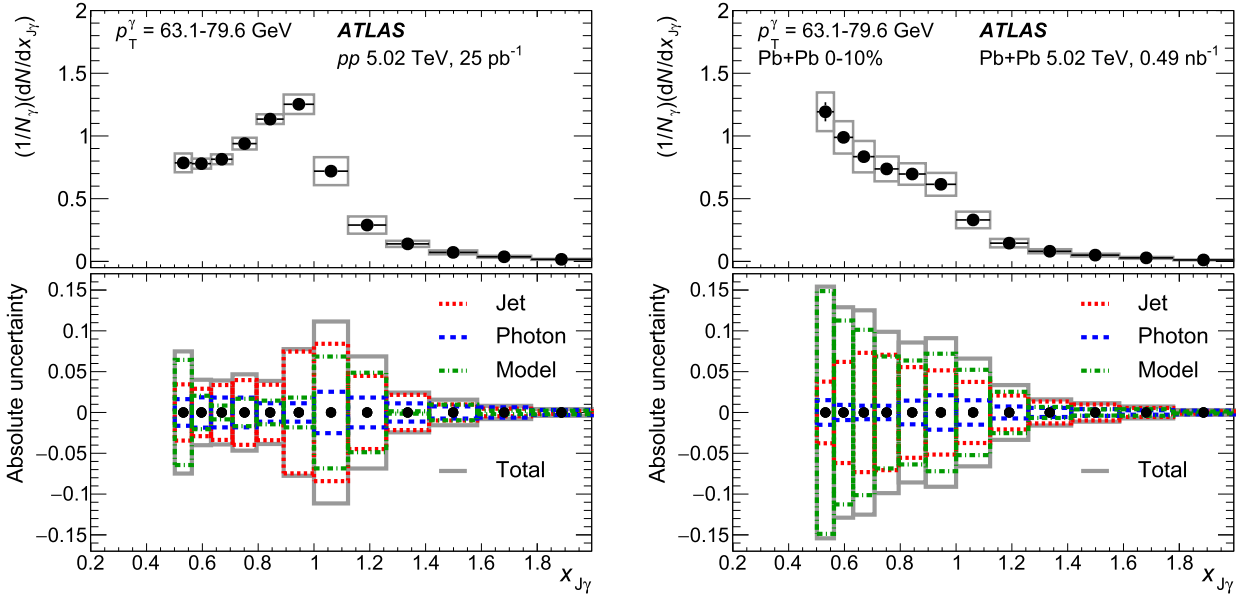


Fig. 2. Unfolded distributions and summary of systematic uncertainties in the per-photon jet-yield measurement for $p_T^\gamma = 63.1\text{--}79.6 \text{ GeV}$ in (left) pp events and (right) 0–10% centrality $\text{Pb} + \text{Pb}$ events. Top panels show the photon-jet p_T -balance $x_{J\gamma}$ distributions and total uncertainties, while the bottom panels show the absolute uncertainties from jet-related, photon-related, and modelling or unfolding sources, as well as the total uncertainty.

pp collisions [53]. All of the above uncertainties apply equally to jets in pp and $\text{Pb} + \text{Pb}$ events. A separate, centrality-dependent uncertainty is included in 0–60% $\text{Pb} + \text{Pb}$ collisions. This uncertainty accounts for a possible modification of the jet response after energy loss and is evaluated through *in situ* comparisons of the charged-particle track-jet and calorimeter-jet p_T values in data and simulation. More details are provided in Refs. [54,57]. No additional uncertainty is included for 60–80% centrality events.

Uncertainties in the photon purity estimate are determined by varying the non-tight identification and isolation criteria used to select hadron background candidates and by considering a possible non-factorisation of the hadron background along the axes used in the double-sideband procedure. The sensitivity to the modelling of photon shower shapes in simulation is evaluated by removing the data-driven corrections to these quantities [50]. Finally, the photon p_T scale and resolution uncertainties are described in detail in Ref. [51], and their impact is evaluated by applying them as variations to the response matrices used in unfolding.

Modelling- or unfolding-related systematic uncertainties arise from several sources. The estimate of the combinatoric photon-jet rate in the data-overlay simulation is sensitive to the requirement on the minimum p_T of a generator-level jet in the classification of a given reconstructed jet as a combinatoric jet, as opposed to a photon-correlated jet. To provide one estimate of the sensitivity to this threshold, it is varied in the range $20 \pm 10 \text{ GeV}$. To assess the sensitivity to the choice of prior, the unfolding is repeated using the alternative priors which are systematically closer to and farther from the original PYTHIA prior. The sensitivity to statistical limitations of the simulation samples is determined through pseudo-experiments, resampling entries in the response matrices according to their uncertainty. Finally, the analysis is repeated using the SHERPA simulation to perform the corrections and unfolding, since this generator provides a different description of photon-jet production topologies.

Fig. 2 summarises the systematic uncertainties in each category, as well as the total uncertainty, for the lowest- p_T^γ interval in pp and 0–10% $\text{Pb} + \text{Pb}$ events. The jet-related uncertainties are generally the dominant ones, except in more central events and

lower- p_T^γ intervals, where the unfolding and modelling uncertainties become co-dominant.

As an additional check on the features in the unfolded $x_{J\gamma}$ distributions observed in data, the analysis was repeated with two modifications which change the signal photon-jet definition. First, the photon-jet $\Delta\phi$ requirement was changed from $> 7\pi/8$ to $> 3\pi/4$. With this alteration, the correlated jet yield changes only by a small amount, while the combinatoric background, which is constant in $\Delta\phi$, doubles. Second, the analysis was repeated, but selecting only the leading (highest- p_T) jet in the event if it fell within the $\Delta\phi$ window. In this case, the combinatoric background contribution is no longer purely additive and the inefficiency when a higher- p_T uncorrelated jet is selected instead of the photon-correlated jet must be accounted for, similar to Ref. [12]. In both cases, the distributions in $\text{Pb} + \text{Pb}$ exhibit a qualitatively similar modification pattern compared to the main results as a function of $x_{J\gamma}$.

7. Results

The unfolded $(1/N_\gamma)(dN/dx_{J\gamma})$ distributions in pp collisions are shown for each p_T^γ interval in Fig. 3. The distributions are reported for all $x_{J\gamma}$ bins where the jet minimum p_T requirement is fully efficient. Also shown are the corresponding generator-level distributions from the PYTHIA, SHERPA and HERWIG samples. Each generator describes the data fairly well, with HERWIG generally overpredicting the yield at large- $x_{J\gamma}$ and SHERPA showing the best agreement over the full $x_{J\gamma}$ range.

The unfolded $(1/N_\gamma)(dN/dx_{J\gamma})$ distributions in $\text{Pb} + \text{Pb}$ collisions are presented in Figs. 4 through 7, with each figure representing a different p_T^γ interval. Since the results are fully corrected, they may be directly compared with the analogous $x_{J\gamma}$ distributions in pp collisions, which are reproduced in each panel for convenience.

For all p_T^γ intervals, the $x_{J\gamma}$ distributions in $\text{Pb} + \text{Pb}$ collisions evolve smoothly with centrality. For peripheral collisions with centrality 50–80%, they are similar to those measured in pp collisions. However, in increasingly more central collisions, the distributions become progressively more modified. For the $p_T^\gamma < 100 \text{ GeV}$ in-

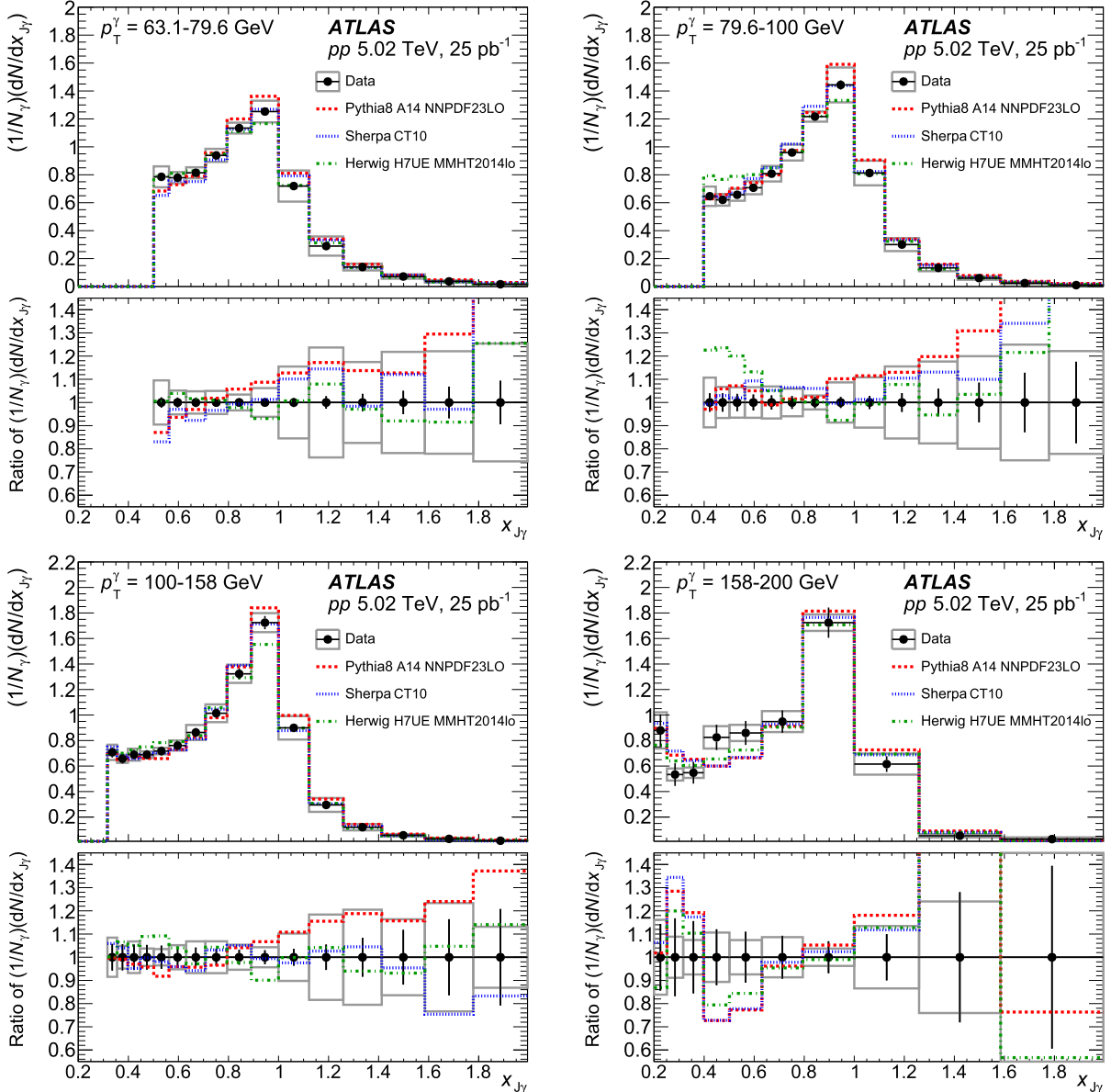


Fig. 3. Photon-jet p_T -balance distributions $(1/N_\gamma)(dN/dx_{J\gamma})$ in pp collisions, each panel showing a different photon- p_T interval. The unfolded results are compared with the particle-level distributions from three Monte Carlo event generators. Bottom panels show the ratios of the generators to the pp data. Total systematic uncertainties are shown as boxes, while statistical uncertainties are shown as vertical bars.

ervals shown in Figs. 4 and 5, the $x_{J\gamma}$ distributions in the most central 0–10% events are so strongly modified that they decrease monotonically over the measured $x_{J\gamma}$ range and no peak is observed. For the $p_T^\gamma > 100$ GeV region shown in Fig. 6, the $x_{J\gamma}$ distributions retain a peak at or near $x_{J\gamma} \approx 0.9$ even in the most central collisions. However, the magnitude of the peak is lower and significantly wider than the sharp peak in pp events. In both cases, the jet yield at small $x_{J\gamma}$ is systematically higher than that in pp collisions, by up to a factor of two. In less central events, a peak-like structure develops at the same position as the maximum in pp events, near $x_{J\gamma} \approx 0.9$. For the lowest- p_T^γ interval, this occurs only for 50–80% centrality events, while in the highest two p_T^γ intervals the distribution in 0–10% events is consistent with a local peak.

As another way of characterising how the modified $x_{J\gamma}$ distributions depend on centrality and p_T^γ , Fig. 8 presents their mean value, $\langle x_{J\gamma} \rangle$, and integral, R^γ , with both values calculated in the

region $x_{J\gamma} > 0.5$. These quantities are shown as a function of the mean number of participating nucleons N_{part} in the corresponding centrality selection, and are plotted for the first three p_T^γ intervals where they have small statistical uncertainties. When measured in the region $x_{J\gamma} > 0.5$, the value of $\langle x_{J\gamma} \rangle$ in pp collisions is observed to be ≈ 0.89 for all p_T^γ intervals. Simulation studies show that, at generator level, the jet yield at $x_{J\gamma} > 0.5$ corresponds to only the leading (highest- p_T) photon-correlated jet in each event. Thus, $\langle x_{J\gamma} \rangle$ can be interpreted as a conditional per-jet fractional energy loss, and R^γ can be interpreted as the fraction of photons with a leading jet above $x_{J\gamma} = 0.5$. In pp collisions, R^γ ranges from 0.65 to 0.75 in the three p_T^γ intervals shown, which is below unity due to the jet selection criteria ($\Delta\phi > 7\pi/8$, $|\eta| < 2.8$).

In Pb + Pb events, $\langle x_{J\gamma} \rangle$ decreases monotonically from the value in pp collisions as the collisions become more central. In the most central collisions, it is below the pp value by 0.04–0.06, depending on the p_T^γ interval, while in peripheral collisions it reaches a

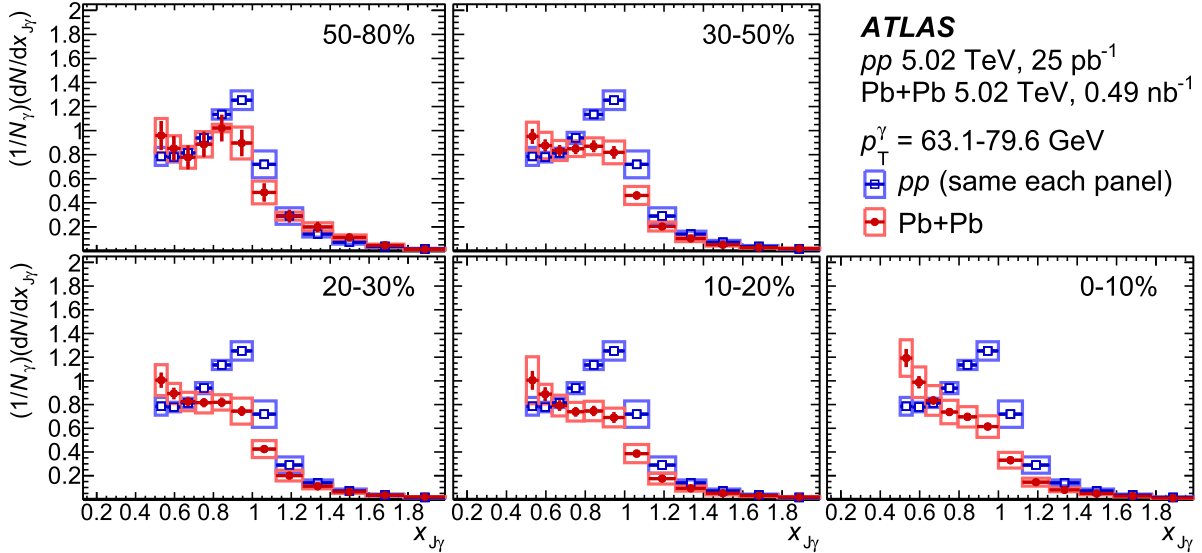


Fig. 4. Photon-jet p_T -balance distributions $(1/N_\gamma)(dN/dx_\gamma)$ in $\text{Pb} + \text{Pb}$ events (red circles) with each panel showing a different centrality selection compared to that in pp events (blue squares). These panels show results for $p_T^\gamma = 63.1\text{--}79.6 \text{ GeV}$. Total systematic uncertainties are shown as boxes, while statistical uncertainties are shown as vertical bars.

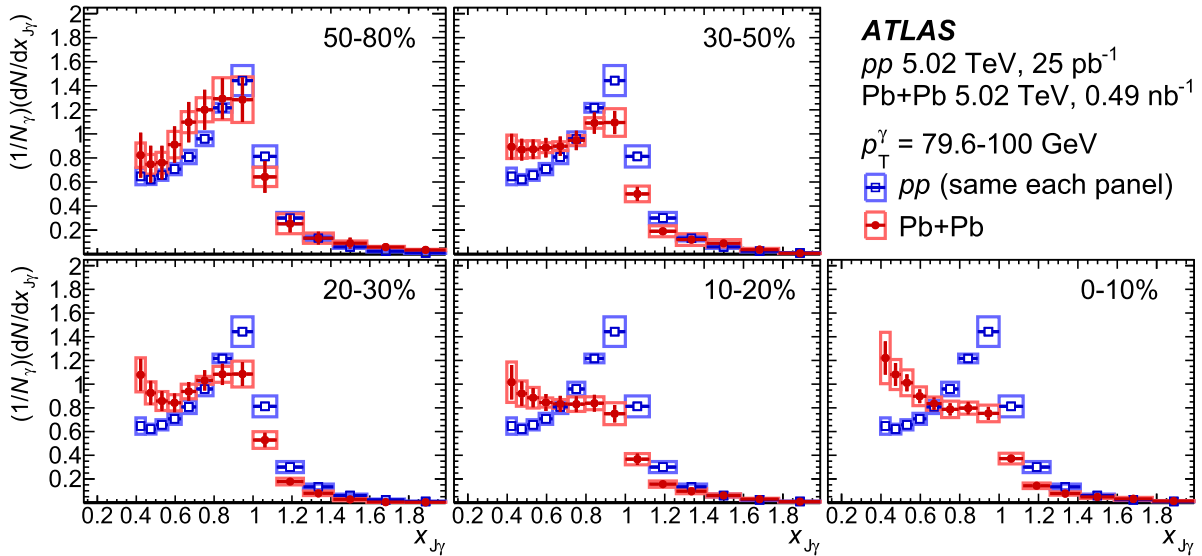


Fig. 5. Photon-jet p_T -balance distributions $(1/N_\gamma)(dN/dx_\gamma)$ in $\text{Pb} + \text{Pb}$ events (red circles) with each panel showing a different centrality selection compared to that in pp events (blue squares). These panels show results for $p_T^\gamma = 79.6\text{--}100 \text{ GeV}$. Total systematic uncertainties are shown as boxes, while statistical uncertainties are shown as vertical bars.

value which is statistically compatible with that in pp events. The R^γ value also decreases monotonically as the collisions become more central, reflecting the overall shift of the $x_{J\gamma}$ value of leading jets below $x_{J\gamma} = 0.5$. At low p_T^γ in central $\text{Pb} + \text{Pb}$ collisions, R^γ reaches the value of 0.5, which is only $\approx 75\%$ of its value in pp collisions.

The results are compared with the following theoretical predictions which include Monte Carlo generators and analytical calculations of jet energy loss: (1) a pQCD calculation which includes Sudakov resummation to describe the vacuum distributions and energy loss in $\text{Pb} + \text{Pb}$ collisions as described in the BDMPS-Z formalism [26], (2) a perturbative calculation within the framework of soft-collinear effective field theory with Glauber gluons (SCET_G) in the soft gluon emission (energy-loss) limit [27], (3) the JEWEL Monte Carlo event generator which simulates QCD jet evolution in heavy-ion collisions and includes energy-loss effects from

radiative and elastic scattering processes [28], and (4) the Hybrid Strong/Weak Coupling model [29] which combines initial production using PYTHIA with a parameterisation of energy loss derived from holographic methods, and includes back-reaction effects.

Figs. 9 and 10 compare a selection of the measured $x_{J\gamma}$ distributions with the results of these theoretical predictions, where possible. Before testing the description of energy-loss effects in $\text{Pb} + \text{Pb}$ events, the predicted $x_{J\gamma}$ distributions are compared with pp data in Fig. 9. The Hybrid model and JEWEL, which use PYTHIA for the photon-jet production in vacuum, give a good description of pp events over the measured $x_{J\gamma}$ range in both p_T^γ intervals shown. The BDMPS-Z and SCET_G perturbative calculations capture the general features but predict distributions that are more and less peaked, respectively, than those in data.

In $\text{Pb} + \text{Pb}$ events with low p_T^γ , shown in the left panel of Fig. 10, the JEWEL, Hybrid, and SCET_G models successfully capture

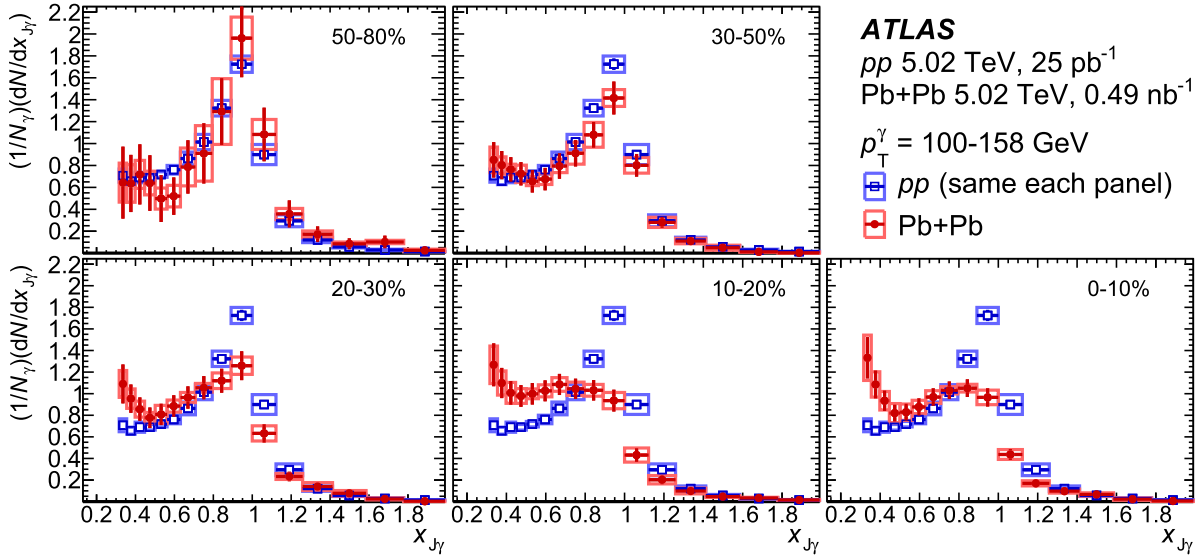


Fig. 6. Photon-jet p_T -balance distributions $(1/N_\gamma)(dN/dx_{J\gamma})$ in $Pb + Pb$ events (red circles) with each panel showing a different centrality selection compared to that in pp events (blue squares). These panels show results for $p_T^\gamma = 100\text{--}158 \text{ GeV}$. Total systematic uncertainties are shown as boxes, while statistical uncertainties are shown as vertical bars.

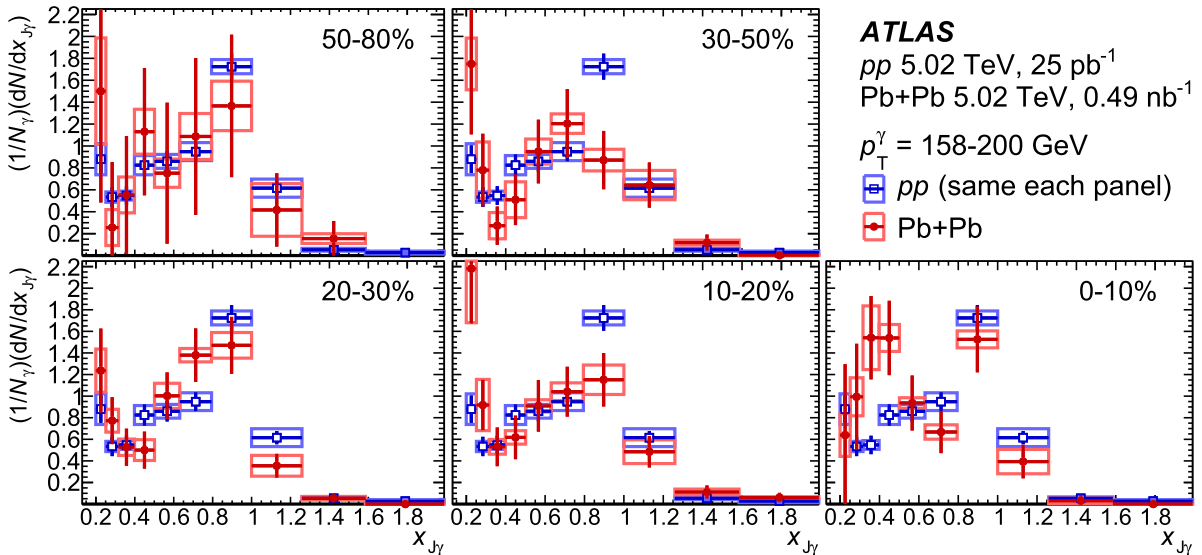


Fig. 7. Photon-jet p_T -balance distributions $(1/N_\gamma)(dN/dx_{J\gamma})$ in $Pb + Pb$ events (red circles) with each panel showing a different centrality selection compared to that in pp events (blue squares). These panels show results for $p_T^\gamma = 158\text{--}200 \text{ GeV}$. Total systematic uncertainties are shown as boxes, while statistical uncertainties are shown as vertical bars.

several key features of the $x_{J\gamma}$ distribution, including the absence of a visible peak, and the monotonically increasing behaviour with decreasing $x_{J\gamma}$. The BDMPS-Z model predicts a suppression of the yield near $x_{J\gamma} \approx 0.9$ relative to what is predicted in pp events, consistent with the trend in data. However, it underestimates the yield at low $x_{J\gamma}$ in both pp and $Pb + Pb$ collisions. In the higher- p_T^γ interval, the Hybrid model and JEWEL successfully describe the reappearance of a localised peak near $x_{J\gamma} \approx 0.9$. However, none of the models considered here describe the increase of the jet yield at $x_{J\gamma} < 0.5$ above that observed in pp events. Additional comparisons between these data and theoretical calculations which are differential in both p_T^γ and centrality will further constrain the description of the strongly coupled medium in these models.

8. Conclusion

This Letter presents a study of photon-jet transverse momentum correlations for photons with $63.1 < p_T^\gamma < 200 \text{ GeV}$ in $Pb + Pb$ collisions at $\sqrt{s_{NN}} = 5.02 \text{ TeV}$ and pp collisions at $\sqrt{s} = 5.02 \text{ TeV}$. The data were recorded with the ATLAS detector at the LHC and correspond to integrated luminosities of 0.49 nb^{-1} and 25 pb^{-1} , respectively. The data are corrected for the presence of combinatoric photon-jet pairs and of dijet pairs where one of the jets is misidentified as a photon. The measured quantities in data are fully corrected for detector effects and reported at the particle level. Per-photon distributions of the jet-to-photon p_T ratio, $x_{J\gamma} = p_T^{\text{jet}}/p_T^\gamma$, are measured for pairs with an azimuthally balanced configuration, $\Delta\phi > 7\pi/8$. In pp events, the data are well reproduced by event generators or models that depend on them, but are

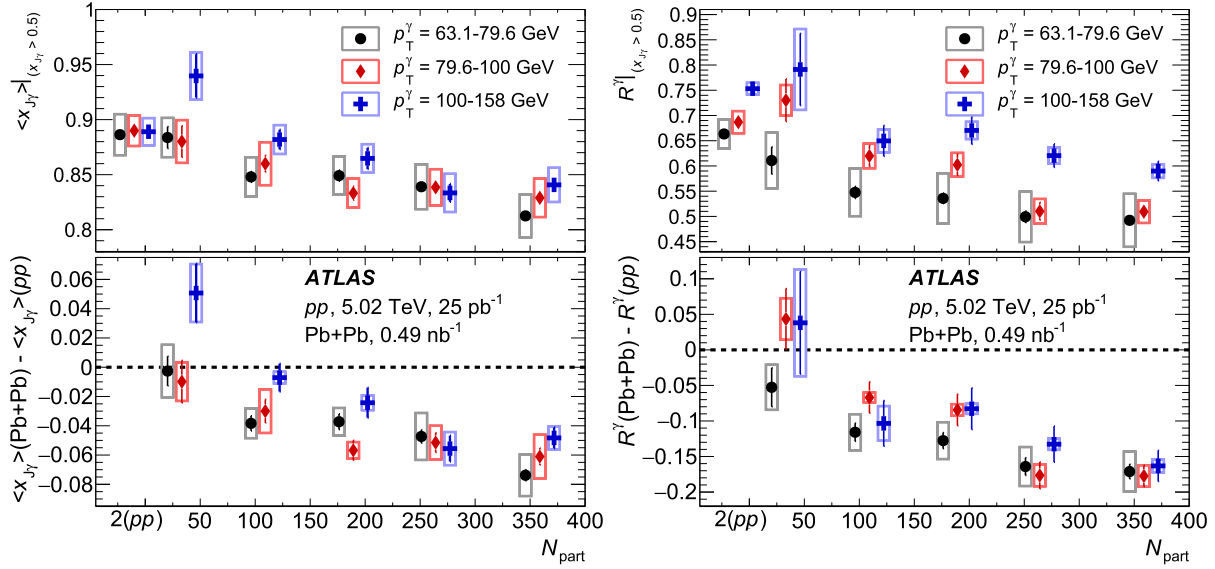


Fig. 8. Summary of (left) the mean jet-to-photon p_T ratio ($\langle x_{J\gamma} \rangle$) and (right) the total per-photon jet yield R^γ , calculated in the region $x_{J\gamma} > 0.5$. The values are presented as a function of the mean number of participating nucleons N_{part} in top panels. Each colour and symbol represents a different p_T^γ interval, where the lowest and highest intervals are displaced horizontally for clarity. The points plotted at $N_{\text{part}} = 2$ correspond to pp collisions. The bottom panels show the difference between the $\text{Pb} + \text{Pb}$ centrality selection and pp collisions. Boxes show the total systematic uncertainty while the vertical bars represent statistical uncertainties.

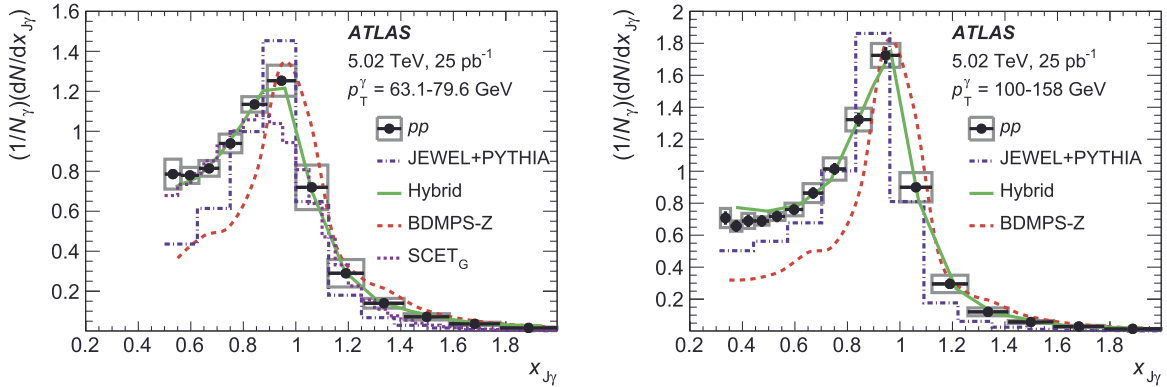


Fig. 9. Photon-jet p_T -balance distributions $(1/N_\gamma)(dN/dx_{J\gamma})$ in pp collisions for (left) $p_T^\gamma = 63.1\text{--}79.6 \text{ GeV}$ and (right) $p_T^\gamma = 100\text{--}158 \text{ GeV}$. The unfolded results are compared with the theoretical calculations shown as dashed coloured lines (see text). Total systematic uncertainties are shown as boxes, while statistical uncertainties are shown as vertical bars.

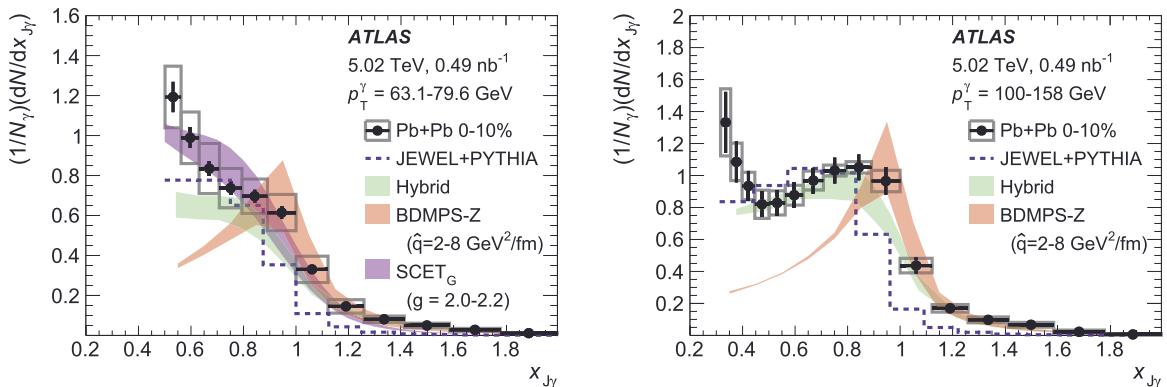


Fig. 10. Photon-jet p_T -balance distributions $(1/N_\gamma)(dN/dx_{J\gamma})$ in $0\text{--}10\%$ $\text{Pb} + \text{Pb}$ collisions for (left) $p_T^\gamma = 63.1\text{--}79.6 \text{ GeV}$ and (right) $p_T^\gamma = 100\text{--}158 \text{ GeV}$. The unfolded results are compared with the theoretical calculations shown as dashed coloured lines denoting central values or coloured bands which correspond to a range of theoretical parameters (see text). Total systematic uncertainties are shown as boxes, while statistical uncertainties are shown as vertical bars.

not fully described in detail by approaches based on perturbative calculations.

In $\text{Pb} + \text{Pb}$ collisions, $x_{\gamma\gamma}$ distributions are observed to have a significantly modified total yield and shape compared with those in pp collisions. These modifications have a smooth onset as a function of $\text{Pb} + \text{Pb}$ event centrality and p_T^γ . In peripheral collisions at high p_T^γ , the distributions in $\text{Pb} + \text{Pb}$ are statistically compatible with those in pp . In the most central $\text{Pb} + \text{Pb}$ events at low p_T^γ , the yield decreases monotonically with increasing $x_{\gamma\gamma}$ over the measured range, in strong contrast to the sharply peaked distributions in pp events. However, in less central events or in higher- p_T^γ intervals, the $x_{\gamma\gamma}$ distributions retain a peak-like excess at an $x_{\gamma\gamma}$ value similar to that in pp collisions but with a smaller per-photon yield. This last observation suggests that the amount of energy lost by jets in single events has a broad distribution, with a small but significant population of jets retaining a pp -like p_T correlation with the photon because they do not lose an appreciable amount of energy.

These results are sensitive to how partons initially produced opposite to a high- p_T photon lose energy in their interactions with the hot nuclear medium. Taken together with other measurements of single-jet and dijet production, the data provide new, complementary information about how energy loss in the strongly coupled medium varies with the initial parton flavour and p_T .

Acknowledgements

We thank CERN for the very successful operation of the LHC, as well as the support staff from our institutions without whom ATLAS could not be operated efficiently.

We acknowledge the support of ANPCyT, Argentina; YerPhI, Armenia; ARC, Australia; BMWFW and FWF, Austria; ANAS, Azerbaijan; SSTC, Belarus; CNPq and FAPESP, Brazil; NSERC, NRC and CFI, Canada; CERN; CONICYT, Chile; CAS, MOST and NSFC, China; COLCIENCIAS, Colombia; MSMT CR, MPO CR and VSC CR, Czech Republic; DNRF and DNSRC, Denmark; IN2P3-CNRS, CEA-DRF/IRFU, France; SRNSFG, Georgia; BMBF, HGF, and MPG, Germany; GSRT, Greece; RGCC, Hong Kong SAR, China; ISF and Benoziyo Center, Israel; INFN, Italy; MEXT and JSPS, Japan; CNRST, Morocco; NWO, Netherlands; RCN, Norway; MNiSW and NCN, Poland; FCT, Portugal; MNE/IFA, Romania; MES of Russia and NRC KI, Russian Federation; JINR; MESTD, Serbia; MSSR, Slovakia; ARRS and MIZŠ, Slovenia; DST/NRF, South Africa; MINECO, Spain; SRC and Wallenberg Foundation, Sweden; SERI, SNSF and Cantons of Bern and Geneva, Switzerland; MOST, Taiwan; TAEK, Turkey; STFC, United Kingdom; DOE and NSF, United States of America. In addition, individual groups and members have received support from BCKDF, Canarie, CRC and Compute Canada, Canada; COST, ERC, ERDF, Horizon 2020, and Marie Skłodowska-Curie Actions, European Union; Investissements d' Avenir Labex and Idex, ANR, France; DFG and AvH Foundation, Germany; Herakleitos, Thales and Aristeia programmes co-financed by EU-ESF and the Greek NSRF, Greece; BSF-NSF and GIF, Israel; CERCA Programme Generalitat de Catalunya, Spain; The Royal Society and Leverhulme Trust, United Kingdom.

The crucial computing support from all WLCG partners is acknowledged gratefully, in particular from CERN, the ATLAS Tier-1 facilities at TRIUMF (Canada), NDGF (Denmark, Norway, Sweden), CC-IN2P3 (France), KIT/GridKA (Germany), INFN-CNAF (Italy), NL-T1 (Netherlands), PIC (Spain), ASGC (Taiwan), RAL (UK) and BNL (USA), the Tier-2 facilities worldwide and large non-WLCG resource providers. Major contributors of computing resources are listed in Ref. [61].

References

- [1] X.-N. Wang, Z. Huang, I. Sarcevic, Jet quenching in the direction opposite to a tagged photon in high-energy heavy-ion collisions, *Phys. Rev. Lett.* **77** (1996) 231, arXiv:hep-ph/9605213.
- [2] X.-N. Wang, Z. Huang, Medium-induced parton energy loss in $\gamma + \text{jet}$ events of high-energy heavy-ion collisions, *Phys. Rev. C* **55** (1997) 3047, arXiv:hep-ph/9701227.
- [3] G.-Y. Qin, J. Ruppert, C. Gale, S. Jeon, G.D. Moore, Jet energy loss, photon production, and photon-hadron correlations at energies available at the BNL Relativistic Heavy Ion Collider (RHIC), *Phys. Rev. C* **80** (2009) 054909, arXiv: 0906.3280 [hep-ph].
- [4] T. Renk, γ -hadron correlations as a tool to trace the flow of energy lost from hard partons in heavy-ion collisions, *Phys. Rev. C* **80** (2009) 014901, arXiv:0904.3806 [hep-ph].
- [5] G.-Y. Qin, Parton shower evolution in medium and nuclear modification of photon-tagged jets in $\text{Pb} + \text{Pb}$ collisions at the LHC, *Eur. Phys. J. C* **74** (2014) 2959, arXiv:1210.6610 [hep-ph].
- [6] X.-N. Wang, Y. Zhu, Medium modification of γ -jets in high-energy heavy-ion collisions, *Phys. Rev. Lett.* **111** (2013) 062301, arXiv:1302.5874 [hep-ph].
- [7] W. Dai, I. Vitev, B.-W. Zhang, Momentum imbalance of isolated photon-tagged jet production at RHIC and LHC, *Phys. Rev. Lett.* **110** (2013) 142001, arXiv:1207.5177 [hep-ph].
- [8] PHENIX Collaboration, Measurement of direct photons in $\text{Au} + \text{Au}$ collisions at $\sqrt{s_{\text{NN}}} = 200$ GeV, *Phys. Rev. Lett.* **109** (2012) 152302, arXiv:1205.5759 [nucl-ex].
- [9] ATLAS Collaboration, Centrality, rapidity and transverse momentum dependence of isolated prompt photon production in lead-lead collisions at $\sqrt{s_{\text{NN}}} = 2.76$ TeV measured with the ATLAS detector, *Phys. Rev. C* **93** (2016) 034914, arXiv:1506.08552 [hep-ex].
- [10] F. Arleo, K.J. Eskola, H. Paukkunen, C.A. Salgado, Inclusive prompt photon production in nuclear collisions at RHIC and LHC, *J. High Energy Phys.* **04** (2011) 055, arXiv:1103.1471 [hep-ph].
- [11] ATLAS Collaboration, Observation of a centrality-dependent dijet asymmetry in lead-lead collisions at $\sqrt{s_{\text{NN}}} = 2.76$ TeV with the ATLAS detector at the LHC, *Phys. Rev. Lett.* **105** (2010) 252303, arXiv:1011.6182 [hep-ex].
- [12] ATLAS Collaboration, Measurement of jet p_T correlations in $\text{Pb} + \text{Pb}$ and pp collisions at $\sqrt{s_{\text{NN}}} = 2.76$ TeV with the ATLAS detector, *Phys. Lett. B* **774** (2017) 379, arXiv:1706.09363 [hep-ex].
- [13] CMS Collaboration, Observation and studies of jet quenching in PbPb collisions at $\sqrt{s_{\text{NN}}} = 2.76$ TeV, *Phys. Rev. C* **84** (2011) 024906, arXiv:1102.1957 [nucl-ex].
- [14] ATLAS Collaboration, Measurement of the jet radius and transverse momentum dependence of inclusive jet suppression in lead-lead collisions at $\sqrt{s_{\text{NN}}} = 2.76$ TeV with the ATLAS detector, *Phys. Lett. B* **719** (2013) 220, arXiv:1208.1967 [hep-ex].
- [15] ATLAS Collaboration, Measurements of the nuclear modification factor for jets in $\text{Pb} + \text{Pb}$ collisions at $\sqrt{s_{\text{NN}}} = 2.76$ TeV with the ATLAS detector, *Phys. Rev. Lett.* **114** (2015) 072302, arXiv:1411.2357 [hep-ex].
- [16] CMS Collaboration, Jet momentum dependence of jet quenching in PbPb collisions at $\sqrt{s_{\text{NN}}} = 2.76$ TeV, *Phys. Lett. B* **712** (2012) 176, arXiv:1202.5022 [nucl-ex].
- [17] ATLAS Collaboration, Measurement of charged-particle spectra in $\text{Pb} + \text{Pb}$ collisions at $\sqrt{s_{\text{NN}}} = 2.76$ TeV with the ATLAS detector at the LHC, *J. High Energy Phys.* **09** (2015) 050, arXiv:1504.04337 [hep-ex].
- [18] CMS Collaboration, Charged-particle nuclear modification factors in PbPb and $p\text{Pb}$ collisions at $\sqrt{s_{\text{NN}}} = 5.02$ TeV, *J. High Energy Phys.* **04** (2017) 039, arXiv: 1611.01664 [hep-ex].
- [19] ALICE Collaboration, Transverse momentum spectra and nuclear modification factors of charged particles in pp , $p + \text{Pb}$ and $\text{Pb} + \text{Pb}$ collisions at the LHC, arXiv: 1802.09145 [nucl-ex], 2018.
- [20] PHENIX Collaboration, Photon-hadron jet correlations in $p + p$ and $\text{Au} + \text{Au}$ collisions at $\sqrt{s_{\text{NN}}} = 200$ GeV, *Phys. Rev. C* **80** (2009) 024908, arXiv:0903.3399 [nucl-ex].
- [21] PHENIX Collaboration, Medium modification of jet fragmentation in $\text{Au} + \text{Au}$ collisions at $\sqrt{s_{\text{NN}}} = 200$ GeV measured in direct photon-hadron correlations, *Phys. Rev. Lett.* **111** (2013) 032301, arXiv:1212.3323 [nucl-ex].
- [22] STAR Collaboration, Jet-like correlations with direct-photon and neutral-pion Triggers at $\sqrt{s_{\text{NN}}} = 200$ GeV, *Phys. Lett. B* **760** (2016) 689, arXiv:1604.01117 [nucl-ex].
- [23] CMS Collaboration, Studies of jet quenching using isolated-photon + jet correlations in PbPb and pp collisions at $\sqrt{s_{\text{NN}}} = 2.76$ TeV, *Phys. Lett. B* **718** (2013) 773, arXiv:1205.0206 [nucl-ex].
- [24] CMS Collaboration, Study of jet quenching with isolated-photon + jet correlations in PbPb and pp collisions at $\sqrt{s_{\text{NN}}} = 5.02$ TeV, *Phys. Lett. B* **785** (2018) 14, arXiv:1711.09738 [nucl-ex].
- [25] ATLAS Collaboration, Measurement of jet fragmentation in $\text{Pb} + \text{Pb}$ and pp collisions at $\sqrt{s_{\text{NN}}} = 2.76$ TeV with the ATLAS detector at the LHC, *Eur. Phys. J. C* **77** (2017) 379, arXiv:1702.00674 [hep-ex].

- [26] L. Chen, et al., Study of isolated-photon and jet momentum imbalance in pp and $PbPb$ collisions, Nucl. Phys. B 933 (2018) 306, arXiv:1803.10533 [hep-ph].
- [27] Z.-B. Kang, I. Vitev, H. Xing, Vector-boson-tagged jet production in heavy ion collisions at energies available at the CERN large hadron collider, Phys. Rev. C 96 (2017) 014912, arXiv:1702.07276 [hep-ph].
- [28] R. Kunnawalkam Elayavalli, K.C. Zapp, Simulating $V +$ jet processes in heavy ion collisions with JEWEL, Eur. Phys. J. C 76 (2016) 695, arXiv:1608.03099 [hep-ph].
- [29] J. Casalderrey-Solana, D.C. Gulhan, J.G. Milhano, D. Pablos, K. Rajagopal, Predictions for boson-jet observables and fragmentation function ratios from a hybrid strong/weak coupling model for jet quenching, J. High Energy Phys. 03 (2016) 053, arXiv:1508.00815 [hep-ph].
- [30] ATLAS Collaboration, The ATLAS experiment at the CERN large hadron collider, J. Instrum. 3 (2008) S08003.
- [31] ATLAS Collaboration, Performance of the ATLAS trigger system in 2015, Eur. Phys. J. C 77 (2017) 317, arXiv:1611.09661 [hep-ex].
- [32] ATLAS Collaboration, Measurement of longitudinal flow de-correlations in $Pb + Pb$ collisions at $\sqrt{s_{NN}} = 2.76$ and 5.02 TeV with the ATLAS detector, Eur. Phys. J. C 78 (2018) 142, arXiv:1709.02301 [nucl-ex].
- [33] ATLAS Collaboration, Measurement of the pseudorapidity and transverse momentum dependence of the elliptic flow of charged particles in lead-lead collisions at $\sqrt{s_{NN}} = 2.76$ TeV with the ATLAS detector, Phys. Lett. B 707 (2012) 330, arXiv:1108.6018 [hep-ex].
- [34] M.L. Miller, K. Reigers, S.J. Sanders, P. Steinberg, Glauber modeling in high energy nuclear collisions, Annu. Rev. Nucl. Part. Sci. 57 (2007) 205, arXiv: nucl-ex/0701025 [nucl-ex].
- [35] ATLAS Collaboration, Prompt and non-prompt J/ψ and $\psi(2S)$ suppression at high transverse momentum in 5.02 TeV $Pb + Pb$ collisions with the ATLAS experiment, Eur. Phys. J. C 78 (2018) 762, arXiv:1805.04077 [nucl-ex].
- [36] S. Agostinelli, et al., GEANT4: a simulation toolkit, Nucl. Instrum. Methods, Sect. A 506 (2003) 250.
- [37] ATLAS Collaboration, The ATLAS simulation infrastructure, Eur. Phys. J. C 70 (2010) 823, arXiv:1005.4568 [physics.ins-det].
- [38] T. Sjöstrand, S. Mrenna, P.Z. Skands, A brief introduction to PYTHIA 8.1, Comput. Phys. Commun. 178 (2008) 852, arXiv:0710.3820 [hep-ph].
- [39] R.D. Ball, et al., Parton distributions with LHC data, Nucl. Phys. B 867 (2013) 244, arXiv:1207.1303 [hep-ph].
- [40] ATLAS Collaboration, ATLAS Pythia 8 tunes to 7 TeV data, ATL-PHYS-PUB-2014-021, <https://cds.cern.ch/record/1966419>, 2014.
- [41] T. Gleisberg, et al., Event generation with SHERPA 1.1, J. High Energy Phys. 02 (2009) 007, arXiv:0811.4622 [hep-ph].
- [42] H.-L. Lai, et al., New parton distributions for collider physics, Phys. Rev. D 82 (2010) 074024, arXiv:1007.2241 [hep-ph].
- [43] J. Bellm, et al., Herwig 7.0/Herwig++ 3.0 release note, Eur. Phys. J. C 76 (2016) 196, arXiv:1512.01178 [hep-ph].
- [44] L.A. Harland-Lang, A.D. Martin, P. Motylinski, R.S. Thorne, Parton distributions in the LHC era: MMHT 2014 PDFs, Eur. Phys. J. C 75 (2015) 204, arXiv:1412.3989 [hep-ph].
- [45] M. Cacciari, G.P. Salam, G. Soyez, The anti- k_t jet clustering algorithm, J. High Energy Phys. 04 (2008) 063, arXiv:0802.1189 [hep-ph].
- [46] M. Cacciari, G.P. Salam, G. Soyez, Fastjet user manual, Eur. Phys. J. C 72 (2012) 1896, arXiv:1111.6097 [hep-ph].
- [47] ATLAS Collaboration, Jet energy measurement with the ATLAS detector in proton-proton collisions at $\sqrt{s} = 7$ TeV, Eur. Phys. J. C 73 (2013) 2304, arXiv: 1112.6426 [hep-ex].
- [48] ATLAS Collaboration, Measurement of the inclusive isolated prompt photon cross section in pp collisions at $\sqrt{s} = 8$ TeV with the ATLAS detector, J. High Energy Phys. 08 (2016) 005, arXiv:1605.03495 [hep-ex].
- [49] ATLAS Collaboration, Measurement of the cross section for inclusive isolated-photon production in pp collisions at $\sqrt{s} = 13$ TeV using the ATLAS detector, Phys. Lett. B 770 (2017) 473, arXiv:1701.06882 [hep-ex].
- [50] ATLAS Collaboration, Photon identification in 2015 ATLAS, data ATL-PHYS-PUB-2016-014, <https://cds.cern.ch/record/2203125>, 2016.
- [51] ATLAS Collaboration, Electron and photon energy calibration with the ATLAS detector using data collected in 2015 at $\sqrt{s} = 13$ TeV, ATL-PHYS-PUB-2016-015, <https://cds.cern.ch/record/2203514>, 2016.
- [52] ATLAS Collaboration, Centrality and rapidity dependence of inclusive jet production in $\sqrt{s_{NN}} = 5.02$ TeV proton-lead collisions with the ATLAS detector, Phys. Lett. B 748 (2015) 392, arXiv:1412.4092 [hep-ex].
- [53] ATLAS Collaboration, Jet energy scale measurements and their systematic uncertainties in proton-proton collisions at $\sqrt{s} = 13$ TeV with the ATLAS detector, Phys. Rev. D 96 (2017) 072002, arXiv:1703.09665 [hep-ex].
- [54] ATLAS Collaboration, Measurement of the nuclear modification factor for inclusive jets in $Pb + Pb$ collisions at $\sqrt{s_{NN}} = 5.02$ TeV with the ATLAS detector, arXiv:1805.05635 [nucl-ex], 2018.
- [55] G. D'Agostini, A multidimensional unfolding method based on Bayes' theorem, Nucl. Instrum. Methods, Sect. A 362 (1995) 487.
- [56] T. Adye, Unfolding algorithms and tests using RooUnfold, arXiv:1105.1160 [physics.data-an], 2011.
- [57] ATLAS Collaboration, Jet energy scale and its uncertainty for jets reconstructed using the ATLAS heavy ion jet algorithm, ATLAS-CONF-2015-016, <https://cds.cern.ch/record/2008677>, 2015.
- [58] ATLAS Collaboration, Measurement of jet fragmentation in $Pb + Pb$ and pp collisions at $\sqrt{s_{NN}} = 5.02$ TeV with the ATLAS detector, Phys. Rev. C 98 (2018) 024908, arXiv:1805.05424 [nucl-ex].
- [59] ATLAS Collaboration, Jet calibration and systematic uncertainties for jets reconstructed in the ATLAS detector at $\sqrt{s} = 13$ TeV, ATL-PHYS-PUB-2015-015, <https://cds.cern.ch/record/2037613>, 2015.
- [60] ATLAS Collaboration, Data-driven determination of the energy scale and resolution of jets reconstructed in the ATLAS calorimeters using dijet and multijet events at $\sqrt{s} = 8$ TeV, ATLAS-CONF-2015-017, <https://cds.cern.ch/record/2008678>, 2015.
- [61] ATLAS Collaboration, ATLAS computing acknowledgements 2016–2017, ATL-GEN-PUB-2016-002, <https://cds.cern.ch/record/2202407>.

The ATLAS Collaboration

- M. Aaboud ^{34d}, G. Aad ⁹⁹, B. Abbott ¹²⁴, O. Abdinov ^{13,*}, B. Abelsoos ¹²⁸, D.K. Abhayasinghe ⁹¹, S.H. Abidi ¹⁶⁴, O.S. AbouZeid ³⁹, N.L. Abraham ¹⁵³, H. Abramowicz ¹⁵⁸, H. Abreu ¹⁵⁷, Y. Abulaiti ⁶, B.S. Acharya ^{64a,64b,n}, S. Adachi ¹⁶⁰, L. Adamczyk ^{81a}, J. Adelman ¹¹⁹, M. Adersberger ¹¹², A. Adiguzel ^{12c}, T. Adye ¹⁴¹, A.A. Affolder ¹⁴³, Y. Afik ¹⁵⁷, C. Agheorghiesei ^{27c}, J.A. Aguilar-Saavedra ^{136f,136a}, F. Ahmadov ^{77,ad}, G. Aielli ^{71a,71b}, S. Akatsuka ⁸³, T.P.A. Åkesson ⁹⁴, E. Akilli ⁵², A.V. Akimov ¹⁰⁸, G.L. Alberghi ^{23b,23a}, J. Albert ¹⁷³, P. Albicocco ⁴⁹, M.J. Alconada Verzini ⁸⁶, S. Alderweireldt ¹¹⁷, M. Aleksić ³⁵, I.N. Aleksandrov ⁷⁷, C. Alexa ^{27b}, T. Alexopoulos ¹⁰, M. Alhroob ¹²⁴, B. Ali ¹³⁸, G. Alimonti ^{66a}, J. Alison ³⁶, S.P. Alkire ¹⁴⁵, C. Allaire ¹²⁸, B.M.M. Allbrooke ¹⁵³, B.W. Allen ¹²⁷, P.P. Allport ²¹, A. Aloisio ^{67a,67b}, A. Alonso ³⁹, F. Alonso ⁸⁶, C. Alpigiani ¹⁴⁵, A.A. Alshehri ⁵⁵, M.I. Alstaty ⁹⁹, B. Alvarez Gonzalez ³⁵, D. Álvarez Piqueras ¹⁷¹, M.G. Alvaggi ^{67a,67b}, B.T. Amadio ¹⁸, Y. Amaral Coutinho ^{78b}, L. Ambroz ¹³¹, C. Amelung ²⁶, D. Amidei ¹⁰³, S.P. Amor Dos Santos ^{136a,136c}, S. Amoroso ⁴⁴, C.S. Amrouche ⁵², C. Anastopoulos ¹⁴⁶, L.S. Ancu ⁵², N. Andari ¹⁴², T. Andeen ¹¹, C.F. Anders ^{59b}, J.K. Anders ²⁰, K.J. Anderson ³⁶, A. Andreazza ^{66a,66b}, V. Andrei ^{59a}, C.R. Anelli ¹⁷³, S. Angelidakis ³⁷, I. Angelozzi ¹¹⁸, A. Angerami ³⁸, A.V. Anisenkov ^{120b,120a}, A. Annovi ^{69a}, C. Antel ^{59a}, M.T. Anthony ¹⁴⁶, M. Antonelli ⁴⁹, D.J.A. Antrim ¹⁶⁸, F. Anulli ^{70a}, M. Aoki ⁷⁹, J.A. Aparisi Pozo ¹⁷¹, L. Aperio Bella ³⁵, G. Arabidze ¹⁰⁴, J.P. Araque ^{136a}, V. Araujo Ferraz ^{78b}, R. Araujo Pereira ^{78b}, A.T.H. Arce ⁴⁷, R.E. Ardell ⁹¹, F.A. Arduh ⁸⁶, J-F. Arguin ¹⁰⁷, S. Argyropoulos ⁷⁵, A.J. Armbruster ³⁵, L.J. Armitage ⁹⁰, A. Armstrong ¹⁶⁸, O. Arnaez ¹⁶⁴, H. Arnold ¹¹⁸, M. Arratia ³¹, O. Arslan ²⁴, A. Artamonov ^{109,*}, G. Artoni ¹³¹, S. Artz ⁹⁷,

- S. Asai ¹⁶⁰, N. Asbah ⁵⁷, A. Ashkenazi ¹⁵⁸, E.M. Asimakopoulou ¹⁶⁹, L. Asquith ¹⁵³, K. Assamagan ²⁹, R. Astalos ^{28a}, R.J. Atkin ^{32a}, M. Atkinson ¹⁷⁰, N.B. Atlay ¹⁴⁸, K. Augsten ¹³⁸, G. Avolio ³⁵, R. Avramidou ^{58a}, M.K. Ayoub ^{15a}, G. Azuelos ^{107,ap}, A.E. Baas ^{59a}, M.J. Baca ²¹, H. Bachacou ¹⁴², K. Bachas ^{65a,65b}, M. Backes ¹³¹, P. Bagnaia ^{70a,70b}, M. Bahmani ⁸², H. Bahrasemani ¹⁴⁹, A.J. Bailey ¹⁷¹, J.T. Baines ¹⁴¹, M. Bajic ³⁹, C. Bakalis ¹⁰, O.K. Baker ¹⁸⁰, P.J. Bakker ¹¹⁸, D. Bakshi Gupta ⁹³, E.M. Baldin ^{120b,120a}, P. Balek ¹⁷⁷, F. Balli ¹⁴², W.K. Balunas ¹³³, J. Balz ⁹⁷, E. Banas ⁸², A. Bandyopadhyay ²⁴, S. Banerjee ^{178,j}, A.A.E. Bannoura ¹⁷⁹, L. Barak ¹⁵⁸, W.M. Barbe ³⁷, E.L. Barberio ¹⁰², D. Barberis ^{53b,53a}, M. Barbero ⁹⁹, T. Barillari ¹¹³, M-S. Barisits ³⁵, J. Barkeloo ¹²⁷, T. Barklow ¹⁵⁰, N. Barlow ³¹, R. Barnea ¹⁵⁷, S.L. Barnes ^{58c}, B.M. Barnett ¹⁴¹, R.M. Barnett ¹⁸, Z. Barnovska-Blenessy ^{58a}, A. Baroncelli ^{72a}, G. Barone ²⁶, A.J. Barr ¹³¹, L. Barranco Navarro ¹⁷¹, F. Barreiro ⁹⁶, J. Barreiro Guimarães da Costa ^{15a}, R. Bartoldus ¹⁵⁰, A.E. Barton ⁸⁷, P. Bartos ^{28a}, A. Basalaev ¹³⁴, A. Bassalat ¹²⁸, R.L. Bates ⁵⁵, S.J. Batista ¹⁶⁴, S. Batlamous ^{34e}, J.R. Batley ³¹, M. Battaglia ¹⁴³, M. Bauce ^{70a,70b}, F. Bauer ¹⁴², K.T. Bauer ¹⁶⁸, H.S. Bawa ^{150,l}, J.B. Beacham ¹²², T. Beau ¹³², P.H. Beauchemin ¹⁶⁷, P. Bechtle ²⁴, H.C. Beck ⁵¹, H.P. Beck ^{20,p}, K. Becker ⁵⁰, M. Becker ⁹⁷, C. Becot ⁴⁴, A. Beddall ^{12d}, A.J. Beddall ^{12a}, V.A. Bednyakov ⁷⁷, M. Bedognetti ¹¹⁸, C.P. Bee ¹⁵², T.A. Beermann ³⁵, M. Begalli ^{78b}, M. Begel ²⁹, A. Behera ¹⁵², J.K. Behr ⁴⁴, A.S. Bell ⁹², G. Bella ¹⁵⁸, L. Bellagamba ^{23b}, A. Bellerive ³³, M. Bellomo ¹⁵⁷, P. Bellos ⁹, K. Belotskiy ¹¹⁰, N.L. Belyaev ¹¹⁰, O. Benary ^{158,*}, D. Benchekroun ^{34a}, M. Bender ¹¹², N. Benekos ¹⁰, Y. Benhammou ¹⁵⁸, E. Benhar Noccioli ¹⁸⁰, J. Benitez ⁷⁵, D.P. Benjamin ⁴⁷, M. Benoit ⁵², J.R. Bensinger ²⁶, S. Bentvelsen ¹¹⁸, L. Beresford ¹³¹, M. Beretta ⁴⁹, D. Berge ⁴⁴, E. Bergeaas Kuutmann ¹⁶⁹, N. Berger ⁵, L.J. Bergsten ²⁶, J. Beringer ¹⁸, S. Berlendis ⁷, N.R. Bernard ¹⁰⁰, G. Bernardi ¹³², C. Bernius ¹⁵⁰, F.U. Bernlochner ²⁴, T. Berry ⁹¹, P. Berta ⁹⁷, C. Bertella ^{15a}, G. Bertoli ^{43a,43b}, I.A. Bertram ⁸⁷, G.J. Besjes ³⁹, O. Bessidskaia Bylund ¹⁷⁹, M. Bessner ⁴⁴, N. Besson ¹⁴², A. Bethani ⁹⁸, S. Bethke ¹¹³, A. Betti ²⁴, A.J. Bevan ⁹⁰, J. Beyer ¹¹³, R.M.B. Bianchi ¹³⁵, O. Biebel ¹¹², D. Biedermann ¹⁹, R. Bielski ³⁵, K. Bierwagen ⁹⁷, N.V. Biesuz ^{69a,69b}, M. Biglietti ^{72a}, T.R.V. Billoud ¹⁰⁷, M. Bindi ⁵¹, A. Bingul ^{12d}, C. Bini ^{70a,70b}, S. Biondi ^{23b,23a}, M. Birman ¹⁷⁷, T. Bisanz ⁵¹, J.P. Biswal ¹⁵⁸, C. Bittrich ⁴⁶, D.M. Bjergaard ⁴⁷, J.E. Black ¹⁵⁰, K.M. Black ²⁵, T. Blazek ^{28a}, I. Bloch ⁴⁴, C. Blocker ²⁶, A. Blue ⁵⁵, U. Blumenschein ⁹⁰, Dr. Blunier ^{144a}, G.J. Bobbink ¹¹⁸, V.S. Bobrovnikov ^{120b,120a}, S.S. Bocchetta ⁹⁴, A. Bocci ⁴⁷, D. Boerner ¹⁷⁹, D. Bogavac ¹¹², A.G. Bogdanchikov ^{120b,120a}, C. Bohm ^{43a}, V. Boisvert ⁹¹, P. Bokan ^{169,w}, T. Bold ^{81a}, A.S. Boldyrev ¹¹¹, A.E. Bolz ^{59b}, M. Bomben ¹³², M. Bona ⁹⁰, J.S. Bonilla ¹²⁷, M. Boonekamp ¹⁴², A. Borisov ¹⁴⁰, G. Borissov ⁸⁷, J. Bortfeldt ³⁵, D. Bortoletto ¹³¹, V. Bortolotto ^{71a,71b}, D. Boscherini ^{23b}, M. Bosman ¹⁴, J.D. Bossio Sola ³⁰, K. Bouaouda ^{34a}, J. Boudreau ¹³⁵, E.V. Bouhova-Thacker ⁸⁷, D. Boumediene ³⁷, C. Bourdarios ¹²⁸, S.K. Boutle ⁵⁵, A. Boveia ¹²², J. Boyd ³⁵, D. Boye ^{32b}, I.R. Boyko ⁷⁷, A.J. Bozson ⁹¹, J. Bracinik ²¹, N. Brahimi ⁹⁹, A. Brandt ⁸, G. Brandt ¹⁷⁹, O. Brandt ^{59a}, F. Braren ⁴⁴, U. Bratzler ¹⁶¹, B. Brau ¹⁰⁰, J.E. Brau ¹²⁷, W.D. Breaden Madden ⁵⁵, K. Brendlinger ⁴⁴, L. Brenner ⁴⁴, R. Brenner ¹⁶⁹, S. Bressler ¹⁷⁷, B. Brickwedde ⁹⁷, D.L. Briglin ²¹, D. Britton ⁵⁵, D. Britzger ^{59b}, I. Brock ²⁴, R. Brock ¹⁰⁴, G. Brooijmans ³⁸, T. Brooks ⁹¹, W.K. Brooks ^{144b}, E. Brost ¹¹⁹, J.H. Broughton ²¹, P.A. Bruckman de Renstrom ⁸², D. Bruncko ^{28b}, A. Bruni ^{23b}, G. Bruni ^{23b}, L.S. Bruni ¹¹⁸, S. Bruno ^{71a,71b}, B.H. Brunt ³¹, M. Bruschi ^{23b}, N. Bruscino ¹³⁵, P. Bryant ³⁶, L. Bryngemark ⁴⁴, T. Buanes ¹⁷, Q. Buat ³⁵, P. Buchholz ¹⁴⁸, A.G. Buckley ⁵⁵, I.A. Budagov ⁷⁷, F. Buehrer ⁵⁰, M.K. Bugge ¹³⁰, O. Bulekov ¹¹⁰, D. Bullock ⁸, T.J. Burch ¹¹⁹, S. Burdin ⁸⁸, C.D. Burgard ¹¹⁸, A.M. Burger ⁵, B. Burghgrave ¹¹⁹, K. Burka ⁸², S. Burke ¹⁴¹, I. Burmeister ⁴⁵, J.T.P. Burr ¹³¹, D. Büscher ⁵⁰, V. Büscher ⁹⁷, E. Buschmann ⁵¹, P. Bussey ⁵⁵, J.M. Butler ²⁵, C.M. Buttar ⁵⁵, J.M. Butterworth ⁹², P. Butti ³⁵, W. Buttinger ³⁵, A. Buzatu ¹⁵⁵, A.R. Buzykaev ^{120b,120a}, G. Cabras ^{23b,23a}, S. Cabrera Urbán ¹⁷¹, D. Caforio ¹³⁸, H. Cai ¹⁷⁰, V.M.M. Cairo ², O. Cakir ^{4a}, N. Calace ⁵², P. Calafiura ¹⁸, A. Calandri ⁹⁹, G. Calderini ¹³², P. Calfayan ⁶³, G. Callea ^{40b,40a}, L.P. Caloba ^{78b}, S. Calvente Lopez ⁹⁶, D. Calvet ³⁷, S. Calvet ³⁷, T.P. Calvet ¹⁵², M. Calvetti ^{69a,69b}, R. Camacho Toro ¹³², S. Camarda ³⁵, P. Camarri ^{71a,71b}, D. Cameron ¹³⁰, R. Caminal Armadans ¹⁰⁰, C. Camincher ³⁵, S. Campana ³⁵, M. Campanelli ⁹², A. Camplani ³⁹, A. Campoverde ¹⁴⁸, V. Canale ^{67a,67b}, M. Cano Bret ^{58c}, J. Cantero ¹²⁵, T. Cao ¹⁵⁸, Y. Cao ¹⁷⁰, M.D.M. Capeans Garrido ³⁵, I. Caprini ^{27b}, M. Caprini ^{27b}, M. Capua ^{40b,40a}, R.M. Carbone ³⁸, R. Cardarelli ^{71a}, F.C. Cardillo ¹⁴⁶, I. Carli ¹³⁹, T. Carli ³⁵, G. Carlino ^{67a}, B.T. Carlson ¹³⁵, L. Carminati ^{66a,66b}, R.M.D. Carney ^{43a,43b}, S. Caron ¹¹⁷, E. Carquin ^{144b}, S. Carrá ^{66a,66b}, G.D. Carrillo-Montoya ³⁵, D. Casadei ^{32b}, M.P. Casado ^{14,f}, A.F. Casha ¹⁶⁴, D.W. Casper ¹⁶⁸, R. Castelijn ¹¹⁸, F.L. Castillo ¹⁷¹, V. Castillo Gimenez ¹⁷¹, N.F. Castro ^{136a,136e}, A. Catinaccio ³⁵, J.R. Catmore ¹³⁰, A. Cattai ³⁵, J. Caudron ²⁴, V. Cavaliere ²⁹, E. Cavallaro ¹⁴, D. Cavalli ^{66a},

- M. Cavalli-Sforza ¹⁴, V. Cavasinni ^{69a,69b}, E. Celebi ^{12b}, F. Ceradini ^{72a,72b}, L. Cerdà Alberich ¹⁷¹,
 A.S. Cerqueira ^{78a}, A. Cerri ¹⁵³, L. Cerrito ^{71a,71b}, F. Cerutti ¹⁸, A. Cervelli ^{23b,23a}, S.A. Cetin ^{12b},
 A. Chafaq ^{34a}, D. Chakraborty ¹¹⁹, S.K. Chan ⁵⁷, W.S. Chan ¹¹⁸, Y.L. Chan ^{61a}, J.D. Chapman ³¹,
 B. Chargeishvili ^{156b}, D.G. Charlton ²¹, C.C. Chau ³³, C.A. Chavez Barajas ¹⁵³, S. Che ¹²², A. Chegwidden ¹⁰⁴,
 S. Chekanov ⁶, S.V. Chekulaev ^{165a}, G.A. Chelkov ^{77,ao}, M.A. Chelstowska ³⁵, C. Chen ^{58a}, C.H. Chen ⁷⁶,
 H. Chen ²⁹, J. Chen ^{58a}, J. Chen ³⁸, S. Chen ¹³³, S.J. Chen ^{15b}, X. Chen ^{15c,an}, Y. Chen ⁸⁰, Y-H. Chen ⁴⁴,
 H.C. Cheng ¹⁰³, H.J. Cheng ^{15d}, A. Cheplakov ⁷⁷, E. Cheremushkina ¹⁴⁰, R. Cherkaoui El Moursli ^{34e},
 E. Cheu ⁷, K. Cheung ⁶², L. Chevalier ¹⁴², V. Chiarella ⁴⁹, G. Chiarella ^{69a}, G. Chiodini ^{65a}, A.S. Chisholm ³⁵,
 A. Chitan ^{27b}, I. Chiu ¹⁶⁰, Y.H. Chiu ¹⁷³, M.V. Chizhov ⁷⁷, K. Choi ⁶³, A.R. Chomont ¹²⁸, S. Chouridou ¹⁵⁹,
 Y.S. Chow ¹¹⁸, V. Christodoulou ⁹², M.C. Chu ^{61a}, J. Chudoba ¹³⁷, A.J. Chuinard ¹⁰¹, J.J. Chwastowski ⁸²,
 L. Chytka ¹²⁶, D. Cinca ⁴⁵, V. Cindro ⁸⁹, I.A. Cioară ²⁴, A. Ciocio ¹⁸, F. Cirotto ^{67a,67b}, Z.H. Citron ¹⁷⁷,
 M. Citterio ^{66a}, A. Clark ⁵², M.R. Clark ³⁸, P.J. Clark ⁴⁸, C. Clement ^{43a,43b}, Y. Coadou ⁹⁹, M. Cobal ^{64a,64c},
 A. Coccaro ^{53b,53a}, J. Cochran ⁷⁶, H. Cohen ¹⁵⁸, A.E.C. Coimbra ¹⁷⁷, L. Colasurdo ¹¹⁷, B. Cole ³⁸,
 A.P. Colijn ¹¹⁸, J. Collot ⁵⁶, P. Conde Muiño ^{136a,136b}, E. Coniavitis ⁵⁰, S.H. Connell ^{32b}, I.A. Connally ⁹⁸,
 S. Constantinescu ^{27b}, F. Conventi ^{67a,aq}, A.M. Cooper-Sarkar ¹³¹, F. Cormier ¹⁷², K.J.R. Cormier ¹⁶⁴,
 M. Corradi ^{70a,70b}, E.E. Corrigan ⁹⁴, F. Corriveau ^{101,ab}, A. Cortes-Gonzalez ³⁵, M.J. Costa ¹⁷¹,
 D. Costanzo ¹⁴⁶, G. Cottin ³¹, G. Cowan ⁹¹, B.E. Cox ⁹⁸, J. Crane ⁹⁸, K. Cranmer ¹²¹, S.J. Crawley ⁵⁵,
 R.A. Creager ¹³³, G. Cree ³³, S. Crépé-Renaudin ⁵⁶, F. Crescioli ¹³², M. Cristinziani ²⁴, V. Croft ¹²¹,
 G. Crosetti ^{40b,40a}, A. Cueto ⁹⁶, T. Cuhadar Donszelmann ¹⁴⁶, A.R. Cukierman ¹⁵⁰, J. Cúth ⁹⁷, S. Czekierda ⁸²,
 P. Czodrowski ³⁵, M.J. Da Cunha Sargedas De Sousa ^{58b,136b}, C. Da Via ⁹⁸, W. Dabrowski ^{81a}, T. Dado ^{28a,w},
 S. Dahbi ^{34e}, T. Dai ¹⁰³, F. Dallaire ¹⁰⁷, C. Dallapiccola ¹⁰⁰, M. Dam ³⁹, G. D'amen ^{23b,23a}, J. Damp ⁹⁷,
 J.R. Dandoy ¹³³, M.F. Daneri ³⁰, N.P. Dang ^{178,j}, N.D. Dann ⁹⁸, M. Danninger ¹⁷², V. Dao ³⁵, G. Darbo ^{53b},
 S. Darmora ⁸, O. Dartsi ⁵, A. Dattagupta ¹²⁷, T. Daubney ⁴⁴, S. D'Auria ⁵⁵, W. Davey ²⁴, C. David ⁴⁴,
 T. Davidek ¹³⁹, D.R. Davis ⁴⁷, E. Dawe ¹⁰², I. Dawson ¹⁴⁶, K. De ⁸, R. De Asmundis ^{67a}, A. De Benedetti ¹²⁴,
 M. De Beurs ¹¹⁸, S. De Castro ^{23b,23a}, S. De Cecco ^{70a,70b}, N. De Groot ¹¹⁷, P. de Jong ¹¹⁸, H. De la Torre ¹⁰⁴,
 F. De Lorenzi ⁷⁶, A. De Maria ^{51,r}, D. De Pedis ^{70a}, A. De Salvo ^{70a}, U. De Sanctis ^{71a,71b},
 M. De Santis ^{71a,71b}, A. De Santo ¹⁵³, K. De Vasconcelos Corga ⁹⁹, J.B. De Vivie De Regie ¹²⁸,
 C. Debenedetti ¹⁴³, D.V. Dedovich ⁷⁷, N. Dehghanian ³, M. Del Gaudio ^{40b,40a}, J. Del Peso ⁹⁶,
 Y. Delabat Diaz ⁴⁴, D. Delgove ¹²⁸, F. Deliot ¹⁴², C.M. Delitzsch ⁷, M. Della Pietra ^{67a,67b}, D. Della Volpe ⁵²,
 A. Dell'Acqua ³⁵, L. Dell'Asta ²⁵, M. Delmastro ⁵, C. Delporte ¹²⁸, P.A. Delsart ⁵⁶, D.A. DeMarco ¹⁶⁴,
 S. Demers ¹⁸⁰, M. Demichev ⁷⁷, S.P. Denisov ¹⁴⁰, D. Denysiuk ¹¹⁸, L. D'Eramo ¹³², D. Derendarz ⁸²,
 J.E. Derkaoui ^{34d}, F. Derue ¹³², P. Dervan ⁸⁸, K. Desch ²⁴, C. Deterre ⁴⁴, K. Dette ¹⁶⁴, M.R. Devesa ³⁰,
 P.O. Deviveiros ³⁵, A. Dewhurst ¹⁴¹, S. Dhaliwal ²⁶, F.A. Di Bello ⁵², A. Di Ciaccio ^{71a,71b}, L. Di Ciaccio ⁵,
 W.K. Di Clemente ¹³³, C. Di Donato ^{67a,67b}, A. Di Girolamo ³⁵, B. Di Micco ^{72a,72b}, R. Di Nardo ¹⁰⁰,
 K.F. Di Petrillo ⁵⁷, R. Di Sipio ¹⁶⁴, D. Di Valentino ³³, C. Diaconu ⁹⁹, M. Diamond ¹⁶⁴, F.A. Dias ³⁹,
 T. Dias Do Vale ^{136a}, M.A. Diaz ^{144a}, J. Dickinson ¹⁸, E.B. Diehl ¹⁰³, J. Dietrich ¹⁹, S. Díez Cornell ⁴⁴,
 A. Dimitrieva ¹⁸, J. Dingfelder ²⁴, F. Dittus ³⁵, F. Djama ⁹⁹, T. Djobava ^{156b}, J.I. Djuvsland ^{59a},
 M.A.B. Do Vale ^{78c}, M. Dobre ^{27b}, D. Dodsworth ²⁶, C. Doglioni ⁹⁴, J. Dolejsi ¹³⁹, Z. Dolezal ¹³⁹,
 M. Donadelli ^{78d}, J. Donini ³⁷, A. D'onofrio ⁹⁰, M. D'Onofrio ⁸⁸, J. Dopke ¹⁴¹, A. Doria ^{67a}, M.T. Dova ⁸⁶,
 A.T. Doyle ⁵⁵, E. Drechsler ⁵¹, E. Dreyer ¹⁴⁹, T. Dreyer ⁵¹, Y. Du ^{58b}, J. Duarte-Campderros ¹⁵⁸, F. Dubinin ¹⁰⁸,
 M. Dubovsky ^{28a}, A. Dubreuil ⁵², E. Duchovni ¹⁷⁷, G. Duckeck ¹¹², A. Ducourthial ¹³², O.A. Ducu ^{107,v},
 D. Duda ¹¹³, A. Dudarev ³⁵, A.C. Dudder ⁹⁷, E.M. Duffield ¹⁸, L. Duflot ¹²⁸, M. Dührssen ³⁵, C. Dülsen ¹⁷⁹,
 M. Dumancic ¹⁷⁷, A.E. Dumitriu ^{27b,d}, A.K. Duncan ⁵⁵, M. Dunford ^{59a}, A. Duperrin ⁹⁹, H. Duran Yildiz ^{4a},
 M. Düren ⁵⁴, A. Durglishvili ^{156b}, D. Duschinger ⁴⁶, B. Dutta ⁴⁴, D. Duvnjak ¹, M. Dyndal ⁴⁴, S. Dysch ⁹⁸,
 B.S. Dziedzic ⁸², C. Eckardt ⁴⁴, K.M. Ecker ¹¹³, R.C. Edgar ¹⁰³, T. Eifert ³⁵, G. Eigen ¹⁷, K. Einsweiler ¹⁸,
 T. Ekelof ¹⁶⁹, M. El Kacimi ^{34c}, R. El Kosseifi ⁹⁹, V. Ellajosyula ⁹⁹, M. Ellert ¹⁶⁹, F. Ellinghaus ¹⁷⁹,
 A.A. Elliot ⁹⁰, N. Ellis ³⁵, J. Elmsheuser ²⁹, M. Elsing ³⁵, D. Emeliyanov ¹⁴¹, Y. Enari ¹⁶⁰, J.S. Ennis ¹⁷⁵,
 M.B. Epland ⁴⁷, J. Erdmann ⁴⁵, A. Ereditato ²⁰, S. Errede ¹⁷⁰, M. Escalier ¹²⁸, C. Escobar ¹⁷¹,
 O. Estrada Pastor ¹⁷¹, A.I. Etienne ¹⁴², E. Etzion ¹⁵⁸, H. Evans ⁶³, A. Ezhilov ¹³⁴, M. Ezzi ^{34e}, F. Fabbri ⁵⁵,
 L. Fabbri ^{23b,23a}, V. Fabiani ¹¹⁷, G. Facini ⁹², R.M. Faisca Rodrigues Pereira ^{136a}, R.M. Fakhrutdinov ¹⁴⁰,
 S. Falciano ^{70a}, P.J. Falke ⁵, S. Falke ⁵, J. Faltova ¹³⁹, Y. Fang ^{15a}, M. Fanti ^{66a,66b}, A. Farbin ⁸, A. Farilla ^{72a},
 E.M. Farina ^{68a,68b}, T. Farooque ¹⁰⁴, S. Farrell ¹⁸, S.M. Farrington ¹⁷⁵, P. Farthouat ³⁵, F. Fassi ^{34e},

- P. Fassnacht ³⁵, D. Fassouliotis ⁹, M. Facci Giannelli ⁴⁸, A. Favareto ^{53b,53a}, W.J. Fawcett ³¹, L. Fayard ¹²⁸, O.L. Fedin ^{134,o}, W. Fedorko ¹⁷², M. Feickert ⁴¹, S. Feigl ¹³⁰, L. Feligioni ⁹⁹, C. Feng ^{58b}, E.J. Feng ³⁵, M. Feng ⁴⁷, M.J. Fenton ⁵⁵, A.B. Fenyuk ¹⁴⁰, L. Feremenga ⁸, J. Ferrando ⁴⁴, A. Ferrari ¹⁶⁹, P. Ferrari ¹¹⁸, R. Ferrari ^{68a}, D.E. Ferreira de Lima ^{59b}, A. Ferrer ¹⁷¹, D. Ferrere ⁵², C. Ferretti ¹⁰³, F. Fiedler ⁹⁷, A. Filipčič ⁸⁹, F. Filthaut ¹¹⁷, K.D. Finelli ²⁵, M.C.N. Fiolhais ^{136a,136c,a}, L. Fiorini ¹⁷¹, C. Fischer ¹⁴, W.C. Fisher ¹⁰⁴, N. Flaschel ⁴⁴, I. Fleck ¹⁴⁸, P. Fleischmann ¹⁰³, R.R.M. Fletcher ¹³³, T. Flick ¹⁷⁹, B.M. Flierl ¹¹², L.M. Flores ¹³³, L.R. Flores Castillo ^{61a}, F.M. Follega ^{73a,73b}, N. Fomin ¹⁷, G.T. Forcolin ⁹⁸, A. Formica ¹⁴², F.A. Förster ¹⁴, A.C. Forti ⁹⁸, A.G. Foster ²¹, D. Fournier ¹²⁸, H. Fox ⁸⁷, S. Fracchia ¹⁴⁶, P. Francavilla ^{69a,69b}, M. Franchini ^{23b,23a}, S. Franchino ^{59a}, D. Francis ³⁵, L. Franconi ¹³⁰, M. Franklin ⁵⁷, M. Frate ¹⁶⁸, M. Fraternali ^{68a,68b}, A.N. Fray ⁹⁰, D. Freeborn ⁹², S.M. Fressard-Batraneanu ³⁵, B. Freund ¹⁰⁷, W.S. Freund ^{78b}, D.C. Frizzell ¹²⁴, D. Froidevaux ³⁵, J.A. Frost ¹³¹, C. Fukunaga ¹⁶¹, E. Fullana Torregrosa ¹⁷¹, T. Fusayasu ¹¹⁴, J. Fuster ¹⁷¹, O. Gabizon ¹⁵⁷, A. Gabrielli ^{23b,23a}, A. Gabrielli ¹⁸, G.P. Gach ^{81a}, S. Gadatsch ⁵², P. Gadow ¹¹³, G. Gagliardi ^{53b,53a}, L.G. Gagnon ¹⁰⁷, C. Galea ^{27b}, B. Galhardo ^{136a,136c}, E.J. Gallas ¹³¹, B.J. Gallop ¹⁴¹, P. Gallus ¹³⁸, G. Galster ³⁹, R. Gamboa Goni ⁹⁰, K.K. Gan ¹²², S. Ganguly ¹⁷⁷, J. Gao ^{58a}, Y. Gao ⁸⁸, Y.S. Gao ^{150,l}, C. García ¹⁷¹, J.E. García Navarro ¹⁷¹, J.A. García Pascual ^{15a}, M. Garcia-Sciveres ¹⁸, R.W. Gardner ³⁶, N. Garelli ¹⁵⁰, V. Garonne ¹³⁰, K. Gasnikova ⁴⁴, A. Gaudiello ^{53b,53a}, G. Gaudio ^{68a}, I.L. Gavrilenko ¹⁰⁸, A. Gavrilyuk ¹⁰⁹, C. Gay ¹⁷², G. Gaycken ²⁴, E.N. Gazis ¹⁰, C.N.P. Gee ¹⁴¹, J. Geisen ⁵¹, M. Geisen ⁹⁷, M.P. Geisler ^{59a}, K. Gellerstedt ^{43a,43b}, C. Gemme ^{53b}, M.H. Genest ⁵⁶, C. Geng ¹⁰³, S. Gentile ^{70a,70b}, S. George ⁹¹, D. Gerbaudo ¹⁴, G. Gessner ⁴⁵, S. Ghasemi ¹⁴⁸, M. Ghasemi Bostanabad ¹⁷³, M. Ghneimat ²⁴, B. Giacobbe ^{23b}, S. Giagu ^{70a,70b}, N. Giangiacomi ^{23b,23a}, P. Giannetti ^{69a}, A. Giannini ^{67a,67b}, S.M. Gibson ⁹¹, M. Gignac ¹⁴³, D. Gillberg ³³, G. Gilles ¹⁷⁹, D.M. Gingrich ^{3,ap}, M.P. Giordani ^{64a,64c}, F.M. Giorgi ^{23b}, P.F. Giraud ¹⁴², P. Giromini ⁵⁷, G. Giugliarelli ^{64a,64c}, D. Giugni ^{66a}, F. Juli ¹³¹, M. Giulini ^{59b}, S. Gkaitatzis ¹⁵⁹, I. Gkialas ^{9,i}, E.L. Gkougkousis ¹⁴, P. Gkountoumis ¹⁰, L.K. Gladilin ¹¹¹, C. Glasman ⁹⁶, J. Glatzer ¹⁴, P.C.F. Glaysher ⁴⁴, A. Glazov ⁴⁴, M. Goblirsch-Kolb ²⁶, J. Godlewski ⁸², S. Goldfarb ¹⁰², T. Golling ⁵², D. Golubkov ¹⁴⁰, A. Gomes ^{136a,136b,136d}, R. Goncalves Gama ^{78a}, R. Gonçalo ^{136a}, G. Gonella ⁵⁰, L. Gonella ²¹, A. Gongadze ⁷⁷, F. Gonnella ²¹, J.L. Gonski ⁵⁷, S. González de la Hoz ¹⁷¹, S. Gonzalez-Sevilla ⁵², L. Goossens ³⁵, P.A. Gorbounov ¹⁰⁹, H.A. Gordon ²⁹, B. Gorini ³⁵, E. Gorini ^{65a,65b}, A. Gorišek ⁸⁹, A.T. Goshaw ⁴⁷, C. Gössling ⁴⁵, M.I. Gostkin ⁷⁷, C.A. Gottardo ²⁴, C.R. Goudet ¹²⁸, D. Goujdami ^{34c}, A.G. Goussiou ¹⁴⁵, N. Govender ^{32b,b}, C. Goy ⁵, E. Gozani ¹⁵⁷, I. Grabowska-Bold ^{81a}, P.O.J. Gradin ¹⁶⁹, E.C. Graham ⁸⁸, J. Gramling ¹⁶⁸, E. Gramstad ¹³⁰, S. Grancagnolo ¹⁹, V. Gratchev ¹³⁴, P.M. Gravila ^{27f}, F.G. Gravilli ^{65a,65b}, C. Gray ⁵⁵, H.M. Gray ¹⁸, Z.D. Greenwood ^{93,ag}, C. Grefe ²⁴, K. Gregersen ⁹⁴, I.M. Gregor ⁴⁴, P. Grenier ¹⁵⁰, K. Grevtsov ⁴⁴, N.A. Grieser ¹²⁴, J. Griffiths ⁸, A.A. Grillo ¹⁴³, K. Grimm ¹⁵⁰, S. Grinstein ^{14,x}, Ph. Gris ³⁷, J.-F. Grivaz ¹²⁸, S. Groh ⁹⁷, E. Gross ¹⁷⁷, J. Grosse-Knetter ⁵¹, G.C. Grossi ⁹³, Z.J. Grout ⁹², C. Grud ¹⁰³, A. Grummer ¹¹⁶, L. Guan ¹⁰³, W. Guan ¹⁷⁸, J. Guenther ³⁵, A. Guerguichon ¹²⁸, F. Guesscini ^{165a}, D. Guest ¹⁶⁸, R. Gugel ⁵⁰, B. Gui ¹²², T. Guillemin ⁵, S. Guindon ³⁵, U. Gul ⁵⁵, C. Gumpert ³⁵, J. Guo ^{58c}, W. Guo ¹⁰³, Y. Guo ^{58a,q}, Z. Guo ⁹⁹, R. Gupta ⁴¹, S. Gurbuz ^{12c}, G. Gustavino ¹²⁴, B.J. Gutelman ¹⁵⁷, P. Gutierrez ¹²⁴, C. Gutschow ⁹², C. Guyot ¹⁴², M.P. Guzik ^{81a}, C. Gwenlan ¹³¹, C.B. Gwilliam ⁸⁸, A. Haas ¹²¹, C. Haber ¹⁸, H.K. Hadavand ⁸, N. Haddad ^{34e}, A. Hadef ^{58a}, S. Hageböck ²⁴, M. Haghjara ¹⁶⁶, H. Hakobyan ^{181,*}, M. Haleem ¹⁷⁴, J. Haley ¹²⁵, G. Halladjian ¹⁰⁴, G.D. Hallewell ⁹⁹, K. Hamacher ¹⁷⁹, P. Hamal ¹²⁶, K. Hamano ¹⁷³, A. Hamilton ^{32a}, G.N. Hamity ¹⁴⁶, K. Han ^{58a,af}, L. Han ^{58a}, S. Han ^{15d}, K. Hanagaki ^{79,t}, M. Hance ¹⁴³, D.M. Handl ¹¹², B. Haney ¹³³, R. Hankache ¹³², P. Hanke ^{59a}, E. Hansen ⁹⁴, J.B. Hansen ³⁹, J.D. Hansen ³⁹, M.C. Hansen ²⁴, P.H. Hansen ³⁹, K. Hara ¹⁶⁶, A.S. Hard ¹⁷⁸, T. Harenberg ¹⁷⁹, S. Harkusha ¹⁰⁵, P.F. Harrison ¹⁷⁵, N.M. Hartmann ¹¹², Y. Hasegawa ¹⁴⁷, A. Hasib ⁴⁸, S. Hassani ¹⁴², S. Haug ²⁰, R. Hauser ¹⁰⁴, L. Hauswald ⁴⁶, L.B. Havener ³⁸, M. Havranek ¹³⁸, C.M. Hawkes ²¹, R.J. Hawkings ³⁵, D. Hayden ¹⁰⁴, C. Hayes ¹⁵², C.P. Hays ¹³¹, J.M. Hays ⁹⁰, H.S. Hayward ⁸⁸, S.J. Haywood ¹⁴¹, M.P. Heath ⁴⁸, V. Hedberg ⁹⁴, L. Heelan ⁸, S. Heer ²⁴, K.K. Heidegger ⁵⁰, J. Heilman ³³, S. Heim ⁴⁴, T. Heim ¹⁸, B. Heinemann ^{44,ak}, J.J. Heinrich ¹¹², L. Heinrich ¹²¹, C. Heinz ⁵⁴, J. Hejbal ¹³⁷, L. Helary ³⁵, A. Held ¹⁷², S. Hellesund ¹³⁰, S. Hellman ^{43a,43b}, C. Helsens ³⁵, R.C.W. Henderson ⁸⁷, Y. Heng ¹⁷⁸, S. Henkelmann ¹⁷², A.M. Henriques Correia ³⁵, G.H. Herbert ¹⁹, H. Herde ²⁶, V. Herget ¹⁷⁴, Y. Hernández Jiménez ^{32c}, H. Herr ⁹⁷, M.G. Herrmann ¹¹², G. Herten ⁵⁰, R. Hertenberger ¹¹², L. Hervas ³⁵, T.C. Herwig ¹³³, G.G. Hesketh ⁹², N.P. Hessey ^{165a}, J.W. Hetherly ⁴¹, S. Higashino ⁷⁹, E. Higón-Rodriguez ¹⁷¹,

- K. Hildebrand ³⁶, E. Hill ¹⁷³, J.C. Hill ³¹, K.K. Hill ²⁹, K.H. Hiller ⁴⁴, S.J. Hillier ²¹, M. Hils ⁴⁶, I. Hinchliffe ¹⁸, M. Hirose ¹²⁹, D. Hirschbuehl ¹⁷⁹, B. Hiti ⁸⁹, O. Hladik ¹³⁷, D.R. Hlaluku ^{32c}, X. Hoad ⁴⁸, J. Hobbs ¹⁵², N. Hod ^{165a}, M.C. Hodgkinson ¹⁴⁶, A. Hoecker ³⁵, M.R. Hoeferkamp ¹¹⁶, F. Hoenig ¹¹², D. Hohn ²⁴, D. Hohov ¹²⁸, T.R. Holmes ³⁶, M. Holzbock ¹¹², M. Homann ⁴⁵, S. Honda ¹⁶⁶, T. Honda ⁷⁹, T.M. Hong ¹³⁵, A. Hönle ¹¹³, B.H. Hooberman ¹⁷⁰, W.H. Hopkins ¹²⁷, Y. Horii ¹¹⁵, P. Horn ⁴⁶, A.J. Horton ¹⁴⁹, L.A. Horyn ³⁶, J-Y. Hostachy ⁵⁶, A. Hostiuc ¹⁴⁵, S. Hou ¹⁵⁵, A. Hoummada ^{34a}, J. Howarth ⁹⁸, J. Hoya ⁸⁶, M. Hrabovsky ¹²⁶, J. Hrdinka ³⁵, I. Hristova ¹⁹, J. Hrivnac ¹²⁸, A. Hrynevich ¹⁰⁶, T. Hrynn'ova ⁵, P.J. Hsu ⁶², S.-C. Hsu ¹⁴⁵, Q. Hu ²⁹, S. Hu ^{58c}, Y. Huang ^{15a}, Z. Hubacek ¹³⁸, F. Hubaut ⁹⁹, M. Huebner ²⁴, F. Huegging ²⁴, T.B. Huffman ¹³¹, E.W. Hughes ³⁸, M. Huhtinen ³⁵, R.F.H. Hunter ³³, P. Huo ¹⁵², A.M. Hupe ³³, N. Huseynov ^{77,ad}, J. Huston ¹⁰⁴, J. Huth ⁵⁷, R. Hyneman ¹⁰³, G. Iacobucci ⁵², G. Iakovidis ²⁹, I. Ibragimov ¹⁴⁸, L. Iconomidou-Fayard ¹²⁸, Z. Idrissi ^{34e}, P. Iengo ³⁵, R. Ignazzi ³⁹, O. Igonkina ^{118,z}, R. Iguchi ¹⁶⁰, T. Iizawa ⁵², Y. Ikegami ⁷⁹, M. Ikeno ⁷⁹, D. Iliadis ¹⁵⁹, N. Ilic ¹⁵⁰, F. Iltzsche ⁴⁶, G. Introzzi ^{68a,68b}, M. Iodice ^{72a}, K. Iordanidou ³⁸, V. Ippolito ^{70a,70b}, M.F. Isacson ¹⁶⁹, N. Ishijima ¹²⁹, M. Ishino ¹⁶⁰, M. Ishitsuka ¹⁶², W. Islam ¹²⁵, C. Issever ¹³¹, S. Istin ¹⁵⁷, F. Ito ¹⁶⁶, J.M. Iturbe Ponce ^{61a}, R. Iuppa ^{73a,73b}, A. Ivina ¹⁷⁷, H. Iwasaki ⁷⁹, J.M. Izen ⁴², V. Izzo ^{67a}, P. Jacka ¹³⁷, P. Jackson ¹, R.M. Jacobs ²⁴, V. Jain ², G. Jäkel ¹⁷⁹, K.B. Jakobi ⁹⁷, K. Jakobs ⁵⁰, S. Jakobsen ⁷⁴, T. Jakoubek ¹³⁷, D.O. Jamin ¹²⁵, D.K. Jana ⁹³, R. Jansky ⁵², J. Janssen ²⁴, M. Janus ⁵¹, P.A. Janus ^{81a}, G. Jarlskog ⁹⁴, N. Javadov ^{77,ad}, T. Javůrek ³⁵, M. Javurkova ⁵⁰, F. Jeanneau ¹⁴², L. Jeanty ¹⁸, J. Jejelava ^{156a,ae}, A. Jelinskas ¹⁷⁵, P. Jenni ^{50,c}, J. Jeong ⁴⁴, S. Jézéquel ⁵, H. Ji ¹⁷⁸, J. Jia ¹⁵², H. Jiang ⁷⁶, Y. Jiang ^{58a}, Z. Jiang ¹⁵⁰, S. Jiggins ⁵⁰, F.A. Jimenez Morales ³⁷, J. Jimenez Pena ¹⁷¹, S. Jin ^{15b}, A. Jinaru ^{27b}, O. Jinnouchi ¹⁶², H. Jivan ^{32c}, P. Johansson ¹⁴⁶, K.A. Johns ⁷, C.A. Johnson ⁶³, W.J. Johnson ¹⁴⁵, K. Jon-And ^{43a,43b}, R.W.L. Jones ⁸⁷, S.D. Jones ¹⁵³, S. Jones ⁷, T.J. Jones ⁸⁸, J. Jongmanns ^{59a}, P.M. Jorge ^{136a,136b}, J. Jovicevic ^{165a}, X. Ju ¹⁸, J.J. Junggeburth ¹¹³, A. Juste Rozas ^{14,x}, A. Kaczmarska ⁸², M. Kado ¹²⁸, H. Kagan ¹²², M. Kagan ¹⁵⁰, T. Kaji ¹⁷⁶, E. Kajomovitz ¹⁵⁷, C.W. Kalderon ⁹⁴, A. Kaluza ⁹⁷, S. Kama ⁴¹, A. Kamenshchikov ¹⁴⁰, L. Kanjir ⁸⁹, Y. Kano ¹⁶⁰, V.A. Kantserov ¹¹⁰, J. Kanzaki ⁷⁹, B. Kaplan ¹²¹, L.S. Kaplan ¹⁷⁸, D. Kar ^{32c}, M.J. Kareem ^{165b}, E. Karentzos ¹⁰, S.N. Karpov ⁷⁷, Z.M. Karpova ⁷⁷, V. Kartvelishvili ⁸⁷, A.N. Karyukhin ¹⁴⁰, L. Kashif ¹⁷⁸, R.D. Kass ¹²², A. Kastanas ¹⁵¹, Y. Kataoka ¹⁶⁰, C. Kato ^{58d,58c}, J. Katzy ⁴⁴, K. Kawade ⁸⁰, K. Kawagoe ⁸⁵, T. Kawamoto ¹⁶⁰, G. Kawamura ⁵¹, E.F. Kay ⁸⁸, V.F. Kazanin ^{120b,120a}, R. Keeler ¹⁷³, R. Kehoe ⁴¹, J.S. Keller ³³, E. Kellermann ⁹⁴, J.J. Kempster ²¹, J. Kendrick ²¹, O. Kepka ¹³⁷, S. Kersten ¹⁷⁹, B.P. Kerševan ⁸⁹, R.A. Keyes ¹⁰¹, M. Khader ¹⁷⁰, F. Khalil-Zada ¹³, A. Khanov ¹²⁵, A.G. Kharlamov ^{120b,120a}, T. Kharlamova ^{120b,120a}, E.E. Khoda ¹⁷², A. Khodinov ¹⁶³, T.J. Khoo ⁵², E. Khramov ⁷⁷, J. Khubua ^{156b}, S. Kido ⁸⁰, M. Kiehn ⁵², C.R. Kilby ⁹¹, Y.K. Kim ³⁶, N. Kimura ^{64a,64c}, O.M. Kind ¹⁹, B.T. King ⁸⁸, D. Kirchmeier ⁴⁶, J. Kirk ¹⁴¹, A.E. Kiryunin ¹¹³, T. Kishimoto ¹⁶⁰, D. Kisielewska ^{81a}, V. Kitali ⁴⁴, O. Kivernyk ⁵, E. Kladiva ^{28b}, T. Klapdor-Kleingrothaus ⁵⁰, M.H. Klein ¹⁰³, M. Klein ⁸⁸, U. Klein ⁸⁸, K. Kleinknecht ⁹⁷, P. Klimek ¹¹⁹, A. Klimentov ²⁹, R. Klingenberg ^{45,*}, T. Klingl ²⁴, T. Klioutchnikova ³⁵, F.F. Klitzner ¹¹², P. Kluit ¹¹⁸, S. Kluth ¹¹³, E. Kneringer ⁷⁴, E.B.F.G. Knoops ⁹⁹, A. Knue ⁵⁰, A. Kobayashi ¹⁶⁰, D. Kobayashi ⁸⁵, T. Kobayashi ¹⁶⁰, M. Kobel ⁴⁶, M. Kocian ¹⁵⁰, P. Kodys ¹³⁹, P.T. Koenig ²⁴, T. Koffas ³³, E. Koffeman ¹¹⁸, N.M. Köhler ¹¹³, T. Koi ¹⁵⁰, M. Kolb ^{59b}, I. Koletsou ⁵, T. Kondo ⁷⁹, N. Kondrashova ^{58c}, K. Köneke ⁵⁰, A.C. König ¹¹⁷, T. Kono ⁷⁹, R. Konoplich ^{121,ah}, V. Konstantinides ⁹², N. Konstantinidis ⁹², B. Konya ⁹⁴, R. Kopeliansky ⁶³, S. Koperny ^{81a}, K. Korcyl ⁸², K. Kordas ¹⁵⁹, G. Koren ¹⁵⁸, A. Korn ⁹², I. Korolkov ¹⁴, E.V. Korolkova ¹⁴⁶, N. Korotkova ¹¹¹, O. Kortner ¹¹³, S. Kortner ¹¹³, T. Kosek ¹³⁹, V.V. Kostyukhin ²⁴, A. Kotwal ⁴⁷, A. Koulouris ¹⁰, A. Kourkoumeli-Charalampidi ^{68a,68b}, C. Kourkoumelis ⁹, E. Kourlitis ¹⁴⁶, V. Kouskoura ²⁹, A.B. Kowalewska ⁸², R. Kowalewski ¹⁷³, T.Z. Kowalski ^{81a}, C. Kozakai ¹⁶⁰, W. Kozanecki ¹⁴², A.S. Kozhin ¹⁴⁰, V.A. Kramarenko ¹¹¹, G. Kramberger ⁸⁹, D. Krasnopalitsev ^{58a}, M.W. Krasny ¹³², A. Krasznahorkay ³⁵, D. Krauss ¹¹³, J.A. Kremer ^{81a}, J. Kretschmar ⁸⁸, P. Krieger ¹⁶⁴, K. Krizka ¹⁸, K. Kroeninger ⁴⁵, H. Kroha ¹¹³, J. Kroll ¹³⁷, J. Kroll ¹³³, J. Krstic ¹⁶, U. Kruchonak ⁷⁷, H. Krüger ²⁴, N. Krumnack ⁷⁶, M.C. Kruse ⁴⁷, T. Kubota ¹⁰², S. Kuday ^{4b}, J.T. Kuechler ¹⁷⁹, S. Kuehn ³⁵, A. Kugel ^{59a}, F. Kuger ¹⁷⁴, T. Kuhl ⁴⁴, V. Kukhtin ⁷⁷, R. Kukla ⁹⁹, Y. Kulchitsky ¹⁰⁵, S. Kuleshov ^{144b}, Y.P. Kulinich ¹⁷⁰, M. Kuna ⁵⁶, T. Kunigo ⁸³, A. Kupco ¹³⁷, T. Kupfer ⁴⁵, O. Kuprash ¹⁵⁸, H. Kurashige ⁸⁰, L.L. Kurchaninov ^{165a}, Y.A. Kurochkin ¹⁰⁵, M.G. Kurth ^{15d}, E.S. Kuwertz ³⁵, M. Kuze ¹⁶², J. Kvita ¹²⁶, T. Kwan ¹⁰¹, A. La Rosa ¹¹³, J.L. La Rosa Navarro ^{78d}, L. La Rotonda ^{40b,40a}, F. La Ruffa ^{40b,40a}, C. Lacasta ¹⁷¹, F. Lacava ^{70a,70b}, J. Lacey ⁴⁴, D.P.J. Lack ⁹⁸, H. Lacker ¹⁹, D. Lacour ¹³², E. Ladygin ⁷⁷, R. Lafaye ⁵, B. Laforge ¹³², T. Lagouri ^{32c}, S. Lai ⁵¹, S. Lammers ⁶³,

- W. Lampl ⁷, E. Lançon ²⁹, U. Landgraf ⁵⁰, M.P.J. Landon ⁹⁰, M.C. Lanfermann ⁵², V.S. Lang ⁴⁴, J.C. Lange ¹⁴, R.J. Langenberg ³⁵, A.J. Lankford ¹⁶⁸, F. Lanni ²⁹, K. Lantzsch ²⁴, A. Lanza ^{68a}, A. Lapertosa ^{53b,53a}, S. Laplace ¹³², J.F. Laporte ¹⁴², T. Lari ^{66a}, F. Lasagni Manghi ^{23b,23a}, M. Lassnig ³⁵, T.S. Lau ^{61a}, A. Laudrain ¹²⁸, M. Lavorgna ^{67a,67b}, A.T. Law ¹⁴³, P. Laycock ⁸⁸, M. Lazzaroni ^{66a,66b}, B. Le ¹⁰², O. Le Dortz ¹³², E. Le Guiriec ⁹⁹, E.P. Le Quilleuc ¹⁴², M. LeBlanc ⁷, T. LeCompte ⁶, F. Ledroit-Guillon ⁵⁶, C.A. Lee ²⁹, G.R. Lee ^{144a}, L. Lee ⁵⁷, S.C. Lee ¹⁵⁵, B. Lefebvre ¹⁰¹, M. Lefebvre ¹⁷³, F. Legger ¹¹², C. Leggett ¹⁸, K. Lehmann ¹⁴⁹, N. Lehmann ¹⁷⁹, G. Lehmann Miotto ³⁵, W.A. Leight ⁴⁴, A. Leisos ^{159,u}, M.A.L. Leite ^{78d}, R. Leitner ¹³⁹, D. Lellouch ¹⁷⁷, B. Lemmer ⁵¹, K.J.C. Leney ⁹², T. Lenz ²⁴, B. Lenzi ³⁵, R. Leone ⁷, S. Leone ^{69a}, C. Leonidopoulos ⁴⁸, G. Lerner ¹⁵³, C. Leroy ¹⁰⁷, R. Les ¹⁶⁴, A.A.J. Lesage ¹⁴², C.G. Lester ³¹, M. Levchenko ¹³⁴, J. Levêque ⁵, D. Levin ¹⁰³, L.J. Levinson ¹⁷⁷, D. Lewis ⁹⁰, B. Li ¹⁰³, C-Q. Li ^{58a}, H. Li ^{58b}, L. Li ^{58c}, Q. Li ^{15d}, Q.Y. Li ^{58a}, S. Li ^{58d,58c}, X. Li ^{58c}, Y. Li ¹⁴⁸, Z. Liang ^{15a}, B. Liberti ^{71a}, A. Liblong ¹⁶⁴, K. Lie ^{61c}, S. Liem ¹¹⁸, A. Limosani ¹⁵⁴, C.Y. Lin ³¹, K. Lin ¹⁰⁴, T.H. Lin ⁹⁷, R.A. Linck ⁶³, J.H. Lindon ²¹, B.E. Lindquist ¹⁵², A.L. Lionti ⁵², E. Lipeles ¹³³, A. Lipniacka ¹⁷, M. Lisovyi ^{59b}, T.M. Liss ^{170,am}, A. Lister ¹⁷², A.M. Litke ¹⁴³, J.D. Little ⁸, B. Liu ⁷⁶, B.L. Liu ⁶, H.B. Liu ²⁹, H. Liu ¹⁰³, J.B. Liu ^{58a}, J.K.K. Liu ¹³¹, K. Liu ¹³², M. Liu ^{58a}, P. Liu ¹⁸, Y. Liu ^{15a}, Y.L. Liu ^{58a}, Y.W. Liu ^{58a}, M. Livan ^{68a,68b}, A. Lleres ⁵⁶, J. Llorente Merino ^{15a}, S.L. Lloyd ⁹⁰, C.Y. Lo ^{61b}, F. Lo Sterzo ⁴¹, E.M. Lobodzinska ⁴⁴, P. Loch ⁷, A. Loesle ⁵⁰, T. Lohse ¹⁹, K. Lohwasser ¹⁴⁶, M. Lokajicek ¹³⁷, B.A. Long ²⁵, J.D. Long ¹⁷⁰, R.E. Long ⁸⁷, L. Longo ^{65a,65b}, K.A.Looper ¹²², J.A. Lopez ^{144b}, I. Lopez Paz ¹⁴, A. Lopez Solis ¹⁴⁶, J. Lorenz ¹¹², N. Lorenzo Martinez ⁵, M. Losada ²², P.J. Lösel ¹¹², X. Lou ⁴⁴, X. Lou ^{15a}, A. Lounis ¹²⁸, J. Love ⁶, P.A. Love ⁸⁷, J.J. Lozano Bahilo ¹⁷¹, H. Lu ^{61a}, M. Lu ^{58a}, N. Lu ¹⁰³, Y.J. Lu ⁶², H.J. Lubatti ¹⁴⁵, C. Luci ^{70a,70b}, A. Lucotte ⁵⁶, C. Luedtke ⁵⁰, F. Luehring ⁶³, I. Luise ¹³², L. Luminari ^{70a}, B. Lund-Jensen ¹⁵¹, M.S. Lutz ¹⁰⁰, P.M. Luzi ¹³², D. Lynn ²⁹, R. Lysak ¹³⁷, E. Lytken ⁹⁴, F. Lyu ^{15a}, V. Lyubushkin ⁷⁷, H. Ma ²⁹, L.L. Ma ^{58b}, Y. Ma ^{58b}, G. Maccarrone ⁴⁹, A. Macchiolo ¹¹³, C.M. Macdonald ¹⁴⁶, J. Machado Miguens ^{133,136b}, D. Madaffari ¹⁷¹, R. Madar ³⁷, W.F. Mader ⁴⁶, A. Madsen ⁴⁴, N. Madysa ⁴⁶, J. Maeda ⁸⁰, K. Maekawa ¹⁶⁰, S. Maeland ¹⁷, T. Maeno ²⁹, A.S. Maevskiy ¹¹¹, V. Magerl ⁵⁰, C. Maidantchik ^{78b}, T. Maier ¹¹², A. Maio ^{136a,136b,136d}, O. Majersky ^{28a}, S. Majewski ¹²⁷, Y. Makida ⁷⁹, N. Makovec ¹²⁸, B. Malaescu ¹³², Pa. Malecki ⁸², V.P. Maleev ¹³⁴, F. Malek ⁵⁶, U. Mallik ⁷⁵, D. Malon ⁶, C. Malone ³¹, S. Maltezos ¹⁰, S. Malyukov ³⁵, J. Mamuzic ¹⁷¹, G. Mancini ⁴⁹, I. Mandić ⁸⁹, J. Maneira ^{136a}, L. Manhaes de Andrade Filho ^{78a}, J. Manjarres Ramos ⁴⁶, K.H. Mankinen ⁹⁴, A. Mann ¹¹², A. Manousos ⁷⁴, B. Mansoulie ¹⁴², J.D. Mansour ^{15a}, M. Mantoani ⁵¹, S. Manzoni ^{66a,66b}, G. Marceca ³⁰, L. March ⁵², L. Marchese ¹³¹, G. Marchiori ¹³², M. Marcisovsky ¹³⁷, C.A. Marin Tobon ³⁵, M. Marjanovic ³⁷, D.E. Marley ¹⁰³, F. Marroquim ^{78b}, Z. Marshall ¹⁸, M.U.F Martensson ¹⁶⁹, S. Marti-Garcia ¹⁷¹, C.B. Martin ¹²², T.A. Martin ¹⁷⁵, V.J. Martin ⁴⁸, B. Martin dit Latour ¹⁷, M. Martinez ^{14,x}, V.I. Martinez Outschoorn ¹⁰⁰, S. Martin-Haugh ¹⁴¹, V.S. Martoiu ^{27b}, A.C. Martyniuk ⁹², A. Marzin ³⁵, L. Masetti ⁹⁷, T. Mashimo ¹⁶⁰, R. Mashinistov ¹⁰⁸, J. Masik ⁹⁸, A.L. Maslennikov ^{120b,120a}, L.H. Mason ¹⁰², L. Massa ^{71a,71b}, P. Massarotti ^{67a,67b}, P. Mastrandrea ⁵, A. Mastroberardino ^{40b,40a}, T. Masubuchi ¹⁶⁰, P. Mättig ¹⁷⁹, J. Maurer ^{27b}, B. Maček ⁸⁹, S.J. Maxfield ⁸⁸, D.A. Maximov ^{120b,120a}, R. Mazini ¹⁵⁵, I. Maznas ¹⁵⁹, S.M. Mazza ¹⁴³, N.C. Mc Fadden ¹¹⁶, G. Mc Goldrick ¹⁶⁴, S.P. Mc Kee ¹⁰³, A. McCarn ¹⁰³, T.G. McCarthy ¹¹³, L.I. McClymont ⁹², E.F. McDonald ¹⁰², J.A. McFayden ³⁵, G. Mcchedlidze ⁵¹, M.A. McKay ⁴¹, K.D. McLean ¹⁷³, S.J. McMahon ¹⁴¹, P.C. McNamara ¹⁰², C.J. McNicol ¹⁷⁵, R.A. McPherson ^{173,ab}, J.E. Mdhluli ^{32c}, Z.A. Meadows ¹⁰⁰, S. Meehan ¹⁴⁵, T. Megy ⁵⁰, S. Mehlhase ¹¹², A. Mehta ⁸⁸, T. Meideck ⁵⁶, B. Meirose ⁴², D. Melini ^{171,g}, B.R. Mellado Garcia ^{32c}, J.D. Mellenthin ⁵¹, M. Melo ^{28a}, F. Meloni ⁴⁴, A. Melzer ²⁴, S.B. Menary ⁹⁸, E.D. Mendes Gouveia ^{136a}, L. Meng ⁸⁸, X.T. Meng ¹⁰³, A. Mengarelli ^{23b,23a}, S. Menke ¹¹³, E. Meoni ^{40b,40a}, S. Mergelmeyer ¹⁹, C. Merlassino ²⁰, P. Mermoud ⁵², L. Merola ^{67a,67b}, C. Meroni ^{66a}, F.S. Merritt ³⁶, A. Messina ^{70a,70b}, J. Metcalfe ⁶, A.S. Mete ¹⁶⁸, C. Meyer ¹³³, J. Meyer ¹⁵⁷, J-P. Meyer ¹⁴², H. Meyer Zu Theenhausen ^{59a}, F. Miano ¹⁵³, R.P. Middleton ¹⁴¹, L. Mijović ⁴⁸, G. Mikenberg ¹⁷⁷, M. Mikestikova ¹³⁷, M. Mikuž ⁸⁹, M. Milesi ¹⁰², A. Milic ¹⁶⁴, D.A. Millar ⁹⁰, D.W. Miller ³⁶, A. Milov ¹⁷⁷, D.A. Milstead ^{43a,43b}, A.A. Minaenko ¹⁴⁰, M. Miñano Moya ¹⁷¹, I.A. Minashvili ^{156b}, A.I. Mincer ¹²¹, B. Mindur ^{81a}, M. Mineev ⁷⁷, Y. Minegishi ¹⁶⁰, Y. Ming ¹⁷⁸, L.M. Mir ¹⁴, A. Mirto ^{65a,65b}, K.P. Mistry ¹³³, T. Mitani ¹⁷⁶, J. Mitrevski ¹¹², V.A. Mitsou ¹⁷¹, A. Miucci ²⁰, P.S. Miyagawa ¹⁴⁶, A. Mizukami ⁷⁹, J.U. Mjörnmark ⁹⁴, T. Mkrtchyan ¹⁸¹, M. Mlynárikova ¹³⁹, T. Moa ^{43a,43b}, K. Mochizuki ¹⁰⁷, P. Mogg ⁵⁰, S. Mohapatra ³⁸, S. Molander ^{43a,43b}, R. Moles-Valls ²⁴, M.C. Mondragon ¹⁰⁴, K. Mönig ⁴⁴, J. Monk ³⁹, E. Monnier ⁹⁹, A. Montalbano ¹⁴⁹, J. Montejo Berlingen ³⁵, F. Monticelli ⁸⁶, S. Monzani ^{66a},

- N. Morange ¹²⁸, D. Moreno ²², M. Moreno Llácer ³⁵, P. Morettini ^{53b}, M. Morgenstern ¹¹⁸,
 S. Morgenstern ⁴⁶, D. Mori ¹⁴⁹, M. Morii ⁵⁷, M. Morinaga ¹⁷⁶, V. Morisbak ¹³⁰, A.K. Morley ³⁵,
 G. Mornacchi ³⁵, A.P. Morris ⁹², J.D. Morris ⁹⁰, L. Morvaj ¹⁵², P. Moschovakos ¹⁰, M. Mosidze ^{156b},
 H.J. Moss ¹⁴⁶, J. Moss ^{150,m}, K. Motohashi ¹⁶², R. Mount ¹⁵⁰, E. Mountricha ³⁵, E.J.W. Moyse ¹⁰⁰,
 S. Muanza ⁹⁹, F. Mueller ¹¹³, J. Mueller ¹³⁵, R.S.P. Mueller ¹¹², D. Muenstermann ⁸⁷, G.A. Mullier ²⁰,
 F.J. Munoz Sanchez ⁹⁸, P. Murin ^{28b}, W.J. Murray ^{175,141}, A. Murrone ^{66a,66b}, M. Muškinja ⁸⁹, C. Mwewa ^{32a},
 A.G. Myagkov ^{140,ai}, J. Myers ¹²⁷, M. Myska ¹³⁸, B.P. Nachman ¹⁸, O. Nackenhorst ⁴⁵, K. Nagai ¹³¹,
 K. Nagano ⁷⁹, Y. Nagasaka ⁶⁰, M. Nagel ⁵⁰, E. Nagy ⁹⁹, A.M. Nairz ³⁵, Y. Nakahama ¹¹⁵, K. Nakamura ⁷⁹,
 T. Nakamura ¹⁶⁰, I. Nakano ¹²³, H. Nanjo ¹²⁹, F. Napolitano ^{59a}, R.F. Naranjo Garcia ⁴⁴, R. Narayan ¹¹,
 D.I. Narrias Villar ^{59a}, I. Naryshkin ¹³⁴, T. Naumann ⁴⁴, G. Navarro ²², R. Nayyar ⁷, H.A. Neal ¹⁰³,
 P.Y. Nechaeva ¹⁰⁸, T.J. Neep ¹⁴², A. Negri ^{68a,68b}, M. Negrini ^{23b}, S. Nektarijevic ¹¹⁷, C. Nellist ⁵¹,
 M.E. Nelson ¹³¹, S. Nemecek ¹³⁷, P. Nemethy ¹²¹, M. Nessi ^{35,e}, M.S. Neubauer ¹⁷⁰, M. Neumann ¹⁷⁹,
 P.R. Newman ²¹, T.Y. Ng ^{61c}, Y.S. Ng ¹⁹, H.D.N. Nguyen ⁹⁹, T. Nguyen Manh ¹⁰⁷, E. Nibigira ³⁷,
 R.B. Nickerson ¹³¹, R. Nicolaïdou ¹⁴², J. Nielsen ¹⁴³, N. Nikiforou ¹¹, V. Nikolaenko ^{140,ai},
 I. Nikolic-Audit ¹³², K. Nikolopoulos ²¹, P. Nilsson ²⁹, Y. Ninomiya ⁷⁹, A. Nisati ^{70a}, N. Nishu ^{58c},
 R. Nisius ¹¹³, I. Nitsche ⁴⁵, T. Nitta ¹⁷⁶, T. Nobe ¹⁶⁰, Y. Noguchi ⁸³, M. Nomachi ¹²⁹, I. Nomidis ¹³²,
 M.A. Nomura ²⁹, T. Nooney ⁹⁰, M. Nordberg ³⁵, N. Norjoharuddeen ¹³¹, T. Novak ⁸⁹, O. Novgorodova ⁴⁶,
 R. Novotny ¹³⁸, L. Nozka ¹²⁶, K. Ntekas ¹⁶⁸, E. Nurse ⁹², F. Nuti ¹⁰², F.G. Oakham ^{33,ap}, H. Oberlack ¹¹³,
 T. Obermann ²⁴, J. Ocariz ¹³², A. Ochi ⁸⁰, I. Ochoa ³⁸, J.P. Ochoa-Ricoux ^{144a}, K. O'Connor ²⁶, S. Oda ⁸⁵,
 S. Odaka ⁷⁹, S. Oerdekk ⁵¹, A. Oh ⁹⁸, S.H. Oh ⁴⁷, C.C. Ohm ¹⁵¹, H. Oide ^{53b,53a}, M.L. Ojeda ¹⁶⁴, H. Okawa ¹⁶⁶,
 Y. Okazaki ⁸³, Y. Okumura ¹⁶⁰, T. Okuyama ⁷⁹, A. Olariu ^{27b}, L.F. Oleiro Seabra ^{136a}, S.A. Olivares Pino ^{144a},
 D. Oliveira Damazio ²⁹, J.L. Oliver ¹, M.J.R. Olsson ³⁶, A. Olszewski ⁸², J. Olszowska ⁸², D.C. O'Neil ¹⁴⁹,
 A. Onofre ^{136a,136e}, K. Onogi ¹¹⁵, P.U.E. Onyisi ¹¹, H. Oppen ¹³⁰, M.J. Oreglia ³⁶, Y. Oren ¹⁵⁸,
 D. Orestano ^{72a,72b}, E.C. Orgill ⁹⁸, N. Orlando ^{61b}, A.A. O'Rourke ⁴⁴, R.S. Orr ¹⁶⁴, B. Osculati ^{53b,53a,*},
 V. O'Shea ⁵⁵, R. Ospanov ^{58a}, G. Otero y Garzon ³⁰, H. Otono ⁸⁵, M. Ouchrif ^{34d}, F. Ould-Saada ¹³⁰,
 A. Ouraou ¹⁴², Q. Ouyang ^{15a}, M. Owen ⁵⁵, R.E. Owen ²¹, V.E. Ozcan ^{12c}, N. Ozturk ⁸, J. Pacalt ¹²⁶,
 H.A. Pacey ³¹, K. Pachal ¹⁴⁹, A. Pacheco Pages ¹⁴, L. Pacheco Rodriguez ¹⁴², C. Padilla Aranda ¹⁴,
 S. Pagan Griso ¹⁸, M. Paganini ¹⁸⁰, G. Palacino ⁶³, S. Palazzo ^{40b,40a}, S. Palestini ³⁵, M. Palka ^{81b}, D. Pallin ³⁷,
 I. Panagoulias ¹⁰, C.E. Pandini ³⁵, J.G. Panduro Vazquez ⁹¹, P. Pani ³⁵, G. Panizzo ^{64a,64c}, L. Paolozzi ⁵²,
 T.D. Papadopoulou ¹⁰, K. Papageorgiou ^{9,i}, A. Paramonov ⁶, D. Paredes Hernandez ^{61b},
 S.R. Paredes Saenz ¹³¹, B. Parida ^{58c}, A.J. Parker ⁸⁷, K.A. Parker ⁴⁴, M.A. Parker ³¹, F. Parodi ^{53b,53a},
 J.A. Parsons ³⁸, U. Parzefall ⁵⁰, V.R. Pascuzzi ¹⁶⁴, J.M.P. Pasner ¹⁴³, E. Pasqualucci ^{70a}, S. Passaggio ^{53b},
 F. Pastore ⁹¹, P. Pasuwan ^{43a,43b}, S. Pataraia ⁹⁷, J.R. Pater ⁹⁸, A. Pathak ^{178,j}, T. Pauly ³⁵, B. Pearson ¹¹³,
 M. Pedersen ¹³⁰, L. Pedraza Diaz ¹¹⁷, R. Pedro ^{136a,136b}, S.V. Peleganchuk ^{120b,120a}, O. Penc ¹³⁷, C. Peng ^{15d},
 H. Peng ^{58a}, B.S. Peralva ^{78a}, M.M. Perego ¹⁴², A.P. Pereira Peixoto ^{136a}, D.V. Perepelitsa ²⁹, F. Peri ¹⁹,
 L. Perini ^{66a,66b}, H. Pernegger ³⁵, S. Perrella ^{67a,67b}, V.D. Peshekhonov ^{77,*}, K. Peters ⁴⁴, R.F.Y. Peters ⁹⁸,
 B.A. Petersen ³⁵, T.C. Petersen ³⁹, E. Petit ⁵⁶, A. Petridis ¹, C. Petridou ¹⁵⁹, P. Petroff ¹²⁸, M. Petrov ¹³¹,
 F. Petrucci ^{72a,72b}, M. Pettee ¹⁸⁰, N.E. Pettersson ¹⁰⁰, A. Peyaud ¹⁴², R. Pezoa ^{144b}, T. Pham ¹⁰²,
 F.H. Phillips ¹⁰⁴, P.W. Phillips ¹⁴¹, G. Piacquadio ¹⁵², E. Pianori ¹⁸, A. Picazio ¹⁰⁰, M.A. Pickering ¹³¹,
 R.H. Pickles ⁹⁸, R. Piegaia ³⁰, J.E. Pilcher ³⁶, A.D. Pilkington ⁹⁸, M. Pinamonti ^{71a,71b}, J.L. Pinfold ³,
 M. Pitt ¹⁷⁷, M-A. Pleier ²⁹, V. Pleskot ¹³⁹, E. Plotnikova ⁷⁷, D. Pluth ⁷⁶, P. Podberezko ^{120b,120a},
 R. Poettgen ⁹⁴, R. Poggi ⁵², L. Poggiali ¹²⁸, I. Pogrebnyak ¹⁰⁴, D. Pohl ²⁴, I. Pokharel ⁵¹, G. Polesello ^{68a},
 A. Poley ¹⁸, A. Policicchio ^{70a,70b}, R. Polifka ³⁵, A. Polini ^{23b}, C.S. Pollard ⁴⁴, V. Polychronakos ²⁹,
 D. Ponomarenko ¹¹⁰, L. Pontecorvo ^{70a}, G.A. Popeneciu ^{27d}, D.M. Portillo Quintero ¹³², S. Pospisil ¹³⁸,
 K. Potamianos ⁴⁴, I.N. Potrap ⁷⁷, C.J. Potter ³¹, H. Potti ¹¹, T. Poulsen ⁹⁴, J. Poveda ³⁵, T.D. Powell ¹⁴⁶,
 M.E. Pozo Astigarraga ³⁵, P. Pralavorio ⁹⁹, S. Prell ⁷⁶, D. Price ⁹⁸, M. Primavera ^{65a}, S. Prince ¹⁰¹,
 N. Proklova ¹¹⁰, K. Prokofiev ^{61c}, F. Prokoshin ^{144b}, S. Protopopescu ²⁹, J. Proudfoot ⁶, M. Przybycien ^{81a},
 A. Puri ¹⁷⁰, P. Puzo ¹²⁸, J. Qian ¹⁰³, Y. Qin ⁹⁸, A. Quadt ⁵¹, M. Queitsch-Maitland ⁴⁴, A. Qureshi ¹,
 P. Rados ¹⁰², F. Ragusa ^{66a,66b}, G. Rahal ⁹⁵, J.A. Raine ⁵², S. Rajagopalan ²⁹, A. Ramirez Morales ⁹⁰,
 T. Rashid ¹²⁸, S. Raspopov ⁵, M.G. Ratti ^{66a,66b}, D.M. Rauch ⁴⁴, F. Rauscher ¹¹², S. Rave ⁹⁷, B. Ravina ¹⁴⁶,
 I. Ravinovich ¹⁷⁷, J.H. Rawling ⁹⁸, M. Raymond ³⁵, A.L. Read ¹³⁰, N.P. Readioff ⁵⁶, M. Reale ^{65a,65b},
 D.M. Rebuzzi ^{68a,68b}, A. Redelbach ¹⁷⁴, G. Redlinger ²⁹, R. Reece ¹⁴³, R.G. Reed ^{32c}, K. Reeves ⁴²,

- L. Rehnisch ¹⁹, J. Reichert ¹³³, A. Reiss ⁹⁷, C. Rembser ³⁵, H. Ren ^{15d}, M. Rescigno ^{70a}, S. Resconi ^{66a}, E.D. Resseguei ¹³³, S. Rettie ¹⁷², E. Reynolds ²¹, O.L. Rezanova ^{120b,120a}, P. Reznicek ¹³⁹, E. Ricci ^{73a,73b}, R. Richter ¹¹³, S. Richter ⁹², E. Richter-Was ^{81b}, O. Ricken ²⁴, M. Ridel ¹³², P. Rieck ¹¹³, C.J. Riegel ¹⁷⁹, O. Rifki ⁴⁴, M. Rijssenbeek ¹⁵², A. Rimoldi ^{68a,68b}, M. Rimoldi ²⁰, L. Rinaldi ^{23b}, G. Ripellino ¹⁵¹, B. Ristić ⁸⁷, E. Ritsch ³⁵, I. Riu ¹⁴, J.C. Rivera Vergara ^{144a}, F. Rizatdinova ¹²⁵, E. Rizvi ⁹⁰, C. Rizzi ¹⁴, R.T. Roberts ⁹⁸, S.H. Robertson ^{101,ab}, D. Robinson ³¹, J.E.M. Robinson ⁴⁴, A. Robson ⁵⁵, E. Rocco ⁹⁷, C. Roda ^{69a,69b}, Y. Rodina ⁹⁹, S. Rodriguez Bosca ¹⁷¹, A. Rodriguez Perez ¹⁴, D. Rodriguez Rodriguez ¹⁷¹, A.M. Rodríguez Vera ^{165b}, S. Roe ³⁵, C.S. Rogan ⁵⁷, O. Røhne ¹³⁰, R. Röhrlig ¹¹³, C.P.A. Roland ⁶³, J. Roloff ⁵⁷, A. Romanouk ¹¹⁰, M. Romano ^{23b,23a}, N. Rompotis ⁸⁸, M. Ronzani ¹²¹, L. Roos ¹³², S. Rosati ^{70a}, K. Rosbach ⁵⁰, P. Rose ¹⁴³, N-A. Rosien ⁵¹, E. Rossi ⁴⁴, E. Rossi ^{67a,67b}, L.P. Rossi ^{53b}, L. Rossini ^{66a,66b}, J.H.N. Rosten ³¹, R. Rosten ¹⁴, M. Rotaru ^{27b}, J. Rothberg ¹⁴⁵, D. Rousseau ¹²⁸, D. Roy ^{32c}, A. Rozanov ⁹⁹, Y. Rozen ¹⁵⁷, X. Ruan ^{32c}, F. Rubbo ¹⁵⁰, F. Rühr ⁵⁰, A. Ruiz-Martinez ¹⁷¹, Z. Rurikova ⁵⁰, N.A. Rusakovich ⁷⁷, H.L. Russell ¹⁰¹, J.P. Rutherford ⁷, E.M. Rüttinger ^{44,k}, Y.F. Ryabov ¹³⁴, M. Rybar ¹⁷⁰, G. Rybkin ¹²⁸, S. Ryu ⁶, A. Ryzhov ¹⁴⁰, G.F. Rzehorž ⁵¹, P. Sabatini ⁵¹, G. Sabato ¹¹⁸, S. Sacerdoti ¹²⁸, H.-F.-W. Sadrozinski ¹⁴³, R. Sadykov ⁷⁷, F. Safai Tehrani ^{70a}, P. Saha ¹¹⁹, M. Sahinsoy ^{59a}, A. Sahu ¹⁷⁹, M. Saimpert ⁴⁴, M. Saito ¹⁶⁰, T. Saito ¹⁶⁰, H. Sakamoto ¹⁶⁰, A. Sakharov ^{121,ah}, D. Salamani ⁵², G. Salamanna ^{72a,72b}, J.E. Salazar Loyola ^{144b}, D. Salek ¹¹⁸, P.H. Sales De Bruin ¹⁶⁹, D. Salihagic ¹¹³, A. Salnikov ¹⁵⁰, J. Salt ¹⁷¹, D. Salvatore ^{40b,40a}, F. Salvatore ¹⁵³, A. Salvucci ^{61a,61b,61c}, A. Salzburger ³⁵, J. Samarati ³⁵, D. Sammel ⁵⁰, D. Sampsonidis ¹⁵⁹, D. Sampsonidou ¹⁵⁹, J. Sánchez ¹⁷¹, A. Sanchez Pineda ^{64a,64c}, H. Sandaker ¹³⁰, C.O. Sander ⁴⁴, M. Sandhoff ¹⁷⁹, C. Sandoval ²², D.P.C. Sankey ¹⁴¹, M. Sannino ^{53b,53a}, Y. Sano ¹¹⁵, A. Sansoni ⁴⁹, C. Santoni ³⁷, H. Santos ^{136a}, I. Santoyo Castillo ¹⁵³, A. Santra ¹⁷¹, A. Sapronov ⁷⁷, J.G. Saraiva ^{136a,136d}, O. Sasaki ⁷⁹, K. Sato ¹⁶⁶, E. Sauvan ⁵, P. Savard ^{164,ap}, N. Savic ¹¹³, R. Sawada ¹⁶⁰, C. Sawyer ¹⁴¹, L. Sawyer ^{93,ag}, C. Sbarra ^{23b}, A. Sbrizzi ^{23b,23a}, T. Scanlon ⁹², J. Schaarschmidt ¹⁴⁵, P. Schacht ¹¹³, B.M. Schachtner ¹¹², D. Schaefer ³⁶, L. Schaefer ¹³³, J. Schaeffer ⁹⁷, S. Schaepe ³⁵, U. Schäfer ⁹⁷, A.C. Schaffer ¹²⁸, D. Schaile ¹¹², R.D. Schamberger ¹⁵², N. Scharnberg ⁹⁸, V.A. Schegelsky ¹³⁴, D. Scheirich ¹³⁹, F. Schenck ¹⁹, M. Schernau ¹⁶⁸, C. Schiavi ^{53b,53a}, S. Schier ¹⁴³, L.K. Schildgen ²⁴, Z.M. Schillaci ²⁶, E.J. Schioppa ³⁵, M. Schioppa ^{40b,40a}, K.E. Schleicher ⁵⁰, S. Schlenker ³⁵, K.R. Schmidt-Sommerfeld ¹¹³, K. Schmieden ³⁵, C. Schmitt ⁹⁷, S. Schmitt ⁴⁴, S. Schmitz ⁹⁷, J.C. Schmoekel ⁴⁴, U. Schnoor ⁵⁰, L. Schoeffel ¹⁴², A. Schoening ^{59b}, E. Schopf ²⁴, M. Schott ⁹⁷, J.F.P. Schouwenberg ¹¹⁷, J. Schovancova ³⁵, S. Schramm ⁵², A. Schulte ⁹⁷, H.-C. Schultz-Coulon ^{59a}, M. Schumacher ⁵⁰, B.A. Schumm ¹⁴³, Ph. Schune ¹⁴², A. Schwartzman ¹⁵⁰, T.A. Schwarz ¹⁰³, H. Schweiger ⁹⁸, Ph. Schwemling ¹⁴², R. Schwienhorst ¹⁰⁴, A. Sciandra ²⁴, G. Sciolla ²⁶, M. Scornajenghi ^{40b,40a}, F. Scuri ^{69a}, F. Scutti ¹⁰², L.M. Scyboz ¹¹³, J. Searcy ¹⁰³, C.D. Sebastiani ^{70a,70b}, P. Seema ²⁴, S.C. Seidel ¹¹⁶, A. Seiden ¹⁴³, T. Seiss ³⁶, J.M. Seixas ^{78b}, G. Sekhniaidze ^{67a}, K. Sekhon ¹⁰³, S.J. Sekula ⁴¹, N. Semprini-Cesari ^{23b,23a}, S. Sen ⁴⁷, S. Senkin ³⁷, C. Serfon ¹³⁰, L. Serin ¹²⁸, L. Serkin ^{64a,64b}, M. Sessa ^{72a,72b}, H. Severini ¹²⁴, F. Sforza ¹⁶⁷, A. Sfyrla ⁵², E. Shabalina ⁵¹, J.D. Shahinian ¹⁴³, N.W. Shaikh ^{43a,43b}, L.Y. Shan ^{15a}, R. Shang ¹⁷⁰, J.T. Shank ²⁵, M. Shapiro ¹⁸, A.S. Sharma ¹, A. Sharma ¹³¹, P.B. Shatalov ¹⁰⁹, K. Shaw ¹⁵³, S.M. Shaw ⁹⁸, A. Shcherbakova ¹³⁴, Y. Shen ¹²⁴, N. Sherafati ³³, A.D. Sherman ²⁵, P. Sherwood ⁹², L. Shi ^{155,al}, S. Shimizu ⁷⁹, C.O. Shimmin ¹⁸⁰, M. Shimojima ¹¹⁴, I.P.J. Shipsey ¹³¹, S. Shirabe ⁸⁵, M. Shiyakova ⁷⁷, J. Shlomi ¹⁷⁷, A. Shmeleva ¹⁰⁸, D. Shoaleh Saadi ¹⁰⁷, M.J. Shochet ³⁶, S. Shojaei ¹⁰², D.R. Shope ¹²⁴, S. Shrestha ¹²², E. Shulga ¹¹⁰, P. Sicho ¹³⁷, A.M. Sickles ¹⁷⁰, P.E. Sidebo ¹⁵¹, E. Sideras Haddad ^{32c}, O. Sidiropoulou ³⁵, A. Sidoti ^{23b,23a}, F. Siegert ⁴⁶, Dj. Sijacki ¹⁶, J. Silva ^{136a}, M. Silva Jr. ¹⁷⁸, M.V. Silva Oliveira ^{78a}, S.B. Silverstein ^{43a}, L. Simic ⁷⁷, S. Simion ¹²⁸, E. Simioni ⁹⁷, M. Simon ⁹⁷, R. Simoniello ⁹⁷, P. Sinervo ¹⁶⁴, N.B. Sinev ¹²⁷, M. Sioli ^{23b,23a}, G. Siragusa ¹⁷⁴, I. Siral ¹⁰³, S.Yu. Sivoklokov ¹¹¹, J. Sjölin ^{43a,43b}, P. Skubic ¹²⁴, M. Slater ²¹, T. Slavicek ¹³⁸, M. Slawinska ⁸², K. Sliwa ¹⁶⁷, R. Slovak ¹³⁹, V. Smakhtin ¹⁷⁷, B.H. Smart ⁵, J. Smiesko ^{28a}, N. Smirnov ¹¹⁰, S.Yu. Smirnov ¹¹⁰, Y. Smirnov ¹¹⁰, L.N. Smirnova ¹¹¹, O. Smirnova ⁹⁴, J.W. Smith ⁵¹, M.N.K. Smith ³⁸, M. Smizanska ⁸⁷, K. Smolek ¹³⁸, A. Smykiewicz ⁸², A.A. Snesarev ¹⁰⁸, I.M. Snyder ¹²⁷, S. Snyder ²⁹, R. Sobie ^{173,ab}, A.M. Soffa ¹⁶⁸, A. Soffer ¹⁵⁸, A. Søgaard ⁴⁸, D.A. Soh ¹⁵⁵, G. Sokhrannyi ⁸⁹, C.A. Solans Sanchez ³⁵, M. Solar ¹³⁸, E.Yu. Soldatov ¹¹⁰, U. Soldevila ¹⁷¹, A.A. Solodkov ¹⁴⁰, A. Soloshenko ⁷⁷, O.V. Solovyev ¹⁴⁰, V. Solovyev ¹³⁴, P. Sommer ¹⁴⁶, H. Son ¹⁶⁷, W. Song ¹⁴¹, W.Y. Song ^{165b}, A. Sopczak ¹³⁸, F. Sopkova ^{28b}, D. Sosa ^{59b}, C.L. Sotiropoulou ^{69a,69b}, S. Sottocornola ^{68a,68b}, R. Soualah ^{64a,64c,h}, A.M. Soukharev ^{120b,120a},

- D. South 44, B.C. Sowden 91, S. Spagnolo 65a, 65b, M. Spalla 113, M. Spangenberg 175, F. Spanò 91,
 D. Sperlich 19, F. Spettel 113, T.M. Spieker 59a, R. Spighi 23b, G. Spigo 35, L.A. Spiller 102, D.P. Spiteri 55,
 M. Spousta 139, A. Stabile 66a, 66b, R. Stamen 59a, S. Stamm 19, E. Stanecka 82, R.W. Stanek 6, C. Stanescu 72a,
 B. Stanislaus 131, M.M. Stanitzki 44, B.S. Stapf 118, S. Stapnes 130, E.A. Starchenko 140, G.H. Stark 36,
 J. Stark 56, S.H. Stark 39, P. Staroba 137, P. Starovoitov 59a, S. Stärz 35, R. Staszewski 82, M. Stegler 44,
 P. Steinberg 29, B. Stelzer 149, H.J. Stelzer 35, O. Stelzer-Chilton 165a, H. Stenzel 54, T.J. Stevenson 90,
 G.A. Stewart 55, M.C. Stockton 127, G. Stoicea 27b, P. Stolte 51, S. Stonjek 113, A. Straessner 46,
 J. Strandberg 151, S. Strandberg 43a, 43b, M. Strauss 124, P. Strizenec 28b, R. Ströhmer 174, D.M. Strom 127,
 R. Stroynowski 41, A. Strubig 48, S.A. Stucci 29, B. Stugu 17, J. Stupak 124, N.A. Styles 44, D. Su 150, J. Su 135,
 S. Suchek 59a, Y. Sugaya 129, M. Suk 138, V.V. Sulin 108, D.M.S. Sultan 52, S. Sultansoy 4c, T. Sumida 83,
 S. Sun 103, X. Sun 3, K. Suruliz 153, C.J.E. Suster 154, M.R. Sutton 153, S. Suzuki 79, M. Svatos 137,
 M. Swiatlowski 36, S.P. Swift 2, A. Sydorenko 97, I. Sykora 28a, T. Sykora 139, D. Ta 97, K. Tackmann 44,y,
 J. Taenzer 158, A. Taffard 168, R. Tafirout 165a, E. Tahirovic 90, N. Taiblum 158, H. Takai 29, R. Takashima 84,
 E.H. Takasugi 113, K. Takeda 80, T. Takeshita 147, Y. Takubo 79, M. Talby 99, A.A. Talyshев 120b, 120a,
 J. Tanaka 160, M. Tanaka 162, R. Tanaka 128, B.B. Tannenwald 122, S. Tapia Araya 144b, S. Tapprogge 97,
 A. Tarek Abouelfadl Mohamed 132, S. Tarem 157, G. Tarna 27b,d, G.F. Tartarelli 66a, P. Tas 139,
 M. Tasevsky 137, T. Tashiro 83, E. Tassi 40b, 40a, A. Tavares Delgado 136a, 136b, Y. Tayalati 34e, A.C. Taylor 116,
 A.J. Taylor 48, G.N. Taylor 102, P.T.E. Taylor 102, W. Taylor 165b, A.S. Tee 87, P. Teixeira-Dias 91, H. Ten Kate 35,
 P.K. Teng 155, J.J. Teoh 118, F. Tepel 179, S. Terada 79, K. Terashi 160, J. Terron 96, S. Terzo 14, M. Testa 49,
 R.J. Teuscher 164, ab, S.J. Thais 180, T. Theveneaux-Pelzer 44, F. Thiele 39, D.W. Thomas 91, J.P. Thomas 21,
 A.S. Thompson 55, P.D. Thompson 21, L.A. Thomsen 180, E. Thomson 133, Y. Tian 38, R.E. Ticse Torres 51,
 V.O. Tikhomirov 108, aj, Yu.A. Tikhonov 120b, 120a, S. Timoshenko 110, P. Tipton 180, S. Tisserant 99,
 K. Todome 162, S. Todorova-Nova 5, S. Todt 46, J. Tojo 85, S. Tokár 28a, K. Tokushuku 79, E. Tolley 122,
 K.G. Tomiwa 32c, M. Tomoto 115, L. Tompkins 150, K. Toms 116, B. Tong 57, P. Tornambe 50, E. Torrence 127,
 H. Torres 46, E. Torró Pastor 145, C. Tosciri 131, J. Toth 99, aa, F. Touchard 99, D.R. Tovey 146, C.J. Treado 121,
 T. Trefzger 174, F. Tresoldi 153, A. Tricoli 29, I.M. Trigger 165a, S. Trincaz-Duvold 132, M.F. Tripiana 14,
 W. Trischuk 164, B. Trocmé 56, A. Trofymov 128, C. Troncon 66a, M. Trovatelli 173, F. Trovato 153,
 L. Truong 32b, M. Trzebinski 82, A. Trzupek 82, F. Tsai 44, J.-C.L. Tseng 131, P.V. Tsiareshka 105, A. Tsirigotis 159,
 N. Tsirintanis 9, V. Tsiskaridze 152, E.G. Tskhadadze 156a, I.I. Tsukerman 109, V. Tsulaia 18, S. Tsuno 79,
 D. Tsybychev 152, 163, Y. Tu 61b, A. Tudorache 27b, V. Tudorache 27b, T.T. Tulbure 27a, A.N. Tuna 57,
 S. Turchikhin 77, D. Turgeman 177, I. Turk Cakir 4b,s, R. Turra 66a, P.M. Tuts 38, E. Tzovara 97,
 G. Ucchielli 23b, 23a, I. Ueda 79, M. Ughetto 43a, 43b, F. Ukegawa 166, G. Unal 35, A. Undrus 29, G. Unel 168,
 F.C. Ungaro 102, Y. Unno 79, K. Uno 160, J. Urban 28b, P. Urquijo 102, P. Urrejola 97, G. Usai 8, J. Usui 79,
 L. Vacavant 99, V. Vacek 138, B. Vachon 101, K.O.H. Vadla 130, A. Vaidya 92, C. Valderanis 112,
 E. Valdes Santurio 43a, 43b, M. Valente 52, S. Valentineti 23b, 23a, A. Valero 171, L. Valéry 44, R.A. Vallance 21,
 A. Vallier 5, J.A. Valls Ferrer 171, T.R. Van Daalen 14, H. Van der Graaf 118, P. Van Gemmeren 6,
 J. Van Nieuwkoop 149, I. Van Vulpen 118, M. Vanadia 71a, 71b, W. Vandelli 35, A. Vaniachine 163,
 P. Vankov 118, R. Vari 70a, E.W. Varnes 7, C. Varni 53b, 53a, T. Varol 41, D. Varouchas 128, K.E. Varvell 154,
 G.A. Vasquez 144b, J.G. Vasquez 180, F. Vazeille 37, D. Vazquez Furelos 14, T. Vazquez Schroeder 101,
 J. Veatch 51, V. Vecchio 72a, 72b, L.M. Veloce 164, F. Veloso 136a, 136c, S. Veneziano 70a, A. Ventura 65a, 65b,
 M. Venturi 173, N. Venturi 35, V. Vercesi 68a, M. Verducci 72a, 72b, C.M. Vergel Infante 76, C. Vergis 24,
 W. Verkerke 118, A.T. Vermeulen 118, J.C. Vermeulen 118, M.C. Vetterli 149, ap, N. Viaux Maira 144b,
 M. Vicente Barreto Pinto 52, I. Vichou 170, *, T. Vickey 146, O.E. Vickey Boeriu 146, G.H.A. Viehhauser 131,
 S. Viel 18, L. Vigani 131, M. Villa 23b, 23a, M. Villaplana Perez 66a, 66b, E. Vilucchi 49, M.G. Vincter 33,
 V.B. Vinogradov 77, A. Vishwakarma 44, C. Vittori 23b, 23a, I. Vivarelli 153, S. Vlachos 10, M. Vogel 179,
 P. Vokac 138, G. Volpi 14, S.E. Von Buddenbrock 32c, E. Von Toerne 24, V. Vorobel 139, K. Vorobev 110,
 M. Vos 171, J.H. Vossebeld 88, N. Vranjes 16, M. Vranjes Milosavljevic 16, V. Vrba 138, M. Vreeswijk 118,
 T. Šfiligoj 89, R. Vuillermet 35, I. Vukotic 36, T. Ženiš 28a, L. Živković 16, P. Wagner 24, W. Wagner 179,
 J. Wagner-Kuhr 112, H. Wahlberg 86, S. Wahr mund 46, K. Wakamiya 80, V.M. Walbrecht 113, J. Walder 87,
 R. Walker 112, S.D. Walker 91, W. Walkowiak 148, V. Wallangen 43a, 43b, A.M. Wang 57, C. Wang 58b, d,
 F. Wang 178, H. Wang 18, H. Wang 3, J. Wang 154, J. Wang 59b, P. Wang 41, Q. Wang 124, R.-J. Wang 132,
 R. Wang 58a, R. Wang 6, S.M. Wang 155, W.T. Wang 58a, W. Wang 15b, ac, W.X. Wang 58a, ac, Y. Wang 58a,

- Z. Wang ^{58c}, C. Wanotayaroj ⁴⁴, A. Warburton ¹⁰¹, C.P. Ward ³¹, D.R. Wardrope ⁹², A. Washbrook ⁴⁸, P.M. Watkins ²¹, A.T. Watson ²¹, M.F. Watson ²¹, G. Watts ¹⁴⁵, S. Watts ⁹⁸, B.M. Waugh ⁹², A.F. Webb ¹¹, S. Webb ⁹⁷, C. Weber ¹⁸⁰, M.S. Weber ²⁰, S.A. Weber ³³, S.M. Weber ^{59a}, A.R. Weidberg ¹³¹, B. Weinert ⁶³, J. Weingarten ⁵¹, M. Weirich ⁹⁷, C. Weiser ⁵⁰, P.S. Wells ³⁵, T. Wenaus ²⁹, T. Wengler ³⁵, S. Wenig ³⁵, N. Wermes ²⁴, M.D. Werner ⁷⁶, P. Werner ³⁵, M. Wessels ^{59a}, T.D. Weston ²⁰, K. Whalen ¹²⁷, N.L. Whallon ¹⁴⁵, A.M. Wharton ⁸⁷, A.S. White ¹⁰³, A. White ⁸, M.J. White ¹, R. White ^{144b}, D. Whiteson ¹⁶⁸, B.W. Whitmore ⁸⁷, F.J. Wickens ¹⁴¹, W. Wiedenmann ¹⁷⁸, M. Wielers ¹⁴¹, C. Wiglesworth ³⁹, L.A.M. Wiik-Fuchs ⁵⁰, A. Wildauer ¹¹³, F. Wilk ⁹⁸, H.G. Wilkens ³⁵, L.J. Wilkins ⁹¹, H.H. Williams ¹³³, S. Williams ³¹, C. Willis ¹⁰⁴, S. Willocq ¹⁰⁰, J.A. Wilson ²¹, I. Wingerter-Seez ⁵, E. Winkels ¹⁵³, F. Winklmeier ¹²⁷, O.J. Winston ¹⁵³, B.T. Winter ²⁴, M. Wittgen ¹⁵⁰, M. Wobisch ⁹³, A. Wolf ⁹⁷, T.M.H. Wolf ¹¹⁸, R. Wolff ⁹⁹, M.W. Wolter ⁸², H. Wolters ^{136a,136c}, V.W.S. Wong ¹⁷², N.L. Woods ¹⁴³, S.D. Worm ²¹, B.K. Wosiek ⁸², K.W. Woźniak ⁸², K. Wright ⁵⁵, M. Wu ³⁶, S.L. Wu ¹⁷⁸, X. Wu ⁵², Y. Wu ^{58a}, T.R. Wyatt ⁹⁸, B.M. Wynne ⁴⁸, S. Xella ³⁹, Z. Xi ¹⁰³, L. Xia ¹⁷⁵, D. Xu ^{15a}, H. Xu ^{58a}, L. Xu ²⁹, T. Xu ¹⁴², W. Xu ¹⁰³, B. Yabsley ¹⁵⁴, S. Yacoob ^{32a}, K. Yajima ¹²⁹, D.P. Yallup ⁹², D. Yamaguchi ¹⁶², Y. Yamaguchi ¹⁶², A. Yamamoto ⁷⁹, T. Yamanaka ¹⁶⁰, F. Yamane ⁸⁰, M. Yamatani ¹⁶⁰, T. Yamazaki ¹⁶⁰, Y. Yamazaki ⁸⁰, Z. Yan ²⁵, H.J. Yang ^{58c,58d}, H.T. Yang ¹⁸, S. Yang ⁷⁵, Y. Yang ¹⁶⁰, Z. Yang ¹⁷, W-M. Yao ¹⁸, Y.C. Yap ⁴⁴, Y. Yasu ⁷⁹, E. Yatsenko ^{58c,58d}, J. Ye ⁴¹, S. Ye ²⁹, I. Yeletskikh ⁷⁷, E. Yigitbasi ²⁵, E. Yildirim ⁹⁷, K. Yorita ¹⁷⁶, K. Yoshihara ¹³³, C.J.S. Young ³⁵, C. Young ¹⁵⁰, J. Yu ⁸, J. Yu ⁷⁶, X. Yue ^{59a}, S.P.Y. Yuen ²⁴, B. Zabinski ⁸², G. Zacharis ¹⁰, E. Zaffaroni ⁵², R. Zaidan ¹⁴, A.M. Zaitsev ^{140,ai}, T. Zakareishvili ^{156b}, N. Zakharchuk ⁴⁴, J. Zalieckas ¹⁷, S. Zambito ⁵⁷, D. Zanzi ³⁵, D.R. Zaripovas ⁵⁵, S.V. Zeißner ⁴⁵, C. Zeitnitz ¹⁷⁹, G. Zemaityte ¹³¹, J.C. Zeng ¹⁷⁰, Q. Zeng ¹⁵⁰, O. Zenin ¹⁴⁰, D. Zerwas ¹²⁸, M. Zgubić ¹³¹, D.F. Zhang ^{58b}, D. Zhang ¹⁰³, F. Zhang ¹⁷⁸, G. Zhang ^{58a}, H. Zhang ^{15b}, J. Zhang ⁶, L. Zhang ^{15b}, L. Zhang ^{58a}, M. Zhang ¹⁷⁰, P. Zhang ^{15b}, R. Zhang ^{58a}, R. Zhang ²⁴, X. Zhang ^{58b}, Y. Zhang ^{15d}, Z. Zhang ¹²⁸, X. Zhao ⁴¹, Y. Zhao ^{58b,128,af}, Z. Zhao ^{58a}, A. Zhemchugov ⁷⁷, B. Zhou ¹⁰³, C. Zhou ¹⁷⁸, L. Zhou ⁴¹, M.S. Zhou ^{15d}, M. Zhou ¹⁵², N. Zhou ^{58c}, Y. Zhou ⁷, C.G. Zhu ^{58b}, H.L. Zhu ^{58a}, H. Zhu ^{15a}, J. Zhu ¹⁰³, Y. Zhu ^{58a}, X. Zhuang ^{15a}, K. Zhukov ¹⁰⁸, V. Zhulanov ^{120b,120a}, A. Zibell ¹⁷⁴, D. Ziemińska ⁶³, N.I. Zimine ⁷⁷, S. Zimmermann ⁵⁰, Z. Zinonos ¹¹³, M. Zinser ⁹⁷, M. Ziolkowski ¹⁴⁸, G. Zobernig ¹⁷⁸, A. Zoccoli ^{23b,23a}, K. Zoch ⁵¹, T.G. Zorbas ¹⁴⁶, R. Zou ³⁶, M. Zur Nedden ¹⁹, L. Zwaliński ³⁵

¹ Department of Physics, University of Adelaide, Adelaide, Australia² Physics Department, SUNY Albany, Albany, NY, United States of America³ Department of Physics, University of Alberta, Edmonton, AB, Canada⁴ ^(a) Department of Physics, Ankara University, Ankara; ^(b) Istanbul Aydin University, Istanbul; ^(c) Division of Physics, TOBB University of Economics and Technology, Ankara, Turkey⁵ LAPP, Université Grenoble Alpes, Université Savoie Mont Blanc, CNRS/IN2P3, Annecy, France⁶ High Energy Physics Division, Argonne National Laboratory, Argonne, IL, United States of America⁷ Department of Physics, University of Arizona, Tucson, AZ, United States of America⁸ Department of Physics, University of Texas at Arlington, Arlington, TX, United States of America⁹ Physics Department, National and Kapodistrian University of Athens, Athens, Greece¹⁰ Physics Department, National Technical University of Athens, Zografou, Greece¹¹ Department of Physics, University of Texas at Austin, Austin, TX, United States of America¹² ^(a) Bahçeşehir University, Faculty of Engineering and Natural Sciences, Istanbul; ^(b) İstanbul Bilgi University, Faculty of Engineering and Natural Sciences, Istanbul; ^(c) Department of Physics, Bogaziçi University, Istanbul; ^(d) Department of Physics Engineering, Gaziantep University, Gaziantep, Turkey¹³ Institute of Physics, Azerbaijan Academy of Sciences, Baku, Azerbaijan¹⁴ Institut de Física d'Altes Energies (IFAE), Barcelona Institute of Science and Technology, Barcelona, Spain¹⁵ ^(a) Institute of High Energy Physics, Chinese Academy of Sciences, Beijing; ^(b) Department of Physics, Nanjing University, Nanjing; ^(c) Physics Department, Tsinghua University, Beijing;^(d) University of Chinese Academy of Science (UCAS), Beijing, China¹⁶ Institute of Physics, University of Belgrade, Belgrade, Serbia¹⁷ Department for Physics and Technology, University of Bergen, Bergen, Norway¹⁸ Physics Division, Lawrence Berkeley National Laboratory and University of California, Berkeley, CA, United States of America¹⁹ Institut für Physik, Humboldt Universität zu Berlin, Berlin, Germany²⁰ Albert Einstein Center for Fundamental Physics and Laboratory for High Energy Physics, University of Bern, Bern, Switzerland²¹ School of Physics and Astronomy, University of Birmingham, Birmingham, United Kingdom²² Centro de Investigaciones, Universidad Antonio Nariño, Bogota, Colombia²³ ^(a) Dipartimento di Fisica e Astronomia, Università di Bologna, Bologna; ^(b) INFN Sezione di Bologna, Italy²⁴ Physikalisches Institut, Universität Bonn, Bonn, Germany²⁵ Department of Physics, Boston University, Boston, MA, United States of America²⁶ Department of Physics, Brandeis University, Waltham, MA, United States of America²⁷ ^(a) Transilvania University of Brasov, Brasov; ^(b) Horia Hulubei National Institute of Physics and Nuclear Engineering, Bucharest; ^(c) Department of Physics, Alexandru Ioan Cuza University of Iasi, Iasi; ^(d) National Institute for Research and Development of Isotopic and Molecular Technologies, Physics Department, Cluj-Napoca; ^(e) University Politehnica Bucharest, Bucharest; ^(f) West University in Timisoara, Timisoara, Romania²⁸ ^(a) Faculty of Mathematics, Physics and Informatics, Comenius University, Bratislava; ^(b) Department of Subnuclear Physics, Institute of Experimental Physics of the Slovak Academy of Sciences, Kosice, Slovak Republic²⁹ Physics Department, Brookhaven National Laboratory, Upton, NY, United States of America³⁰ Departamento de Física, Universidad de Buenos Aires, Buenos Aires, Argentina³¹ Cavendish Laboratory, University of Cambridge, Cambridge, United Kingdom

- 32 ^(a) Department of Physics, University of Cape Town, Cape Town; ^(b) Department of Mechanical Engineering Science, University of Johannesburg, Johannesburg; ^(c) School of Physics, University of the Witwatersrand, Johannesburg, South Africa
- 33 Department of Physics, Carleton University, Ottawa, ON, Canada
- 34 ^(a) Faculté des Sciences Ain Chock, Réseau Universitaire de Physique des Hautes Energies – Université Hassan II, Casablanca; ^(b) Centre National de l'Energie des Sciences Techniques Nucléaires (CNESTEN), Rabat; ^(c) Faculté des Sciences Semlalia, Université Cadi Ayyad, LPHEA, Marrakech; ^(d) Faculté des Sciences, Université Mohamed Premier and LPTPM, Oujda; ^(e) Faculté des sciences, Université Mohammed V, Rabat, Morocco
- 35 CERN, Geneva, Switzerland
- 36 Enrico Fermi Institute, University of Chicago, Chicago, IL, United States of America
- 37 LPC, Université Clermont Auvergne, CNRS/IN2P3, Clermont-Ferrand, France
- 38 Nevis Laboratory, Columbia University, Irvington, NY, United States of America
- 39 Niels Bohr Institute, University of Copenhagen, Copenhagen, Denmark
- 40 ^(a) Dipartimento di Fisica, Università della Calabria, Rende; ^(b) INFN Gruppo Collegato di Cosenza, Laboratori Nazionali di Frascati, Italy
- 41 Physics Department, Southern Methodist University, Dallas, TX, United States of America
- 42 Physics Department, University of Texas at Dallas, Richardson, TX, United States of America
- 43 ^(a) Department of Physics, Stockholm University; ^(b) Oskar Klein Centre, Stockholm, Sweden
- 44 Deutsches Elektronen-Synchrotron DESY, Hamburg and Zeuthen, Germany
- 45 Lehrstuhl für Experimentelle Physik IV, Technische Universität Dortmund, Dortmund, Germany
- 46 Institut für Kern- und Teilchenphysik, Technische Universität Dresden, Dresden, Germany
- 47 Department of Physics, Duke University, Durham, NC, United States of America
- 48 SUPA – School of Physics and Astronomy, University of Edinburgh, Edinburgh, United Kingdom
- 49 INFN e Laboratori Nazionali di Frascati, Frascati, Italy
- 50 Physikalisches Institut, Albert-Ludwigs-Universität Freiburg, Freiburg, Germany
- 51 II. Physikalisches Institut, Georg-August-Universität Göttingen, Göttingen, Germany
- 52 Département de Physique Nucléaire et Corpusculaire, Université de Genève, Genève, Switzerland
- 53 ^(a) Dipartimento di Fisica, Università di Genova, Genova; ^(b) INFN Sezione di Genova, Italy
- 54 II. Physikalisches Institut, Justus-Liebig-Universität Giessen, Giessen, Germany
- 55 SUPA – School of Physics and Astronomy, University of Glasgow, Glasgow, United Kingdom
- 56 LPSC, Université Grenoble Alpes, CNRS/IN2P3, Grenoble INP, Grenoble, France
- 57 Laboratory for Particle Physics and Cosmology, Harvard University, Cambridge, MA, United States of America
- 58 ^(a) Department of Modern Physics and State Key Laboratory of Particle Detection and Electronics, University of Science and Technology of China, Hefei, China; ^(b) Institute of Frontier and Interdisciplinary Science and Key Laboratory of Particle Physics and Particle Irradiation (MOE), Shandong University, Qingdao; ^(c) School of Physics and Astronomy, Shanghai Jiao Tong University, KLPAC-MoE, SKLPPC, Shanghai; ^(d) Tsung-Dao Lee Institute, Shanghai, China
- 59 ^(a) Kirchhoff-Institut für Physik, Ruprecht-Karls-Universität Heidelberg, Heidelberg; ^(b) Physikalisches Institut, Ruprecht-Karls-Universität Heidelberg, Heidelberg, Germany
- 60 Faculty of Applied Information Science, Hiroshima Institute of Technology, Hiroshima, Japan
- 61 ^(a) Department of Physics, Chinese University of Hong Kong, Shatin, N.T., Hong Kong; ^(b) Department of Physics, University of Hong Kong, Hong Kong; ^(c) Department of Physics and Institute for Advanced Study, Hong Kong University of Science and Technology, Clear Water Bay, Kowloon, Hong Kong, China
- 62 Department of Physics, National Tsing Hua University, Hsinchu, Taiwan
- 63 Department of Physics, Indiana University, Bloomington, IN, United States of America
- 64 ^(a) INFN Gruppo Collegato di Udine, Sezione di Trieste, Udine; ^(b) ICTP, Trieste; ^(c) Dipartimento di Chimica, Fisica e Ambiente, Università di Udine, Udine, Italy
- 65 ^(a) INFN Sezione di Lecce; ^(b) Dipartimento di Matematica e Fisica, Università del Salento, Lecce, Italy
- 66 ^(a) INFN Sezione di Milano; ^(b) Dipartimento di Fisica, Università di Milano, Milano, Italy
- 67 ^(a) INFN Sezione di Napoli; ^(b) Dipartimento di Fisica, Università di Napoli, Napoli, Italy
- 68 ^(a) INFN Sezione di Pavia; ^(b) Dipartimento di Fisica, Università di Pavia, Pavia, Italy
- 69 ^(a) INFN Sezione di Pisa; ^(b) Dipartimento di Fisica E. Fermi, Università di Pisa, Pisa, Italy
- 70 ^(a) INFN Sezione di Roma; ^(b) Dipartimento di Fisica, Sapienza Università di Roma, Roma, Italy
- 71 ^(a) INFN Sezione di Roma Tor Vergata; ^(b) Dipartimento di Fisica, Università di Roma Tor Vergata, Roma, Italy
- 72 ^(a) INFN Sezione di Roma Tre; ^(b) Dipartimento di Matematica e Fisica, Università Roma Tre, Roma, Italy
- 73 ^(a) INFN-TIFPA; ^(b) Università degli Studi di Trento, Trento, Italy
- 74 Institut für Astro- und Teilchenphysik, Leopold-Franzens-Universität, Innsbruck, Austria
- 75 University of Iowa, Iowa City, IA, United States of America
- 76 Department of Physics and Astronomy, Iowa State University, Ames, IA, United States of America
- 77 Joint Institute for Nuclear Research, Dubna, Russia
- 78 ^(a) Departamento de Engenharia Elétrica, Universidade Federal de Juiz de Fora (UFJF), Juiz de Fora; ^(b) Universidade Federal do Rio De Janeiro COPPE/EE/IF, Rio de Janeiro; ^(c) Universidade Federal de São João del Rei (UFSJ), São João del Rei; ^(d) Instituto de Física, Universidade de São Paulo, São Paulo, Brazil
- 79 KEK, High Energy Accelerator Research Organization, Tsukuba, Japan
- 80 Graduate School of Science, Kobe University, Kobe, Japan
- 81 ^(a) AGH University of Science and Technology, Faculty of Physics and Applied Computer Science, Krakow; ^(b) Marian Smoluchowski Institute of Physics, Jagiellonian University, Krakow, Poland
- 82 Institute of Nuclear Physics Polish Academy of Sciences, Krakow, Poland
- 83 Faculty of Science, Kyoto University, Kyoto, Japan
- 84 Kyoto University of Education, Kyoto, Japan
- 85 Research Center for Advanced Particle Physics and Department of Physics, Kyushu University, Fukuoka, Japan
- 86 Instituto de Física La Plata, Universidad Nacional de La Plata and CONICET, La Plata, Argentina
- 87 Physics Department, Lancaster University, Lancaster, United Kingdom
- 88 Oliver Lodge Laboratory, University of Liverpool, Liverpool, United Kingdom
- 89 Department of Experimental Particle Physics, Jožef Stefan Institute and Department of Physics, University of Ljubljana, Ljubljana, Slovenia
- 90 School of Physics and Astronomy, Queen Mary University of London, London, United Kingdom
- 91 Department of Physics, Royal Holloway University of London, Egham, United Kingdom
- 92 Department of Physics and Astronomy, University College London, London, United Kingdom
- 93 Louisiana Tech University, Ruston, LA, United States of America
- 94 Fysiska institutionen, Lunds universitet, Lund, Sweden
- 95 Centre de Calcul de l'Institut National de Physique Nucléaire et de Physique des Particules (IN2P3), Villeurbanne, France
- 96 Departamento de Física Teórica C-15 and CIAFF, Universidad Autónoma de Madrid, Madrid, Spain
- 97 Institut für Physik, Universität Mainz, Mainz, Germany
- 98 School of Physics and Astronomy, University of Manchester, Manchester, United Kingdom
- 99 CPPM, Aix-Marseille Université, CNRS/IN2P3, Marseille, France
- 100 Department of Physics, University of Massachusetts, Amherst, MA, United States of America
- 101 Department of Physics, McGill University, Montreal, QC, Canada
- 102 School of Physics, University of Melbourne, Victoria, Australia

- ¹⁰³ Department of Physics, University of Michigan, Ann Arbor, MI, United States of America
¹⁰⁴ Department of Physics and Astronomy, Michigan State University, East Lansing, MI, United States of America
¹⁰⁵ B.I. Stepanov Institute of Physics, National Academy of Sciences of Belarus, Minsk, Belarus
¹⁰⁶ Research Institute for Nuclear Problems of Byelorussian State University, Minsk, Belarus
¹⁰⁷ Group of Particle Physics, University of Montreal, Montreal, QC, Canada
¹⁰⁸ P.N. Lebedev Physical Institute of the Russian Academy of Sciences, Moscow, Russia
¹⁰⁹ Institute for Theoretical and Experimental Physics (ITEP), Moscow, Russia
¹¹⁰ National Research Nuclear University MEPhI, Moscow, Russia
¹¹¹ D.V. Skobeltsyn Institute of Nuclear Physics, M.V. Lomonosov Moscow State University, Moscow, Russia
¹¹² Fakultät für Physik, Ludwig-Maximilians-Universität München, München, Germany
¹¹³ Max-Planck-Institut für Physik (Werner-Heisenberg-Institut), München, Germany
¹¹⁴ Nagasaki Institute of Applied Science, Nagasaki, Japan
¹¹⁵ Graduate School of Science and Kobayashi-Maskawa Institute, Nagoya University, Nagoya, Japan
¹¹⁶ Department of Physics and Astronomy, University of New Mexico, Albuquerque, NM, United States of America
¹¹⁷ Institute for Mathematics, Astrophysics and Particle Physics, Radboud University Nijmegen/Nikhef, Nijmegen, Netherlands
¹¹⁸ Nikhef National Institute for Subatomic Physics and University of Amsterdam, Amsterdam, Netherlands
¹¹⁹ Department of Physics, Northern Illinois University, DeKalb, IL, United States of America
¹²⁰ ^(a) Budker Institute of Nuclear Physics, SB RAS, Novosibirsk; ^(b) Novosibirsk State University Novosibirsk, Russia
¹²¹ Department of Physics, New York University, New York, NY, United States of America
¹²² Ohio State University, Columbus, OH, United States of America
¹²³ Faculty of Science, Okayama University, Okayama, Japan
¹²⁴ Homer L. Dodge Department of Physics and Astronomy, University of Oklahoma, Norman, OK, United States of America
¹²⁵ Department of Physics, Oklahoma State University, Stillwater, OK, United States of America
¹²⁶ Palacký University, RCPMT, Joint Laboratory of Optics, Olomouc, Czech Republic
¹²⁷ Center for High Energy Physics, University of Oregon, Eugene, OR, United States of America
¹²⁸ LAL, Université Paris-Sud, CNRS/IN2P3, Université Paris-Saclay, Orsay, France
¹²⁹ Graduate School of Science, Osaka University, Osaka, Japan
¹³⁰ Department of Physics, University of Oslo, Oslo, Norway
¹³¹ Department of Physics, Oxford University, Oxford, United Kingdom
¹³² LPNHE, Sorbonne Université, Paris Diderot Sorbonne Paris Cité, CNRS/IN2P3, Paris, France
¹³³ Department of Physics, University of Pennsylvania, Philadelphia, PA, United States of America
¹³⁴ Konstantinov Nuclear Physics Institute of National Research Centre "Kurchatov Institute", PNPI, St. Petersburg, Russia
¹³⁵ Department of Physics and Astronomy, University of Pittsburgh, Pittsburgh, PA, United States of America
¹³⁶ ^(a) Laboratório de Instrumentação e Física Experimental de Partículas – LIP; ^(b) Departamento de Física, Faculdade de Ciências, Universidade de Lisboa, Lisboa; ^(c) Departamento de Física, Universidade de Coimbra, Coimbra; ^(d) Centro de Física Nuclear da Universidade de Lisboa, Lisboa; ^(e) Departamento de Física, Universidade do Minho, Braga; ^(f) Departamento de Física Teórica y del Cosmos, Universidad de Granada, Granada (Spain); ^(g) Dep Física and CEFITEC of Faculdade de Ciências e Tecnologia, Universidade Nova de Lisboa, Caparica, Portugal
¹³⁷ Institute of Physics, Academy of Sciences of the Czech Republic, Prague, Czech Republic
¹³⁸ Czech Technical University in Prague, Prague, Czech Republic
¹³⁹ Charles University, Faculty of Mathematics and Physics, Prague, Czech Republic
¹⁴⁰ State Research Center Institute for High Energy Physics, NRC KI, Protvino, Russia
¹⁴¹ Particle Physics Department, Rutherford Appleton Laboratory, Didcot, United Kingdom
¹⁴² IRFU, CEA, Université Paris-Saclay, Gif-sur-Yvette, France
¹⁴³ Santa Cruz Institute for Particle Physics, University of California Santa Cruz, Santa Cruz, CA, United States of America
¹⁴⁴ ^(a) Departamento de Física, Pontificia Universidad Católica de Chile, Santiago, Chile; ^(b) Departamento de Física, Universidad Técnica Federico Santa María, Valparaíso, Chile
¹⁴⁵ Department of Physics, University of Washington, Seattle, WA, United States of America
¹⁴⁶ Department of Physics and Astronomy, University of Sheffield, Sheffield, United Kingdom
¹⁴⁷ Department of Physics, Shinshu University, Nagano, Japan
¹⁴⁸ Department Physik, Universität Siegen, Siegen, Germany
¹⁴⁹ Department of Physics, Simon Fraser University, Burnaby, BC, Canada
¹⁵⁰ SLAC National Accelerator Laboratory, Stanford, CA, United States of America
¹⁵¹ Physics Department, Royal Institute of Technology, Stockholm, Sweden
¹⁵² Departments of Physics and Astronomy, Stony Brook University, Stony Brook, NY, United States of America
¹⁵³ Department of Physics and Astronomy, University of Sussex, Brighton, United Kingdom
¹⁵⁴ School of Physics, University of Sydney, Sydney, Australia
¹⁵⁵ Institute of Physics, Academia Sinica, Taipei, Taiwan
¹⁵⁶ ^(a) E. Andronikashvili Institute of Physics, Iv. Javakhishvili Tbilisi State University, Tbilisi; ^(b) High Energy Physics Institute, Tbilisi State University, Tbilisi, Georgia
¹⁵⁷ Department of Physics, Technion, Israel Institute of Technology, Haifa, Israel
¹⁵⁸ Raymond and Beverly Sackler School of Physics and Astronomy, Tel Aviv University, Tel Aviv, Israel
¹⁵⁹ Department of Physics, Aristotle University of Thessaloniki, Thessaloniki, Greece
¹⁶⁰ International Center for Elementary Particle Physics and Department of Physics, University of Tokyo, Tokyo, Japan
¹⁶¹ Graduate School of Science and Technology, Tokyo Metropolitan University, Tokyo, Japan
¹⁶² Department of Physics, Tokyo Institute of Technology, Tokyo, Japan
¹⁶³ Tomsk State University, Tomsk, Russia
¹⁶⁴ Department of Physics, University of Toronto, Toronto, ON, Canada
¹⁶⁵ ^(a) TRIUMF, Vancouver, BC; ^(b) Department of Physics and Astronomy, York University, Toronto, ON, Canada
¹⁶⁶ Division of Physics and Tomonaga Center for the History of the Universe, Faculty of Pure and Applied Sciences, University of Tsukuba, Tsukuba, Japan
¹⁶⁷ Department of Physics and Astronomy, Tufts University, Medford, MA, United States of America
¹⁶⁸ Department of Physics and Astronomy, University of California Irvine, Irvine, CA, United States of America
¹⁶⁹ Department of Physics and Astronomy, University of Uppsala, Uppsala, Sweden
¹⁷⁰ Department of Physics, University of Illinois, Urbana, IL, United States of America
¹⁷¹ Instituto de Física Corpuscular (IFIC), Centro Mixto Universidad de Valencia – CSIC, Valencia, Spain
¹⁷² Department of Physics, University of British Columbia, Vancouver, BC, Canada
¹⁷³ Department of Physics and Astronomy, University of Victoria, Victoria, BC, Canada
¹⁷⁴ Fakultät für Physik und Astronomie, Julius-Maximilians-Universität Würzburg, Würzburg, Germany
¹⁷⁵ Department of Physics, University of Warwick, Coventry, United Kingdom
¹⁷⁶ Waseda University, Tokyo, Japan
¹⁷⁷ Department of Particle Physics, Weizmann Institute of Science, Rehovot, Israel
¹⁷⁸ Department of Physics, University of Wisconsin, Madison, WI, United States of America
¹⁷⁹ Fakultät für Mathematik und Naturwissenschaften, Fachgruppe Physik, Bergische Universität Wuppertal, Wuppertal, Germany

¹⁸⁰ Department of Physics, Yale University, New Haven, CT, United States of America

¹⁸¹ Yerevan Physics Institute, Yerevan, Armenia

^a Also at Borough of Manhattan Community College, City University of New York, NY, United States of America.

^b Also at Centre for High Performance Computing, CSIR Campus, Rosebank, Cape Town, South Africa.

^c Also at CERN, Geneva, Switzerland.

^d Also at CPPM, Aix-Marseille Université, CNRS/IN2P3, Marseille, France.

^e Also at Département de Physique Nucléaire et Corpusculaire, Université de Genève, Genève, Switzerland.

^f Also at Departament de Física de la Universitat Autònoma de Barcelona, Barcelona, Spain.

^g Also at Departamento de Física Teórica y del Cosmos, Universidad de Granada, Granada (Spain), Spain.

^h Also at Department of Applied Physics and Astronomy, University of Sharjah, Sharjah, United Arab Emirates.

ⁱ Also at Department of Financial and Management Engineering, University of the Aegean, Chios, Greece.

^j Also at Department of Physics and Astronomy, University of Louisville, Louisville, KY, United States of America.

^k Also at Department of Physics and Astronomy, University of Sheffield, Sheffield, United Kingdom.

^l Also at Department of Physics, California State University, Fresno, CA, United States of America.

^m Also at Department of Physics, California State University, Sacramento, CA, United States of America.

ⁿ Also at Department of Physics, King's College London, London, United Kingdom.

^o Also at Department of Physics, St. Petersburg State Polytechnical University, St. Petersburg, Russia.

^p Also at Department of Physics, University of Fribourg, Fribourg, Switzerland.

^q Also at Department of Physics, University of Michigan, Ann Arbor, MI, United States of America.

^r Also at Dipartimento di Fisica E. Fermi, Università di Pisa, Pisa, Italy.

^s Also at Giresun University, Faculty of Engineering, Giresun, Turkey.

^t Also at Graduate School of Science, Osaka University, Osaka, Japan.

^u Also at Hellenic Open University, Patras, Greece.

^v Also at Horia Hulubei National Institute of Physics and Nuclear Engineering, Bucharest, Romania.

^w Also at II. Physikalisches Institut, Georg-August-Universität Göttingen, Göttingen, Germany.

^x Also at Institut Catalana de Recerca i Estudis Avancats, ICREA, Barcelona, Spain.

^y Also at Institut für Experimentalphysik, Universität Hamburg, Hamburg, Germany.

^z Also at Institute for Mathematics, Astrophysics and Particle Physics, Radboud University Nijmegen/Nikhef, Nijmegen, Netherlands.

^{aa} Also at Institute for Particle and Nuclear Physics, Wigner Research Centre for Physics, Budapest, Hungary.

^{ab} Also at Institute of Particle Physics (IPP), Canada.

^{ac} Also at Institute of Physics, Academia Sinica, Taipei, Taiwan.

^{ad} Also at Institute of Physics, Azerbaijan Academy of Sciences, Baku, Azerbaijan.

^{ae} Also at Institute of Theoretical Physics, Ilia State University, Tbilisi, Georgia.

^{af} Also at LAL, Université Paris-Sud, CNRS/IN2P3, Université Paris-Saclay, Orsay, France.

^{ag} Also at Louisiana Tech University, Ruston, LA, United States of America.

^{ah} Also at Manhattan College, New York, NY, United States of America.

^{ai} Also at Moscow Institute of Physics and Technology State University, Dolgoprudny, Russia.

^{aj} Also at National Research Nuclear University MEPhI, Moscow, Russia.

^{ak} Also at Physikalisch-Technische Bundesanstalt, Braunschweig, Germany.

^{al} Also at School of Physics, Sun Yat-sen University, Guangzhou, China.

^{am} Also at The City College of New York, New York, NY, United States of America.

^{an} Also at The Collaborative Innovation Center of Quantum Matter (CICQM), Beijing, China.

^{ao} Also at Tomsk State University, Tomsk, and Moscow Institute of Physics and Technology State University, Dolgoprudny, Russia.

^{ap} Also at TRIUMF, Vancouver, BC, Canada.

^{aq} Also at Università di Napoli Parthenope, Napoli, Italy.

* Deceased.